

HEATED TOOL PROCESSING OF OUT-OF-AUTOCLAVE COMPOSITE MATERIALS

by

Steven Payette

B. Eng, McGill University, 2013

Department of Mechanical Engineering
McGill University

A thesis submitted to
McGill University
in partial fulfilling of the requirements of the degree of
Master's in Engineering



August 2015

© Steven Payette, 2015

ABSTRACT

As aerospace manufacturers continue to incorporate Out-of-Autoclave (OoA) materials into their aircraft designs, the shortcomings of the convection oven become more and more apparent. Similar to the autoclave, the traditional oven for OoA processing relies on convective heat transfer, which induces thermal lag and limits heating rates, thereby increasing cycle times. This research investigates the manufacturing of OoA composites using heated tooling where the mould surface itself is heated via conduction, resulting in improved thermal control. The heating system studied here is the TCX™ heating element, produced by ThermoCeramix inc. Two prototype systems were developed, and used to benchmark both laminate quality and energy consumption, as well as to explore alternate material forms and part structures to expand the tools' processing flexibility. Quality benchmarking studies showed that TCX™ heated tools are capable of producing laminates of similar quality to a traditional oven cure in terms of void content, short-beam strength, and glass transition temperature. The tools' rapid heating capability was also explored, and was shown to have no negative effect on part quality at heating rates up to 50 °C/min. Energy trials demonstrated the potential for 26.1 to 91.6 percent savings, depending on the way the heating technology is implemented. This led to several tool design recommendations to optimize the energy savings of future tools, specifically by avoiding excessive use of high thermal mass substructures, and making every effort to thermally isolate the tool surface from the rest of the mould. The processing flexibility experiments demonstrated that heated tools are not limited to flat, monolithic parts. First, resin film infusion (RFI) was investigated as a possible low-cost, short cycle time application. Heated tools were shown to produce good quality laminates in all configurations but one. This led to the recommendation that heated tool RFI trials make use of a tool-side resin strategy where possible, and a short room temperature vacuum hold prior to infusion when using both rapid heating and an interspaced strategy. Next, both tapered laminates and sandwich structures featuring lightweight materials were investigated. The TCX™ prototypes were found to be able to handle both configurations by implementing multiple heating zones, and a hybrid heating blanket system.

ABRÉGÉ

Avec l'incorporation grandissante des matériaux composites hors autoclaves par les constructeurs aéronautiques pour leurs structures d'aéronefs, les limitations de la mise en œuvre au four à convection deviennent de plus en plus apparentes. Similaire à l'autoclave, le four conventionnel, utilisé pour des fabrications hors autoclave, repose sur le transfert de chaleur par convection. Ce qui induit un décalage thermique et limite les vitesses de chauffage, conduisant à augmenter la durée des cycles de production. Cette recherche porte sur la fabrication de matériaux composites hors autoclave utilisant un outillage chauffant, où la surface du moule est directement chauffée par conduction, ce qui résulte en un meilleur contrôle thermique. Le système étudié est l'élément chauffant TCX™, fabriqué par ThermoCeramix inc. Deux prototypes ont été développés et comparés à un four à convection. La qualité des laminés, la consommation énergétique, ainsi que différentes formes et types de pièces ont été explorées pour accroître la flexibilité d'utilisation de l'outillage chauffant. Des études de qualité comparative ont démontré que les outils chauffants TCX™ sont capables de produire des laminés de qualité similaire à une mise en œuvre traditionnelle au four à convection en termes de niveau de porosité, de la résistance au cisaillement interlaminaire, et de la température de transition vitreuse. La capacité de chauffage rapide des outils a également été étudiée. Il a été démontré que des taux de chauffe jusqu'à 50 °C/min n'ont pas d'effet négatif sur la qualité des pièces composites. Les essais de consommation d'énergie ont démontré des potentiels de 26 à 92 % en économie d'énergie, dépendamment de la façon dont la technologie chauffante était implémentée. Plusieurs recommandations pour la conception d'outillage ont été effectuées afin d'optimiser l'économie d'énergie. En particulier, il convient d'éviter l'utilisation excessive de sous-structures à haute masse thermique, et d'isoler thermiquement la surface du moule du reste du moule. Une étude sur la flexibilité de la mise en forme des outils chauffants a démontré que ceux-ci ne sont pas limités à des pièces monolithiques planes. Premièrement, le procédé d'infusion de films de résine (RFI) a été considéré comme une application à faible coût ayant un temps de production rapide. Les outils chauffants ont été capables de produire des laminés de bonne qualité dans toutes les configurations, sauf une. Il a donc été recommandé que les essais RFI avec outils chauffants fasse l'usage d'une stratégie de résine côté

outil (si possible), et une mise sous vide à température ambiante avant l'infusion lorsque le chauffage rapide et une stratégie espacée sont utilisés conjointement. Enfin, les laminés effilés et les panneaux sandwich avec âme à nid d'abeille ont été étudiés. Les prototypes TCX™ ont été capables de cuire chacune des configurations en implémentant différentes zones de chauffage indépendantes et par l'utilisation d'un système de chauffage hybride à l'aide d'une couverture chauffante.

ACKNOWLEDGEMENTS

To begin, I would like to thank my supervisor, Professor Pascal Hubert, for his guidance throughout my time at McGill. His advice and mentorship were not only instrumental to my Master's project, but to also to my growth as an engineer. My time in the Structures and Composite Materials Laboratory has been amazing, and I believe that is mainly due to the spirit of learning and friendship instilled in the group by Professor Hubert as well as Professor Larry Lessard. I would also like to acknowledge Professor Lessard for giving me my start in the composites lab as an undergraduate all those years ago.

Within the Structures and Composite Materials Laboratory, I'd like to thank everyone who has called MD53A home for the last two years. I've truly appreciated the wonderful environment, and it made my graduate studies a period of my life that I'll never forget. Every member had an impact on my work, be it through lending a hand in the lab or helping to brainstorm ideas, and for that I'll always be grateful. Special thanks go to Adam Smith (for continued support on this project), Olivia Houston (helping with ramp rate trials), and to both Benoit Landry and Mathieu Préau (abstract translation).

This research was made possible thanks to a number of partners. I would like to acknowledge the financial support of the FQRNT, as well as NSERC under the G8 Research Councils Initiative on Multilateral Research Funding. Bombardier Aerospace and Cyttec are also acknowledged for providing the composite materials studied here. In addition, many thanks are owed to the people at ThermoCeramix for the time and expertise they put into developing the heated tools used throughout this research. In particular I'd like to thank Kyle Goyette for his support and friendship throughout this project.

Finally, I would like to thank my family for their constant support and Lauren for her love, patience, and faith in me.

TABLE OF CONTENTS

Abstract.....	II
Abrégé	III
Acknowledgements	V
Table of Contents	VI
List of Figures.....	IX
List of Tables	XI
Nomenclature	XII
Chapter 1: Introduction	1
1.1 Background	1
1.2 Research Objectives and Thesis Organization	4
Chapter 2: Literature Review	6
2.1 Heat Transfer.....	6
2.1.1 Convection	6
2.1.2 Conduction.....	7
2.1.3 Combined Heat Transfer Effects	8
2.2 Traditional Convection-Based Processing.....	10
2.2.1 Autoclave Manufacturing	10
2.2.2 Convection Oven Processing.....	11
2.3 Heated Tool Technologies	13
2.3.1 Traditional Integrated Heaters	13
2.3.2 CFOAM [®]	14
2.3.3 Quickstep [™]	15
2.3.4 TCX [™] Resistive Element.....	17
2.4 Thermo-Chemical Phenomena.....	19
2.4.1 Degree of Cure.....	20
2.4.2 Resin Viscosity	21
2.4.3 Glass Transition Temperature.....	22
2.4.4 Exotherm.....	23
2.5 Summary of Literature Review	24
Chapter 3: Prototype Development.....	27
3.1 Heated Tool Plate Prototype	27

3.1.1	Physical Design.....	27
3.1.2	Control and Monitoring System.....	29
3.2	Multi-Zoned Tool Prototype	30
3.2.1	Physical Design.....	30
3.2.2	Control and Monitoring System.....	32
3.2.3	LabVIEW Control Program.....	33
Chapter 4:	Quality Benchmarking.....	36
4.1	Test Plan.....	36
4.2	Laminate Preparation	36
4.3	Void Content	39
4.3.1	Methodology.....	39
4.3.2	Baseline Oven Comparison.....	40
4.3.3	Heated Tool Ramp Rate Trials	41
4.4	Short-Beam Shear Strength.....	44
4.4.1	Methodology.....	45
4.4.2	Overall Comparison	45
4.5	Glass Transition Temperature	46
4.5.1	Methodology.....	47
4.5.2	Overall Comparison	47
4.6	Summary of Results and Discussion.....	47
Chapter 5:	Energy Consumption	49
5.1	Methodology	49
5.2	Energy Trial Results.....	51
5.2.1	Direct Comparison of Heating Systems.....	53
5.2.2	Effect of Heating Rate	53
5.3	Scaled Comparisons	54
5.3.1	Oven Power Function Scaling	54
5.3.2	Laminate Area Scaling.....	55
5.3.3	Scale Up Considerations.....	56
5.4	Results and Discussion.....	56
Chapter 6:	Processing Flexibility	58
6.1	Resin Film Infusion.....	58
6.1.1	Methodology.....	59
6.1.2	Void Content Results	60
6.1.3	Discussion.....	61
6.2	Tapered Laminates	62

6.2.1	Methodology	63
6.2.2	Laminate Preparation	64
6.2.3	Direct Comparison of Heating Systems.....	65
6.2.4	Power Considerations	68
6.3	Sandwich Structures.....	70
6.3.1	Methodology	70
6.3.2	Laminate Preparation	70
6.3.3	Results and Discussion	72
6.4	Summary of Processing Flexibility Experiments.....	75
Chapter 7: Conclusions and Future Work.....		76
7.1	Conclusions and Contributions	76
7.2	Future Work	77
References.....		79
Appendix I – Quality Benchmarking Data.....		84
Appendix II – Energy Benchmarking Data.....		89

LIST OF FIGURES

Figure 1.1-1: Bell-Boeing V-22 material usage [3]	2
Figure 1.1-2: Boeing 787 material usage [6]	2
Figure 1.1-3: TCX™ multi-layer heating system	3
Figure 2.1-1: Schematic of typical 1-D autoclave/oven heat transfer	9
Figure 2.1-2: Schematic of typical 1-D heated tool heat transfer	9
Figure 2.2-1: Typical autoclave schematic [7]	10
Figure 2.2-2: OoA prepreg air evacuation channels [16]	12
Figure 2.3-1: Integrated heating example temperature distribution [20]	13
Figure 2.3-2: CFOAM® heating setup [22]	14
Figure 2.3-3: Quickstep process schematic [21]	16
Figure 2.3-4: Thermal spray element deposition [30]	17
Figure 2.3-5: TCX™ element trace (left), in service (right) [30]	18
Figure 2.4-1: Thermoset cross-linking during cure [35]	19
Figure 2.4-2: Generalized TTT cure diagram [36]	20
Figure 2.4-3: Example of exotherm during composites manufacturing [5]	24
Figure 3.1-1: HTP trimetric view showing tool surface, vacuum fittings, and support structure	28
Figure 3.1-2: HTP underside showing TCX™ heating element configuration	28
Figure 3.1-3: HTP control system circuit diagram	29
Figure 3.2-1: Multi-zoned TCX™ heating system	30
Figure 3.2-2: MZT underside featuring six heating elements	31
Figure 3.2-3: MZT control system circuit diagram, elements 1-3	32
Figure 3.2-4: LabVIEW control program overview	33
Figure 3.2-5: MZT controller PID output vs. current drawn	34
Figure 4.2-1: Flat laminate bagging scheme, arrows indicating air evacuation direction	37
Figure 4.2-2: Quality benchmarking cure cycles	38
Figure 4.2-3: Typical thermal profile for 3 °C/min HTP heating	38
Figure 4.2-4: Typical thermal profile for 50 °C/min HTP heating	38
Figure 4.3-1: Quality assessment sample locations, arrows indicating micrographed edges	39
Figure 4.3-2: Average laminate void contents, oven vs. HTP at 3 °C/min	40

Figure 4.3-3: Average heating method void contents, Oven vs. HTP at 3 °C/min.....	41
Figure 4.3-4: Average void contents, HTP cure with 3, 10, 30, and 50 °C/min heating	42
Figure 4.3-5: Representative micrograph, HTP 3 °C/min, 1.42% void content	42
Figure 4.3-6: Representative micrograph, HTP 10 °C/min, 2.33% void content	43
Figure 4.3-7: Representative micrograph, HTP 30 °C/min, 1.98% void content	43
Figure 4.3-8: Representative micrograph, HTP 50 °C/min, 3.35% void content	44
Figure 4.4-1: Average short-beam strengths for 3 heating conditions.....	45
Figure 4.4-2: Short-beam strength vs. void content.....	46
Figure 5.2-1: Representative power vs. time for Oven-3C condition.....	51
Figure 5.2-2: Representative power vs. time for HTP-3C condition	51
Figure 5.2-3: Representative power vs. time for HTP-50C condition	52
Figure 5.2-4: Representative power vs. time for MZT-3C condition	52
Figure 5.2-5: Energy consumption per heating system using 3 °C/min heating	53
Figure 5.3-1: Cavity volume vs. maximum power for commercially available ovens.....	54
Figure 6.1-1: Tool-Side RFI layup configuration	59
Figure 6.1-2: Interspaced RFI layup configuration.....	59
Figure 6.1-3: RFI trial 2 sample micrograph, 0.26 % void content	61
Figure 6.1-4: RFI trial 5 sample micrograph, 2.31 % void content	61
Figure 6.2-1: Thermal performance metrics illustrated for a typical one-sided heating cure.....	64
Figure 6.2-2: Tapered laminate layup configuration	65
Figure 6.2-3: Co-cured laminate layup configuration.....	65
Figure 6.2-4: Tapered laminate thermal lag results	66
Figure 6.2-5: Tapered laminate mid-plane temperature deviation results	67
Figure 6.2-6: Tapered laminate through-thickness temperature difference results	67
Figure 6.2-7: Comparison of oven processed co-cured and tapered laminates	68
Figure 6.2-8: Comparison of MZT processed co-cured and tapered laminates.....	68
Figure 6.2-9: MZT tapered laminate power consumption per zone	69
Figure 6.3-1: Sandwich structure laminate configuration.....	71
Figure 6.3-2: Sandwich structure oven cure thermal profile	72
Figure 6.3-3: Sandwich structure heated tool cure thermal profile	73
Figure 6.3-4: Sandwich structure hybrid cure thermal profile.....	73

LIST OF TABLES

Table 2.5-1: Summary of heating technologies	25
Table 4.5-1: Glass transition temperature results with standard deviations	47
Table 4.6-1: Quality benchmarking average results with standard deviations	48
Table 5.1-1: Heating conditions for energy consumption trials	50
Table 5.2-1: Energy trial average results with standard deviations	52
Table 5.3-1: Theoretical oven energy consumption based on power function scaling	55
Table 5.3-2: Oven power function scaling results	55
Table 5.3-3: Laminate area scaling results	56
Table 6.1-1: RFI trial void content results	60
Table 6.3-1: Sandwich structure thermal performance results	74

NOMENCLATURE

ABBREVIATIONS

AC	Alternating current
ANOVA	Analysis of variance
CAD	Computer-aided design
CFOAM [®]	Carbon foam
CFRP	Carbon fibre reinforced polymer
CTE	Coefficient of thermal expansion
DC	Direct current
DMA	Dynamic mechanical analysis
FRP	Fibre reinforced polymer
HTP	Heated tool plate
MZT	Multi-zoned tool
OoA	Out-of-autoclave
PID	Proportional-integral-derivative
Prepreg	Fibre reinforcement pre-impregnated with resin
RFI	Resin film infusion
RMS	Root mean square
SSR	Solid state relay
TTT	Time-Temperature-Transformation
VI	Virtual instrument

CONSTANTS AND VARIABLES

A	Area
c_p	Specific heat capacity
E	Energy
$E_{experimental}$	Experimentally determined energy consumption
$E_{scaled\ oven}$	Energy consumption for a theoretical oven
E_{total}	Total 3-phase energy

$_{gel}T_g$	Glass transition temperature at gelation
h	Heat transfer coefficient
$H(t)$	Heat of reaction at time t
H_T	Total heat of reaction
I_{phase}	Current of 1 phase in 3-phase power
I_{RMS}	Root mean square current
k	Thermal conductivity
P	Power
$P_{heater\ wattage}$	Oven heater wattage
P_{total}	Total 3-phase power
$q_{cond,x}$	Steady-state rate of convective heat transfer, x direction
q_{conv}	Rate of convective heat transfer
RMS	Root mean square
t	Time
t_{cycle}	Length of cure cycle
t_{lag}	Thermal lag
T	Temperature
T_A	Fluid bulk temperature
T_g	Glass transition temperature
T_{g0}	Initial glass transition temperature
$T_{g\infty}$	Glass transition temperature of fully cured resin
T_S	Surface temperature
V_{LL}	Line-to-line voltage
$Vol.$	Oven chamber volume
V_{RMS}	Root mean square voltage
α_C	Degree of cure
α_T	Thermal diffusivity
ΔT_{mp}	Mid-plane temperature deviation
ΔT_{tt}	Through-thickness temperature difference
μ	Viscosity
ρ	Density

CHAPTER 1: INTRODUCTION

As scientists and engineers continue to produce new and exciting materials, designers are faced with many options when considering the base material for a given application. Materials such as metals, ceramics, glasses, and polymers all have their strengths, and are suited to a variety of applications. Another class of materials, known as composites, have been used throughout history but have seen an increase in use in modern times. The American Society of Composites Manufacturers provides a succinct definition of composite materials, which hints at their complicated nature:

Composites are two or more materials with markedly different physical or chemical properties – categorized as “matrix” or “reinforcement” – combined in a way that they act in concert, yet remain separate and distinct at some level because they don’t fully merge or dissolve into one another [1].

This definition is broad enough to encompass many early examples of composites, such as rebar reinforced concrete. Modern composites usually refer to a polymer matrix combined with fibre reinforcements, dubbed Fibre Reinforced Polymers (FRP). Typical matrices include both thermoset and thermoplastic polymers, and the fibre reinforcements can be any of a number of materials including carbon, glass, aramid, and natural fibres. These materials have seen widespread adoption in recent years, across a number of industries. Industries such as aerospace, automotive, biomedical, and sporting goods have turned to FRPs in their search for high performance and economic advantage. Their interest has made these materials a popular topic in engineering research, as FRPs are uniquely suited to tackle a number of engineering challenges.

1.1 BACKGROUND

In the aerospace industry, advancements in composite materials have led to their increased use in both military and commercial aircraft since showing initial promise in the 1960s and 1970s [2]. On the military side, early examples such as the F-15 and F-16 paved the way for more modern applications like the V-22 Osprey and the F-35 Joint Strike Fighter, with composites representing 50% and 35% of their respective structural weights [3; 4]. Manufacturers of commercial aircraft

have also made a push towards these advanced materials, with Boeing moving from 1% to over 50% composites by weight from the 747 to their recent 787 Dreamliner [4]. As engineers have gained experience with these materials, they have been incorporated into more and more components as companies look for every edge over their competition. These materials offer many advantages over conventional materials, such as high specific strength and modulus, tailorable anisotropic properties, long fatigue life, and corrosion resistance [5].

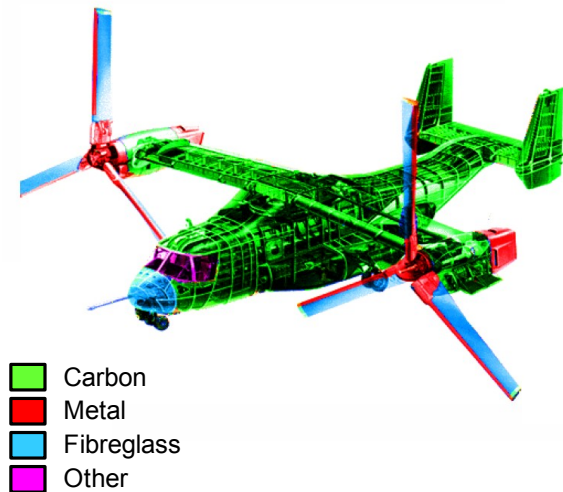


Figure 1.1-1: Bell-Boeing V-22 material usage [3]

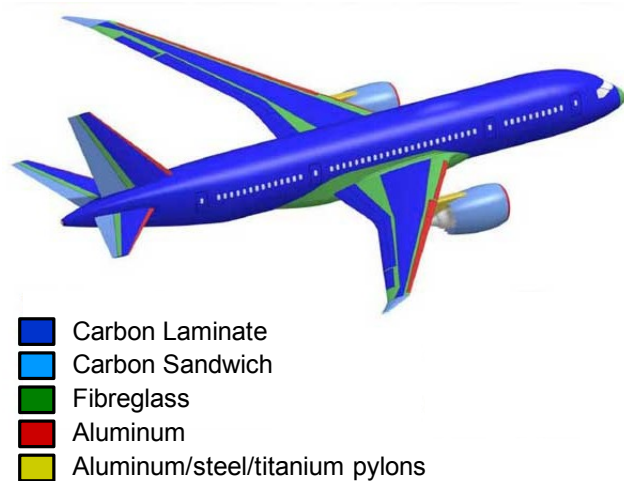


Figure 1.1-2: Boeing 787 material usage [6]

One common combination of fibre and resin seen throughout the aerospace industry is the pairing of carbon and epoxy. Carbon-epoxy materials come in a variety of forms, the most common being fibre reinforcements pre-impregnated with resin (prepreg). Prepregs come as sheets of continuous fibres, unidirectional or woven, already combined with resin. In a typical manufacturing environment, prepreg plies are placed on a rigid tool, compacted under a vacuum bag, and cured. As epoxy is a thermosetting material, all manufacturing techniques using this material require the application of heat to promote the polymerization of the material. What begins as a stack of flexible sheets becomes a rigid structure through the application of heat and pressure, leading to high quality, lightweight parts.

For many applications, this heat and pressure have been supplied by an autoclave, which has long been the most common manufacturing method for advanced composites [7]. The autoclave cure (Section 2.2.1) succeeds at achieving excellent quality mostly due to its high pressure envi-

ronment which compacts the material, preventing the formation of voids within the matrix [8]. However, an autoclave is very expensive to install and operate, which has led to manufacturers seeking more cost-effective alternatives. To that end researchers developed out-of-autoclave (OoA) carbon-epoxy material systems capable of producing autoclave quality parts under atmospheric conditions (Section 2.2.2), greatly reducing costs. Unfortunately, the convection ovens used with these materials feature some of the same drawbacks as the autoclave when it comes to thermal performance. Relying on convective heat transfer leads to considerable thermal lag and limited heating rates, which ultimately limits cycle times [8].

To address the common challenge faced by both autoclave and OoA processing, many alternatives featuring more direct heating have been developed (Section 2.3). One such technology, the TCX™ heating element is the primary subject of this research. This element is composed of multiple layers which can be applied directly to the underside of a mould, and offers many advantages over other heating systems. It is compact, has very low thermal mass, and can be tailored to provide specific amounts of heat to local areas, all of which make it an interesting candidate for use in the aerospace industry. That said, little work has been done proving its potential for composites manufacturing. The coupling of the TCX™ element with OoA processing techniques could potentially provide a cost-effective processing solution for the manufacturing of aerospace components, as will be discussed in this thesis.



Figure 1.1-3: TCX™ multi-layer heating system

1.2 RESEARCH OBJECTIVES AND THESIS ORGANIZATION

The overall motivation of this thesis is to understand how the TCX™ heating element can be successfully integrated into composites manufacturing. For manufacturers to be comfortable working with new technologies such as this element, they need to understand its advantages and its limitations. To this end, three research objectives were identified as the primary goals of this project:

1. To develop TCX™ heated tool prototypes suitable for laboratory scale processing of OoA composite materials.
2. To benchmark these tools against convection oven processing to identify and evaluate any major differences in terms of thermal performance, laminate quality, and energy consumption.
3. To expand the processing flexibility of TCX™ heated tools beyond the processing of flat, monolithic laminates by investigating alternate material forms and part configurations.

Based on these objectives, the organization of this thesis is as follows:

Chapter 2: A review of current literature relevant to the thesis objectives is presented. This includes a summary of the heat transfer and heat driven phenomena involved in composites manufacturing, as well as presenting pertinent models governing these phenomena. A review of the various heating technologies used throughout the aerospace industry is also included.

Chapter 3: Details are provided on the development of two heating systems featuring the TCX™ heating element. This includes the rationale behind the physical design as well as the control and monitoring systems used throughout, including the LabVIEW code developed as part of this project.

Chapter 4: A quality assessment benchmarking regime is implemented, comparing a heated tool prototype to a convection oven in terms of void content, short-beam strength, and glass transition temperature. The effect of heating rate on quality is also studied to evaluate the high ramp rate cure cycles made possible by this heating technology.

Chapter 5: The energy requirements of the two heated tool prototypes developed here are assessed, and compared to a laboratory scale convection oven. The issue of scale is discussed, and two methods are proposed to provide a more fair comparison between heating methods. Based on these results, recommendations are provided for future heated tool designs.

Chapter 6: Three investigations are performed in an effort to increase the processing flexibility of TCX™ heated tools while examining some of the potential challenges of using this technology. These include studies on resin film infusion (RFI), the manufacturing of tapered laminates, and the manufacturing of sandwich structures featuring lightweight core materials.

Chapter 7: The conclusions of this research project are presented, along with suggestions for future work which could further develop the TCX™ heating element as a method for composites processing.

CHAPTER 2: LITERATURE REVIEW

Composites manufacturing is a complex problem, which couples problems of gas transport, resin flow, thermo-chemical reactions, flow-compaction, and stress deformations [9]. Dealing with all of these problems plays a role in successfully using composite materials to produce high quality parts suitable for the aerospace industry. Within the context of this thesis, certain aspects of composites processing require special attention. This chapter presents a literature review of several topics relevant to heated tool processing of composite materials, specifically heat transfer, an introduction to traditional autoclave and OoA processing, an overview of the available heated tool technologies, and thermo-chemical phenomena and pertinent models related to the OoA materials studied here.

2.1 HEAT TRANSFER

Heat transfer seeks to predict the energy transfer that takes place between bodies due to the existence of a temperature difference [10]. In composites processing, it is this energy which drives the manufacturing processes for both thermoset and thermoplastic materials. As the main materials used throughout this research project are thermosetting epoxies, heat transfer as it affects this type of resin merits further exploration. In simple terms, heat is transferred to the resin, accelerating its polymerization. This chemical reaction transforms a liquid resin into a solid part, locking the geometry in place and holding the reinforcing fibres in the correct orientation to carry structural loads. The energy powering this reaction can reach the resin in a variety of ways, and can have a number of effects on the part's quality and manufacturing cycle. The two dominant forms of heat transfer relevant to composites manufacturing are convection and conduction [11]. At higher temperatures, radiation can also play an important role, but it is not be a major contributor at the temperatures required to process thermosets [12].

2.1.1 CONVECTION

In terms of convection, it has been mentioned previously that the autoclave is the predominant manufacturing method for advanced composites [7]. The autoclave relies on the circulation of a hot gas to transfer heat into a composite material and the mould supporting the composite, driv-

ing the cure. This is a typical example of forced convection. Similarly, OoA processing uses a convective oven which again relies on the circulation of a hot gas. Therefore, for both the autoclave and the oven, heat transfer is governed by the classic convection equation. This equation as it applies to composites processing is given in Equation 1:

$$q_{conv} = hA(T_A - T_S) \quad (1)$$

where q_{conv} is the rate of convective heat transfer, A is the surface area, h is the heat transfer coefficient, and T_A and T_S are the temperature of the gas and the surface respectively.

In this simple form, the governing equation cannot easily be applied to most situations for a number of reasons. Foremost among these reasons is the difficulty in determining h , as empirical correlations exist only for very simple cases. In real-world scenarios h must be determined experimentally. Beyond this limitation, heat transfer analysis can prove be difficult for composites processing, as the nature of autoclaves and ovens filled with tools of various shapes and sizes can lead to complex gas flow patterns and variations in both temperature and heat transfer rates [11]. That said, this simple equation does serve to identify the main driving factors in convective heat transfer, namely the heat transfer coefficient, the temperature difference between a surface and the gas, and the area exposed to convection. Beyond these factors, several variables are known to affect convective heat transfer in a closed cavity like an autoclave, such as gas pressure, gas velocity, and gas flow turbulence. Increasing any of these factors will improve convective heat transfer [5].

2.1.2 CONDUCTION

Conduction is the second main form of heat transfer relevant to composites processing. It is especially important here as it is the driving force in a number of heated tooling technologies. These technologies typically apply heat directly to a mould, and thus to a composite via conduction through the tooling material. In one dimension, steady-state conduction is governed by Fourier's Law given in Equation 2:

$$q_{cond,x} = -kA \frac{dT}{dx} \quad (2)$$

where k is the material's thermal conductivity, A is the cross-sectional surface area, and dT/dx is the temperature gradient. This equation shows that the energy transfer per unit area is proportional to the temperature gradient driving the heat flow.

When temperature is changing with time, the steady-state conduction equation cannot be used. Instead, the transient heat equation must be used as given in Equation 3 for 1-D conduction:

$$\frac{\partial T}{\partial t} = \alpha_T \frac{\partial^2 T}{\partial x^2} \quad (3)$$

where α_T is the thermal diffusivity. The value of α is given by:

$$\alpha_T = \frac{k}{\rho c_p} \quad (4)$$

where k is again the thermal conductivity, ρ is the density, and c_p is the specific heat capacity.

2.1.3 COMBINED HEAT TRANSFER EFFECTS

While Equations 1, 2 and 3 are all relatively simple, the heat transfer present in composites manufacturing is in fact fairly complex. These equations are provided in 1 dimension for clarity, but the problem is inherently 3 dimensional. Adding to the complexity is the anisotropic nature of composite materials, meaning that thermal properties will differ in each direction of the material. Beyond that, despite indicating that convection is dominant in autoclave and oven systems, and conduction is dominant in heated tooling, in reality both heat transfer methods play a role in all processes. Figures 2.1-1 and 2.1.2 show the typical 1 dimensional heat flow for autoclave/oven and heated tool scenarios respectively, with wavy, dashed arrows representing convection and straight, solid arrows representing conduction.

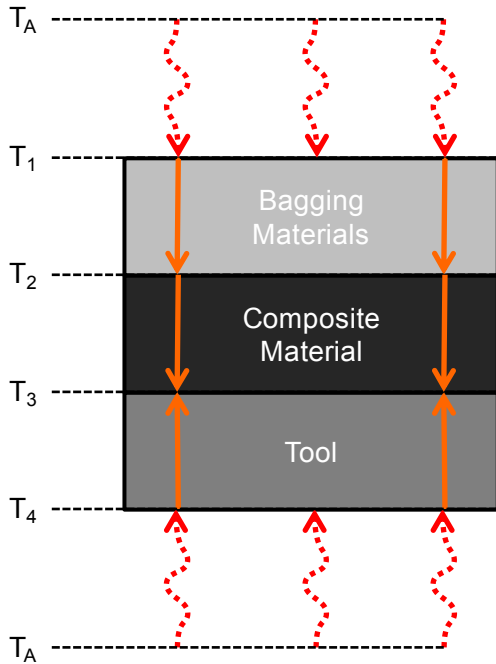


Figure 2.1-1: Schematic of typical 1-D autoclave/oven heat transfer

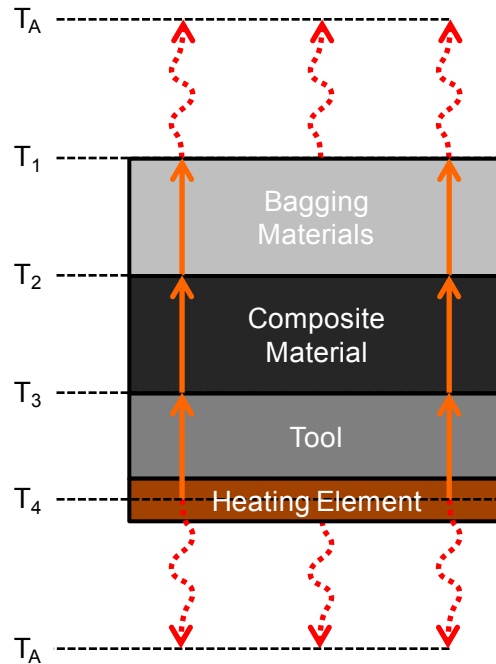


Figure 2.1-2: Schematic of typical 1-D heated tool heat transfer

As shown in Figure 2.1-1, the main driver in both autoclave and oven processing is convective heat transfer to the bottom and the top of the assembled vacuum bag, composite part, and tool (T_A to T_1 and T_4). Within the assembly, conduction transfers heat down through the bagging materials (T_1 to T_2), and up through the tool (T_4 to T_3). The direction of heat flow within the composite depends on the relative thermal mass of each component, but it is generally the tool that heats the slowest and thus heat flows from the composite to the tool (T_2 to T_3). Note that this simplification ignores heat generation within the laminate which will be explored in Section 2.4.4.

In Figure 2.1-2, the main driver is heat transfer away from a heating element. Here there is conduction up through the assembly (T_4 to T_3 , T_3 to T_2 , and T_2 to T_1), and natural convection to the surroundings (T_4 and T_1 to T_A). Again, this simplification ignores heat generation within the laminate.

In all cases, both convective and conductive heat transfer play an important role in transferring energy to the composite. The key is to ensure that the composite itself follows the desired cure cycle, while navigating the complex heat transfer and thermo-chemical phenomena present.

2.2 TRADITIONAL CONVECTION-BASED PROCESSING

As previously mentioned, both oven and autoclave manufacturing techniques rely on convective heat transfer to deliver heat to the material. As these systems serve as a baseline for composites processing, and exploration of their relative strengths and weaknesses serves to highlight some of the areas where heated tooling may be of use to manufacturers.

2.2.1 AUTOCLAVE MANUFACTURING

For high performance aerospace components, the autoclave has long been the most widely used process in composites manufacturing [7]. Autoclaves are essentially a pressurized oven, capable of maintaining high temperatures and pressures during cure. A schematic of a typical autoclave is included in Figure 2.2-1.

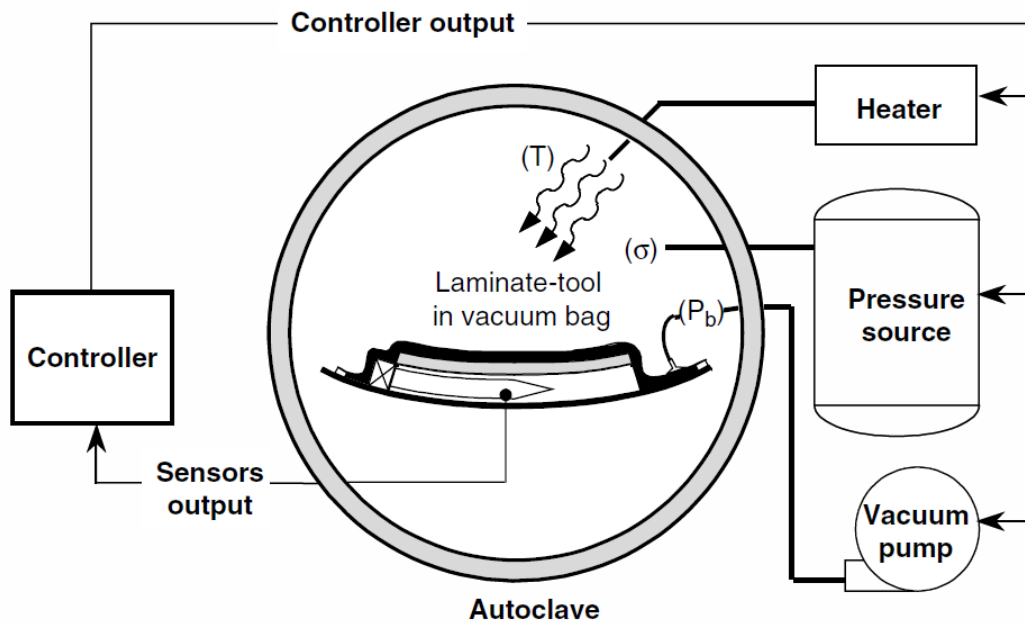


Figure 2.2-1: Typical autoclave schematic [7]

In terms of heating, the autoclave is in no way superior to other processes, but its high pressure environment is extremely attractive. By applying vacuum to the part, and injecting pressurized gas into the autoclave chamber, significant compaction pressure can be applied. A typical autoclave cure involves 6 to 8 atm of pressure, which forces entrapped air out of the part, consolidates the materials, and crushes any volatiles released during cure [7]. This is critical to create a

void-free part and ensure the best possible mechanical properties of the final component. The heating within an autoclave is applied in the same way as a convection oven, typically with electrical resistance heaters producing heat and fans circulating the hot gas. This results in a fairly even temperature distribution throughout the chamber, as well as across the tool [13].

However, autoclave ramp rates tend to be limited to 2 to 4 °C/min, and there can be a substantial lag between the autoclave temperature and the temperature of the tool and the part [8]. This tends to limit the autoclave's ability to maintain high production rates, as each cure requires several hours to heat the compressed gas, and must delay until all parts in the chamber reach the required cure temperature. The count of the material cure time can only begin once everything in the autoclave has reached the desired cure temperature. As such, autoclave manufacturing can often involve lengthy delays while parts wait for autoclave availability. Even with extremely precise planning and scheduling, the production rate can easily be thrown off by errors and unanticipated delays.

Additionally, one of the key detriments to autoclave curing is the high acquisition and operation costs. The high pressure requirements of an autoclave mean it must be a very substantial structure, capable of resisting the high pressure. For large autoclaves capable to curing fuselage size structures, it's not uncommon for the autoclave to be built first, and the rest of the manufacturing facility to be built around it. In terms of operation costs, every run of an autoclave means a compressing a large volume of gas, and heating the entire volume. This is very energy intensive, and contributes to the autoclave's high costs and negative environmental impact. Authors such as Witik *et al.* have studied the costs of autoclaves in an attempt to provide both ways to mitigate these costs, and motivation to switch to other processing techniques [14]. All things considered, while the autoclave is capable of producing high quality parts, there are many drawbacks which make them less appealing for certain applications.

2.2.2 CONVECTION OVEN PROCESSING

Due to the high costs associated with autoclaves, researchers have long sought a cheaper alternative. Using a conventional oven without the high pressure capabilities of an autoclave would have several positive effects. As stated by Ridgard, these would include removing the size con-

straints imposed by an autoclave, reducing costs, and allowing for more suppliers to enter into the aerospace industry [15]. This goal has led to the development of OoA material systems, which are capable of producing autoclave quality parts under atmospheric conditions. Studying these materials has been the focus of significant research in recent years, as they represent a promising future for composites.

However, the standard oven faces many challenges similar to that of an autoclave. The entire volume of air must be heated, so fast ramp rates are generally not possible. In addition, without the consolidation pressure of an autoclave, air entrapped in the part must be removed prior to cure through the addition of a room temperature vacuum hold, which according to Centea *et al.* can be on the order of hours or days for large parts [16]. This limits production rates, as the lengthy vacuum hold greatly increases a part's cycle time. OoA prepregs have been designed to maximize their air evacuation abilities by incorporating dry channels within the material as shown in Figure 2.2-2. These channels allow for air to be drawn out of the material in the plane of the fibres. However, even with these channels, the vacuum hold is a major limitation as large parts require far too long to properly remove the air [16]. As such, while oven cured OoA prepregs have to some extent succeeded in reducing costs, they have not at this stage been able to simultaneously meet the cycle time and part quality requirements.

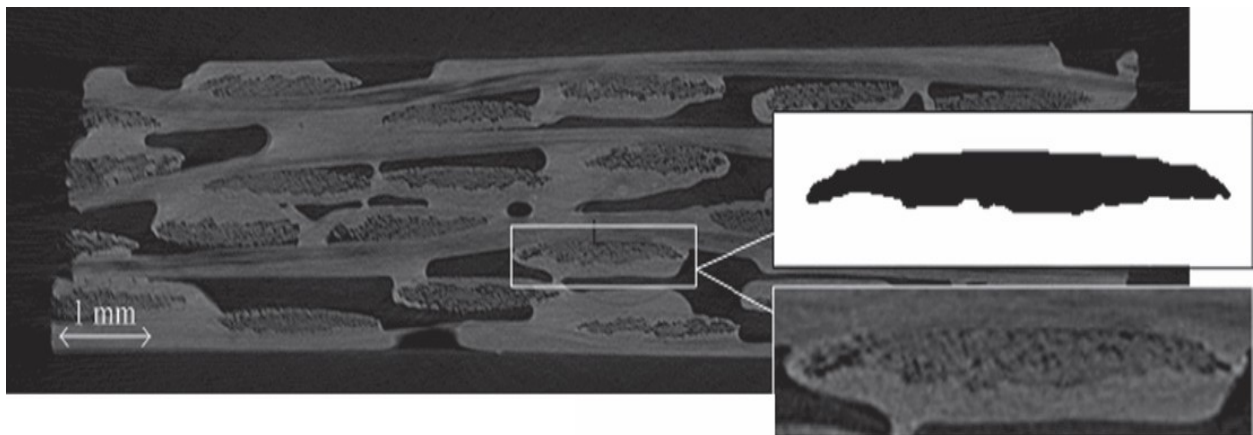


Figure 2.2-2: OoA prepreg air evacuation channels [16]

2.3 HEATED TOOL TECHNOLOGIES

There are many advantages to heating a mould directly rather than indirectly via convection. Over the years many technologies have been examined, including integrated heating fluid circuits, integrated resistive element cartridge heaters, heated fabrics, electrically heated carbon foam (CFOAM[®]) tools, and the Quickstep[™] process. A newly developed heating technology, the TCX[™] resistive element has also been explored, and demonstrates significant promise.

2.3.1 TRADITIONAL INTEGRATED HEATERS

Integrating either electrical heaters, heated fabrics, or heating fluid pipes in a tool provides a straightforward method for directly applying heat to a mould surface. This type of heating has been around for many years, and is commonly used in processes such as resin transfer moulding, compression moulding, and sometimes in conjunction with an autoclave or oven to assist the heating of large parts made with prepreg [8]. Early examples such as Kaufmann's work on nickel coated carbon fibre heating fabrics demonstrate that the idea of directly heating a mould has been around in the aerospace industry for a long time, and is by no means new [17]. While all types of integrated heaters typically allow for increased ramp rates and lower cycle times, specific attributes have hindered their adoption.

For all three integrated heater technologies, obtaining an even heat distribution on the mould's surface has been a challenge. Arney *et al.* demonstrated this effect in their 2004 paper, where they incorporated a heated fabric on the backside of the tool - a common approach for these ma-

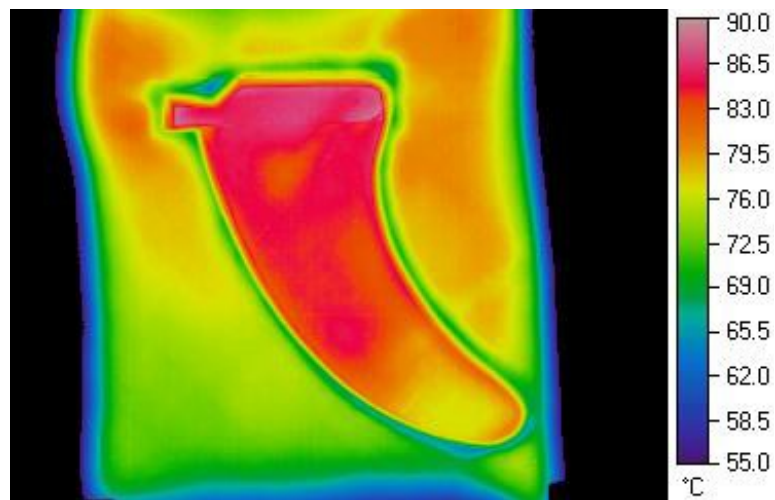


Figure 2.3-1: Integrated heating example temperature distribution [20]

materials [18]. When complex geometries are included in the mould design, it becomes increasingly difficult to obtain uniform temperature distribution across the tool surface using cartridges, fabrics, or fluid circulation. For example, Arney *et al.*'s results show a temperature difference of approximately 10°C across the part's surface during cure. This results in an uneven cure of FRP materials, and a reduction in mechanical properties. An example of the temperature distribution obtained with integrated heaters is included in Figure 2.3-1.

In addition, the tooling required for such setups, circulated heating fluids and cartridge heaters in particular, can be expensive. Incorporating the heating method can result in large, complicated and expensive moulds. In some instances, the increased ramp rates and reduced infrastructure requirements have overcome the deficiencies of these technologies, but they are as of now not in widespread usage across the industry.

2.3.2 CFOAM[®]

A relatively recent advancement in the area of direct heating of composite moulds has been the use of Touchstone Research Laboratory's CFOAM[®] as an electrical heating element. CFOAM[®] was originally developed as a coal-based carbon foam, for use as a rigid, lightweight and easily machined tooling substrate. A tool's support structure could be machined to near net-shape from blocks of CFOAM[®], with a composite mould surface applied on top of the foam structure. As Stewart indicated in his review of new mould technologies, the combination of a carbon based substrate, with a carbon tool surface, and a carbon fibre reinforced polymer (CFRP) part material is extremely attractive. As the coefficient of thermal expansion of all the materials involved are

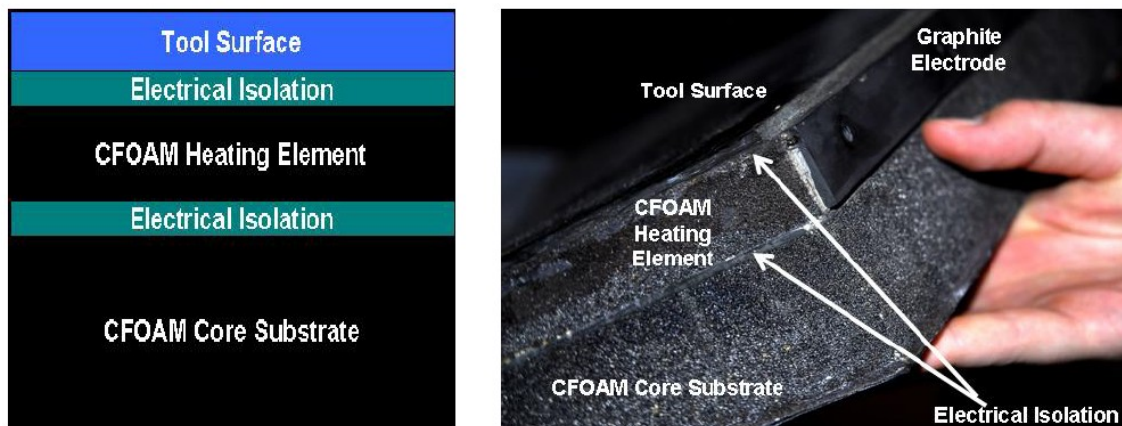


Figure 2.3-2: CFOAM[®] heating setup [22]

very low, dimensional accuracy is extremely high [19]. As the carbon foam is conductive, it was quickly realized that it could be used as a resistive heater to heat the mould surface. By isolating a layer of CFOAM[®] between the mould structure and tool surface, and applying a current across it, heat could be applied across the entire tool surface. An example of this setup is included in Figure 2.3-2.

This method was studied by Blacker *et al.*, who demonstrated that using a constant cross-section thickness of carbon foam as the heater could achieve a uniform temperature distribution on the tool surface [20]. The difficulties they faced came primarily from the management of bonded joints between CFOAM[®] blocks, where the local conductance varied, which could create hot-spots or short circuits. Despite this, the authors were able to show very minimal temperature variations on a complex tool for low ramp rates.

However, while the base materials are inexpensive for this process, significant machining is required to assemble the mould. First, the structure must be assembled out of blocks of foam bonded together to near net-shape. Then a first machining pass is done to bring the blocky surface down to approximately the part geometry. A similar machining pass is done on a separate assembly of CFOAM[®] blocks which will become the constant thickness heating element. These two blocks, essentially a male and female version of each other, are then joined, and the part geometry is again machined into the assembly. Finally, the prepreg tooling surface is applied, which must then be machined to the final part geometry. This results in a total of four complete surface machining passes, which is an expensive process. Despite the complicated machining process, CFOAM[®] tools are very promising and are being investigated by a number of aerospace companies [19].

2.3.3 QUICKSTEP[™]

Another relatively new technology being explored is the Quickstep[™] process. While it is not strictly speaking a heated tooling technology, its heating is very close to direct heating, and it fits under this category of heating better than the traditional autoclave or oven heating. In the Quickstep[™] process, the laminate is assembled and vacuum-bagged in the conventional manner, but on a thin tool without the large support framework seen in oven or autoclave tools. The tool and

laminates are then placed between two flexible membranes in the Quickstep™ pressure chamber. On either side of these membranes, a heat transfer fluid is pressurized, heated and circulated. This provides consolidation pressure and precise temperature control [21]. A schematic of the Quickstep™ process is included in Figure 2.3-3. In addition to the improved temperature control, increased ramp rates of 10-15°C per minute are easily attainable [22; 23]. While this process typically uses prepreg materials, a similar system for liquid composites molding known as Poly-Flex has been developed by École Polytechnique de Montréal. It is very similar to Quickstep™, but allows for dry reinforcements to be combined with a liquid resin within the cavity [24; 25].

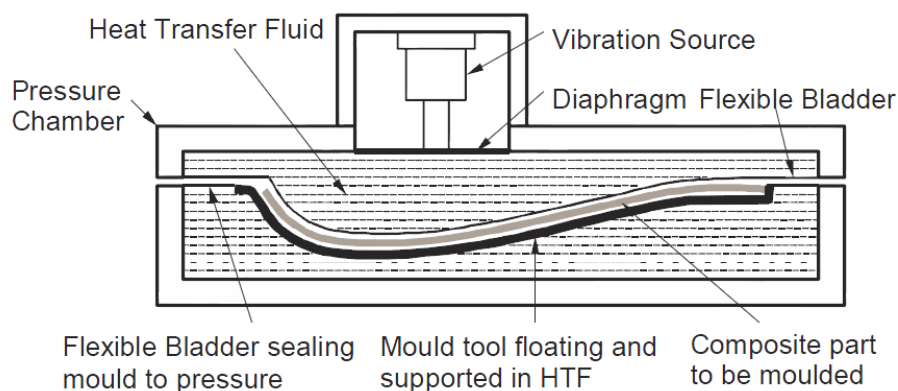


Figure 2.3-3: Quickstep process schematic [21]

In their feasibility study, Coenen *et al.* compared the properties of carbon/epoxy composite panels produced both using Quickstep™ and a traditional autoclave cure. They determined that using the Quickstep™ process, parts of comparable quality to those produced in an autoclave can be produced in roughly 50% of the time, with a cost savings of 82% for tooling alone [21]. This represents remarkable savings and cycle time improvement. Khan *et al.* also indicated that the heat transfer fluid also acts as a thermal sink to dissipate excess heat generated during the cure [23]. This had been previously explored by Schlimbach, Ogale, and Schimmel, who investigated the cure of 30 and 50 mm FRP laminates using a Quickstep™ cure [26]. Davies *et al.* demonstrated this technology's use for rapid composites production by investigating the effect of elevated heating rates on the mechanical properties of epoxy matrix composites, indicating that modified Quickstep™ cure cycles are able to improve quality while shortening cycle times [22].

Despite these apparent advantages, the available research papers do not speak to some of the possible difficulties of implementing this process for large scale parts. In theory, a large Quick-step™ chamber could be used, but that would lead to the same issue of waiting for chamber availability as in an autoclave cure. Additionally, while various authors state significant tooling cost savings, for large parts a substructure would need to be put in place to allow for material layup, which would reintroduce some of the tooling costs.

2.3.4 TCX™ RESISTIVE ELEMENT

A third novel heating technology is the TCX™ element. ThermoCeramix, the developer of the TCX™ element, maintains a number of patents related to resistive heating technologies, centered on the thermal spray application of resistive elements [27; 28; 29]. These patents broadly describe a variety of resistive element systems, all of which share the common trait of being applied via thermal spray. In broad terms, thermal spray involves depositing melted materials onto a surface via a spraying process. ThermoCeramix's elements are a combination of a conductive metallic components and an insulating oxide, nitride, carbide or boride derivative, which are sprayed over an insulating ceramic coating [29]. By varying the balance between the conductor and its derivative insulator during deposition, the resistivity of the element can be finely controlled. The combination of precisely controlled resistivity, and a precise thermal spray process, allows for the creation of a resistive element which can be tuned to deliver a specific amount of heat when a current is applied. A schematic of the thermal spray application can be found in Figure 2.3-4, with images of a serviceable TCX™ tool in Figure 2.3-5.

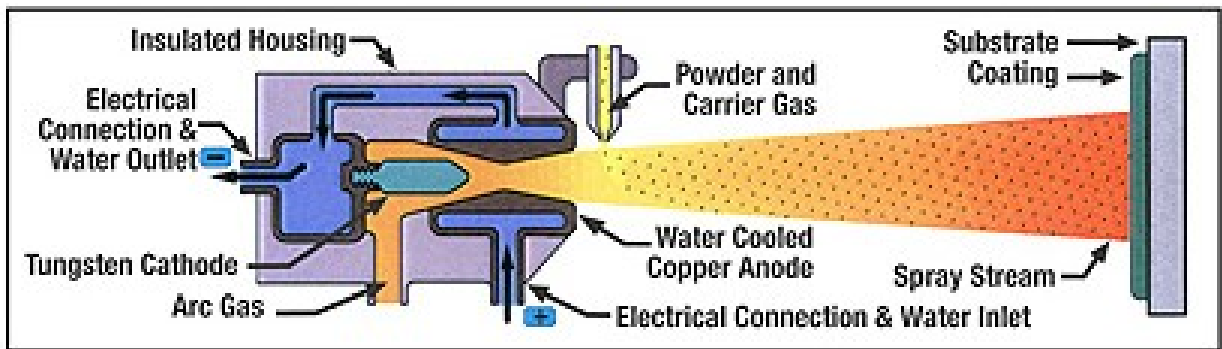


Figure 2.3-4: Thermal spray element deposition [30]

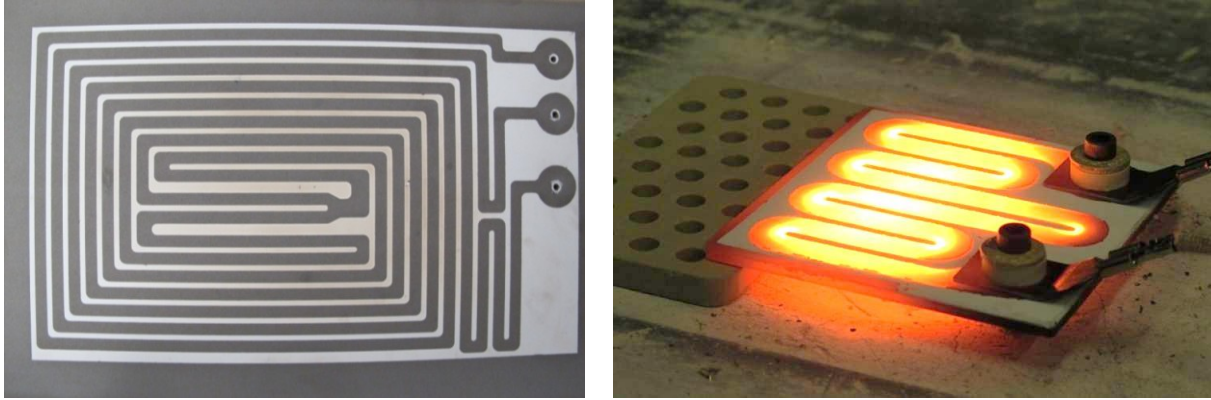


Figure 2.3-5: TCX™ element trace (left), in service (right) [30]

As the TCX™ element can be applied in specifically tailored geometries, it can provide very precise temperature control in the plane of the tool surface. Multiple elements with independent controls can also be used to further reduce any in-plane gradients. This is of particular use for composites manufacturing, as thermal gradients during cure have been shown to result in the development of residual stresses, leading to a reduction in mechanical properties [31]. One risk associated with this type of heating is that the one-sided application of heat could induce a through-thickness temperature gradient, and therefore negatively impact laminate quality.

In their initial study, Smith *et al.* explored the use of a TCX™ resistive element for the processing of an OoA prepreg, and compared it to a conventional oven. Several processing parameters, such as laminate thickness, ramp rate, and the effect of additional insulation were studied. Results were compared in terms of thermal lag, exotherm magnitude, and observed temperature differences through the laminate's thickness as well as in-plane [32]. These experiments showed that the TCX™ element is capable of reducing thermal lag, making the part follow the desired temperature profile more directly, and reducing the exotherm magnitude, which can prevent material degradation. Initial tests showed unacceptable through-thickness thermal gradients, but the addition of insulation on top of the ply stack effectively eliminated this issue. One additional significant finding was that the TCX™ element is capable of ramp rates up to 50 °C/min.

Beyond this initial study, the TCX™ element has numerous interesting applications. It has several unique advantages over other heated tool technologies, some of which include occupying little to no space, applying even heating at lower power than wire heaters, and the ability to be

applied in a range of size, shapes, and heating densities. For composites manufacturing, these characteristics mean that the TCX™ element could be incorporated into moulds which give exceptional process control and economic value. In addition, the high ramp rates could result in reduced cycle time. All things considered, the TCX™ element appears to help meet the requirements of quality and cycle time, while being applicable for a large range of part sizes.

2.4 THERMO-CHEMICAL PHENOMENA

The epoxy resin systems common throughout the aerospace industry are an example of a thermosetting polymer. In their uncured state, thermosets begin as a liquid mix of monomers and additives, including a catalyst [33; 34]. As previously mentioned, when heat is applied the resin will change from a liquid to a solid via a process known as polymerization. Polymerization is ongoing even without the presence of heat, but the heat will activate the catalyst and accelerate the process. Monomers will cross-link, resulting in strong covalent bonds between polymer chains as shown in Figure 2.4-1.

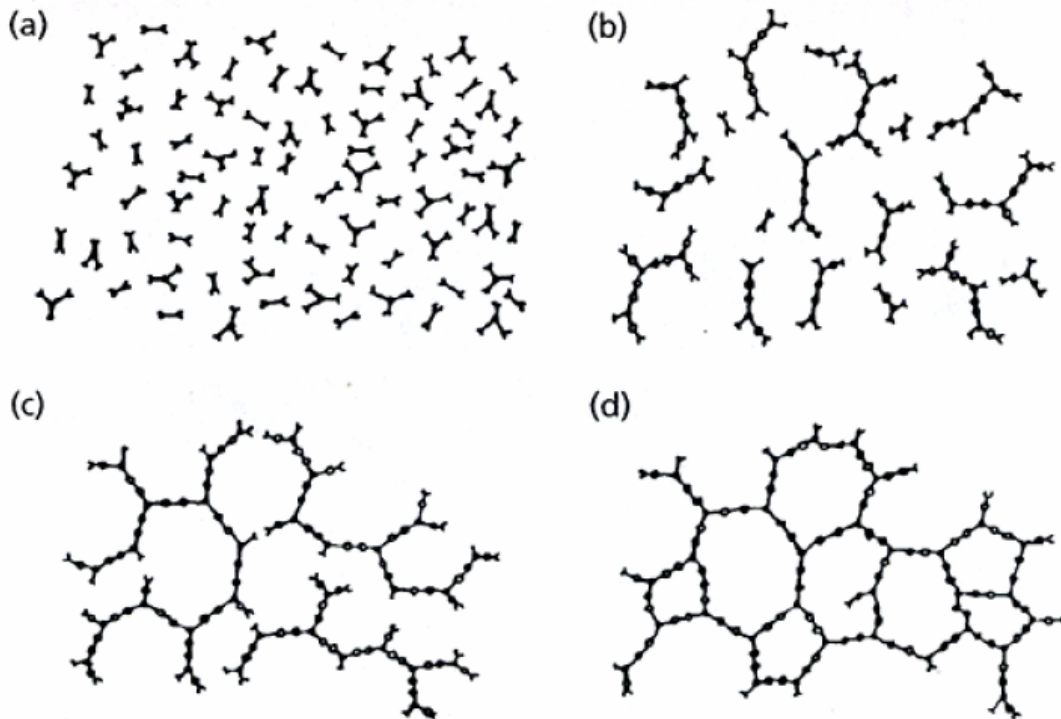


Figure 2.4-1: Thermoset cross-linking during cure [35]

Enns and Gillham presented a Time-Temperature-Transformation (TTT) cure diagram which illustrates a resin's progress through an isothermal cure based on cure temperature, and the various states a thermosetting polymer can reach depending on the cure applied [36]. A typical manufacturing process takes an epoxy resin from liquid to gelled rubber to gelled glass, but poor thermal control or cure cycle selection can result in reaching regions where the polymer hasn't achieved the desired state, or has been damaged by excessive temperatures.

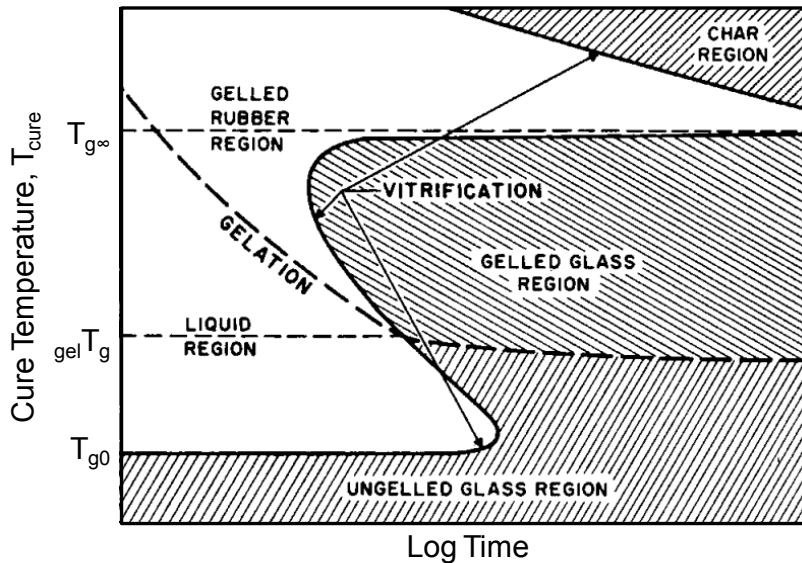


Figure 2.4-2: Generalized TTT cure diagram [36]

Controlling the temperature profile achieved during cure is critical for controlling the polymerization process. Several thermo-chemical phenomena have been shown to have strong links to final part quality, and are in turn controlled by the temperature profile. These phenomena include degree of cure, resin viscosity, glass transition temperature, and exotherm [37; 38].

2.4.1 DEGREE OF CURE

A resin's progress through polymerization can be quantified by its degree of cure, α_c . As previously mentioned, thermoset polymerization is a process which releases heat, and is thus exothermic. As such the degree of cure can be related to the heat released during the reaction:

$$\alpha_c(t) = \frac{H(t)}{H_T} \quad (5)$$

where $H(t)$ is the heat of reaction at time t , and H_T is the total heat of reaction. H_T is the total heat released if the polymer were to be fully reacted, whereas $H(t)$ is the heat released up to a certain point of time during cure. The degree of cure is defined as the ratio between these two values.

Numerous efforts have been made to link temperature history to degree of cure. For the OoA material studied here (CYCOM[®]5320) a cure kinetic model was developed by Kratz *et al.* [38], using a combination of models proposed by Cole *et al.* [39] and Kamal and Sourour [40]. The degree of cure evolution as described by Kratz is shown in Equation 6:

$$\frac{d\alpha_C}{dt} = K_1\alpha_C^{m_1}(1 - \alpha_C)^{n_1} + \frac{K_2\alpha_C^{m_2}(1 - \alpha_C)^{n_2}}{1 + \exp(D(\alpha_C - (\alpha_{C0} + \alpha_{CT})))} \quad (6)$$

Details of this model are not provided here, as they are available in the literature. In this research, this model was implemented using the RAVEN simulation software, from Convergent.

Understanding the link between temperature and degree of cure for a material system is key to successfully working with that material. As heating conditions change, the effect on degree of cure must be understood. In considering heated tooling for OoA applications, the switch to heated tooling must not negatively impact a manufacturer's ability to fully and evenly cure a material.

2.4.2 RESIN VISCOSITY

The viscosity of a resin can be defined as its resistance to flow [5]. During processing of thermosets, the viscosity of the material changes greatly over the course of the process. An initial application of heat lowers the resin's viscosity, allowing the resin to flow. As polymerization proceeds and degree of cure advances, the polymer's viscosity increases with the build up of cross-linked molecules. Eventually, the viscosity profile will approach a vertical asymptote, indicating a rapid increase towards infinity. This is the point known as gelation, where an infinite network of cross-linked polymer molecules has formed, meaning the resin is no longer mobile and viscosity is effectively infinite [36].

Results presented by Kratz *et al.* have shown that the temperature cycle has a significant impact on resin viscosity for the materials studied here [38]. The model developed by Kratz *et al.*, based on techniques presented by Khoun *et al.* [41], links viscosity to degree of cure, which is in turn controlled by the materials temperature history. This viscosity model is given in Equation 7.

$$\mu = \mu_1 + \mu_2 \left(\frac{\alpha_{gel}}{\alpha_{gel} - \alpha_c} \right)^{A+B\alpha+C\alpha^2} \quad (7)$$

Again, details are not presented here as this model was already incorporated in RAVEN. As this model accurately predicts viscosity, it can be used to study the effect of temperature history on resin viscosity. It is well established that increased heating rates result in a lower minimum viscosity, which can improve the wetting of fibres by the resin and therefore increase fibre-resin adhesion and the associated mechanical properties [22; 42]. In the context of heated tooling, aggressive heating rates become available which opens up the possibility of reaching very low minimum viscosities.

For OoA materials, resin viscosity has also been shown to play an important role in fibre impregnation. Centea and Hubert developed a model for the degree of impregnation of CY-COM[®]5320 in which resin viscosity is one of the model inputs. In their study, they demonstrated that the temperature ramp rate had a significant effect on tow impregnation, with faster heating resulting in faster impregnation. This was explained due to high ramp rates providing an ideal combination of high temperature and low degree of cure, resulting in very low viscosity flow [43]. This in turn influences final part quality by reducing the likelihood of flow-induced microvoids developing within the part.

2.4.3 GLASS TRANSITION TEMPERATURE

The glass transition temperature (T_g) of a thermoset polymer can be defined as the temperature at which the material changes from a rubbery state to a hard, glassy state [5]. As polymerization proceeds, the T_g of the system increases with degree of cure. The T_g of a material typically indicates its maximum use temperature, as beyond this point a part will exhibit significantly reduced properties and will no longer behave as designed. In processing of thermosetting composites, it is

important to ensure that a sufficiently advanced T_g has been reached, and that T_g is even throughout the part.

Once again, T_g is a property controlled by the temperature applied to a part during cure. For a typical dwell temperature between the T_g at gelation ($_{gel}T_g$) and the material's fully cured T_g ($T_{g\infty}$), Enns and Gillham's generalized TTT (Figure 2.4-2) can be used to explain the cures progression in the context of T_g . Initially, the material's T_g is below the applied temperature and the resin is in the liquid region. With time, the resin will gel and pass into the gelled rubber region. Next, the T_g will pass the applied cure temperature, a process referred to as vitrification, and the resin will pass into the gelled glass region. The TTT shown in Figure 2.4-2 shows vitrification as an S-shaped solid black line, indicating that the time at which vitrification occurs is linked in a complicated way to the temperature applied.

Kratz *et al.* again provide an appropriate model for CYCOM[®]5320. This T_g model is given by Equation 8.

$$\frac{T_g - T_{g0}}{T_{g\infty} - T_{g0}} = \frac{\lambda \alpha_c}{1 - (1 - \lambda) \alpha_c} \quad (8)$$

2.4.4 EXOTHERM

As thermoset resins release heat during polymerization, there is a risk of exotherm during manufacturing. This constitutes the heat generation term mentioned in Section 2.1.3. In the context of composites manufacturing, exotherm is defined as the part temperature passing the desired set-point due to the build up of heat released during the exothermic reaction. This can result in degradation of resin properties, uneven cure through the thickness of a laminate, matrix cracking, and in severe cases can even result in bagging consumables catching fire [5]. To avoid degradation, manufacturers must ensure that resin temperature does not pass the glass transition temperature of the fully cured resin ($T_{g\infty}$), which becomes a very real risk when processing thick structures [36; 44] Many studies have also linked exothermic overshoot to an increase in residual stresses developed within a part [45; 46]. Exotherm is represented schematically in Figure 2.4-3 **Error! Reference source not found.**

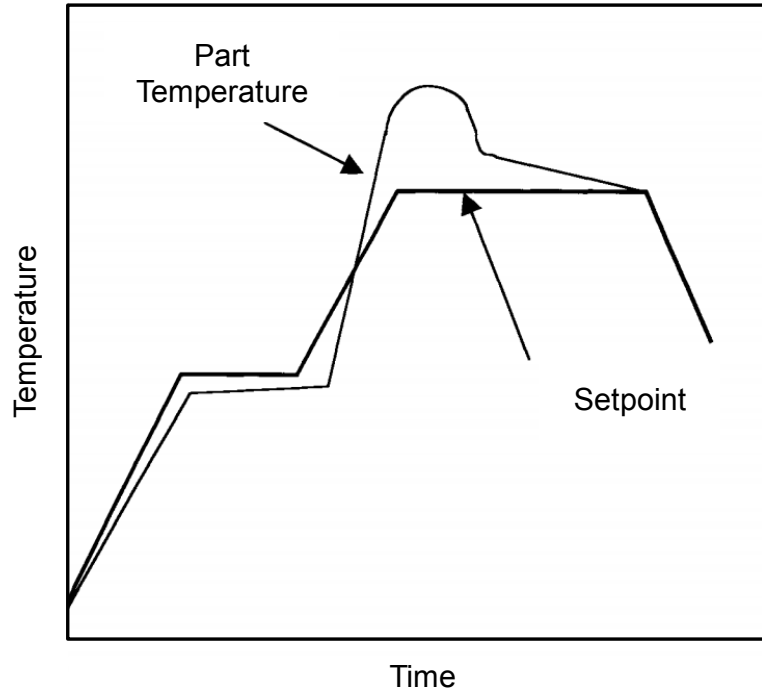


Figure 2.4-3: Example of exotherm during composites manufacturing [5]

To avoid serious exotherms, oven and autoclave cure cycles typically featuring slow heating rates in the realm of 1 to 4 °C/min [22]. In addition, many studies have focused on optimizing cure cycles to try to minimize the effect of exotherm by introducing intermediate dwells, and even intermediate cooling segments [44; 45; 46]. The challenge of controlling an exothermic reaction is clearly non-trivial, especially in the oven/autoclave environment where the surroundings are maintained at elevated temperatures.

2.5 SUMMARY OF LITERATURE REVIEW

As demonstrated throughout this section, there are number of areas which play a role in composites manufacturing. This chapter identifies the key heat transfer mechanisms responsible for promoting polymerization, namely convection and conduction.

The traditional autoclave cure is introduced as the most widespread processing technique for composite materials. Its drawbacks, namely high cost, motivated the development of high quality OoA materials which can be processed in an oven. However, this did not solve the issue of lengthy cycle times, as the oven features the same poor heating as the autoclave, and these new

materials require lengthy room temperature vacuum holds to achieve acceptable part quality. Several alternate methods of applying the required heat are discussed, with the goal of motivating further study of the TCX™ resistive element. The literature presents some positive aspects of the heating technologies discussed, but ultimately hints at the shortcomings and the reasons behind their low adoption rates. A summary of the pros and cons of the heating methods discussed in this section is presented in Table 2.5-1.

Table 2.5-1: Summary of heating technologies

	Pros	Cons
Autoclave	<ul style="list-style-type: none"> – Consistent, high quality parts 	<ul style="list-style-type: none"> – Low heating rates – High acquisition and operation costs
Oven	<ul style="list-style-type: none"> – Low acquisition costs 	<ul style="list-style-type: none"> – Low compaction pressure – Low heating rates – Difficulty achieving consistent part quality
Integrated Heaters <ul style="list-style-type: none"> – Cartridges – Fabrics – Heating pipes 	<ul style="list-style-type: none"> – High heating rates – Good thermal control 	<ul style="list-style-type: none"> – High tooling costs – Difficulty achieving even heat distribution
CFOAM®	<ul style="list-style-type: none"> – Matched CTE of tooling and composite part – Good temperature uniformity 	<ul style="list-style-type: none"> – High machining costs associated with tools – Less durable tools
Quickstep™	<ul style="list-style-type: none"> – High heating rates – High pressure processing 	<ul style="list-style-type: none"> – Difficult to implement for large scale parts
TCX™ Resistive Element	<ul style="list-style-type: none"> – Very high heating rates – Tailorable element design – Good thermal control 	<ul style="list-style-type: none"> – Heaters specific to individual tools – Overall process not yet well established

Finally, this chapter presents numerous thermo-chemical phenomena which are all controlled by the temperature history of a thermoset resin. These factors all have an influence on the final part quality achieved. At this stage, a number of models exist to facilitate working with epoxy resin systems. Presented here are the pertinent models developed for CYCOM®5320. Understanding these phenomena and the models that illustrate their behaviour is only one step in successfully working with composite materials.

To move beyond the autoclave, these OoA materials must be coupled to a heating system capable of rapid heating and precise temperature control, to properly optimize the cure process. The following chapters provide details on the TCX™ tools developed to address this challenge, as well as the experiments performed within the context outlined by this literature review. The results obtained using these new tools will demonstrate heated tooling's applicability to OoA processing, and serve to motivate further work on this type of system.

CHAPTER 3: PROTOTYPE DEVELOPMENT

To investigate the TCX™ heating element's suitability for composites manufacturing, two prototype systems were developed. These systems represent simple manufacturing tools that serve as the first steps in demonstrating the TCX™ element's advantages over other heating methods for the processing of OoA composite materials. This chapter describes the design of these two prototypes, providing details on the design choices made, and the strengths and weaknesses of each system. These systems were used in all of the experiments presented in the subsequent chapters.

3.1 HEATED TOOL PLATE PROTOTYPE

As a first step, a simple flat plate prototype was developed. This first prototype, designated as the Heated Tool Plate (HTP), was produced with the goal of performing very simple lab scale experiments. It served as a first trial in developing a TCX™ heated tool for composites processing. The thermal performance of this system was demonstrated in *Development of a Heated Tooling Solution to Improve Process Flexibility for out-of-Autoclave Prepregs*, presented by Smith *et al.* for SAMPE Tech 2013 [32], as well as in Chapters 4 and 5 of this thesis.

3.1.1 PHYSICAL DESIGN

The HTP system was designed with a 400 mm by 400 mm tool surface, to allow for the processing of panels roughly 200 mm by 200 mm while providing room for the required consumables such as edge breathing and vacuum bagging materials. The decision was made to use MIC6® cast aluminum for the tool surface, as it is available with an extremely smooth surface finish of 0.50 micron smoothness [47] which would ensure a smooth surface of composite panels produced on the HTP. Aluminum is commonly used for prototype moulds, and is a cost-effective material for such applications. Its ease of machining allows for quick polishing to remove any surface damage incurred during use.

Thermally, there are pros and cons to using MIC6® as a tooling material. On one hand, its thermal conductivity of approximately 142 W/m·K [47] is very high compared to other tooling materials such as Invar or CFRP (10.4 – 15.6 and 3.5 – 6 W/m·K, respectively [5]). This results in a

good distribution of heat across the tool surface, which helps in achieving a uniform cure. However, like all aluminum alloys, MIC6® has a very high coefficient of thermal expansion (CTE) of approximately $24.5 \mu\text{m}/\text{m}\cdot\text{K}$ [47]. Invar and CFRP generally feature CTEs an order of magnitude lower ($1.5 - 5.2$ and $3.6 - 9 \mu\text{m}/\text{m}\cdot\text{K}$ respectively [5]). This high CTE presents two problems; introduction of residual stresses into laminates due to CTE mismatch between tool and part, and cyclic loading of the TCX™ element due to CTE mismatch between the element trace and tool substrate. In the context of a flat tool for laboratory scale experiments, it was determined that the advantages of aluminum were enough to outweigh these disadvantages, but they are worth noting. The high CTE of MIC6® potentially limits both the lifespan and the maximum usage temperature of a TCX™ heated tool.

With the tooling material set, a simple support system was added to the tooling surface. The ceramic insulator layer and element trace were added by ThermoCeramix, with high temperature barrel quick disconnect terminals for electrical connections. ISO B hose couplings were installed for application and monitoring of vacuum pressure during cure. Figure 3.1-1 provides an overall view of the HTP, while Figure 3.1-2 shows the tool underside and element configuration. As can be seen from this figure, a single element was applied with a uniform element trace. Varying the width of an element trace results in changes to its resistance, and thus the power density of the element. For this first prototype, a uniform power density of $17.8 \text{ kW}/\text{m}^2$ was used. This decision was made as it provided a simple first design, and would provide an understanding of edge effects. In future works, element geometry could be better tailored to the tool design, but this first prototype would highlight any negative effects of using a uniform power density.



Figure 3.1-1: HTP trimetric view showing tool surface, vacuum fittings, and support structure

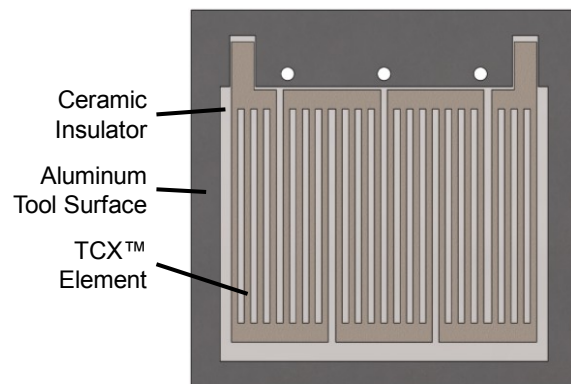


Figure 3.1-2: HTP underside showing TCX™ heating element configuration

To attempt to improve thermal uniformity, insulation was added both below the element, and above the parts being cured. This was done based on results presented by Smith *et al.* which indicated that temperature uniformity, both in-plane and through the thickness of a laminate, was improved when insulation was added to the HTP system [32]. Here, fibreglass was used below the tool, while a stack of polyester breather was used above the tool for ease of handling.

3.1.2 CONTROL AND MONITORING SYSTEM

To provide power and control the tool temperature of the HTP, a controller developed by Bujun was used [32]. This controller consisted of a CN7800 series proportional-integral-derivative (PID) controller, coupled to the TCX™ element via an SSRL240DC25 solid state relay (SSR) and a K-type feedback thermocouple, all from OMEGA. The PID controller measures the tool temperature, compares it against the desired setpoint in a PID control algorithm, and outputs a DC control signal which opens or closes the SSR, controlling the current supplied to the element by the 120 V / 15 A AC source. A circuit diagram of this system is shown in Figure 3.1-3.

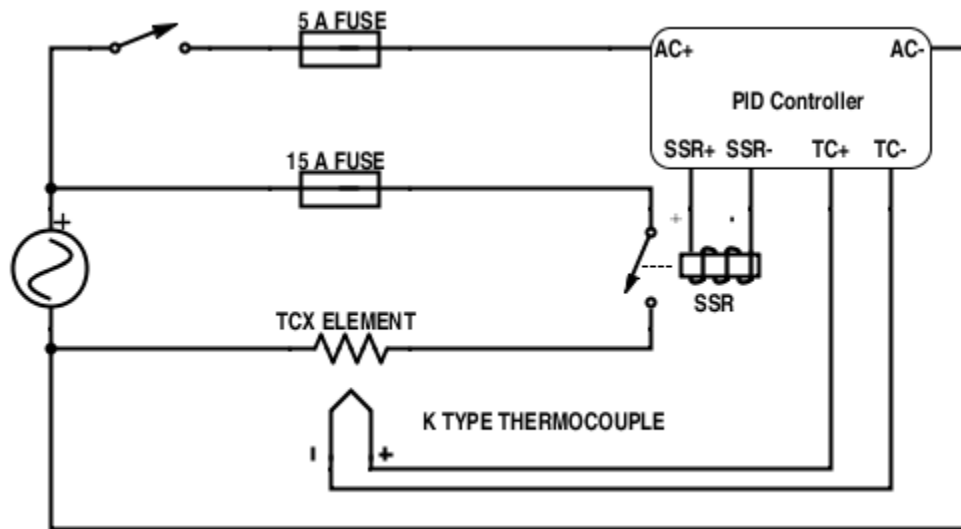


Figure 3.1-3: HTP control system circuit diagram

As this system provided no means of recording temperature data, the SignalExpress data-logging system from National Instruments was used. Using NI 9213 and 9219 modules mounted in an NI 9174 chassis provided a total of 16 thermocouple channels and 4 universal channels for data-logging. In practice, this allowed for the monitoring of both temperature using K-type thermocouples, and pressure using an A-10 4-20 mA pressure transmitter from WIKA.

3.2 MULTI-ZONED TOOL PROTOTYPE

Expanding upon the initial HTP design, a second prototype was developed, designated as the Multi-Zoned Tool (MZT). This tool featured multiple heating zones arranged across its length, which would introduce improved thermal control compared to the HTP, and would be used to investigate certain challenging part configurations. The thermal performance of this system was demonstrated in *Multi-Zoned Heated Tooling for Out-of-Autoclave Processing of Variable Thickness Composite Laminates* [48], and expanded on in Chapter 6 of this thesis.

3.2.1 PHYSICAL DESIGN

The MZT was designed with a slightly larger working surface of 400 mm by 610 mm, allowing for parts of up to 200 mm by 450 mm to be produced. Again, a MIC6® aluminum surface was used for the same reasons given in Section 3.1.1.

Unlike the simple HTP prototype, the MZT design was intentionally made more complicated to demonstrate a real-world solution which would show how this technology could be implemented in industry. First, a more robust extruded aluminum frame was designed. This frame would provide support for the tool surface, create an enclosure for the integrated power supply, and allow for permanent placement of insulation above and below the tool. Additionally, it allowed a reusable vacuum bag to be integrated into the system. A computer-aided design (CAD) drawing of

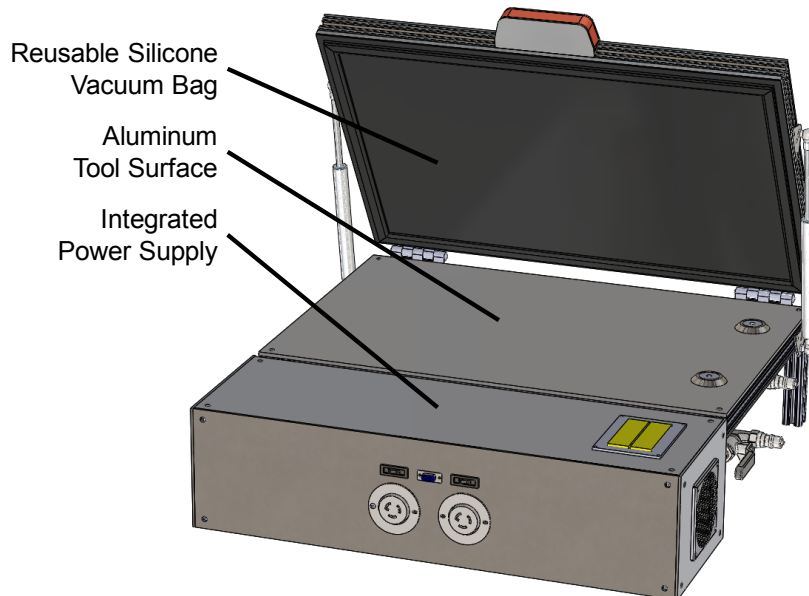


Figure 3.2-1: Multi-zoned TCX™ heating system

the complete assembly of the MZT is shown in Figure 3.2-1.

As shown, the MZT design is in many ways similar to a commercially available vacuum debulk tables. The intention here was to create a system that took advantage of the TCX™ element's heating capabilities and was robust enough to be a useful lab-scale system. To this end, a reusable silicone vacuum bag from Torr technologies was mounted to an 80/20 frame hinged against the tool surface. Fibreglass insulation was placed above this vacuum bag, as well as below the tool surface. All the required electronics were integrated into the design to keep the overall system as clean and compact as possible.

Where the MZT differs most from the HTP, is its element design. As shown in Figure 3.2-2, the MZT features six heating elements arranged along its length. These elements would be independently controlled, to provided full thermal control along the tool's length. Elements were designed by ThermoCeramix in two configurations; 2 edge elements designed with 18 kW/m^2 power density, and 4 central elements with 17.7 kW/m^2 power density. These edge elements were designed to naturally draw slightly more power and minimize edge effects.

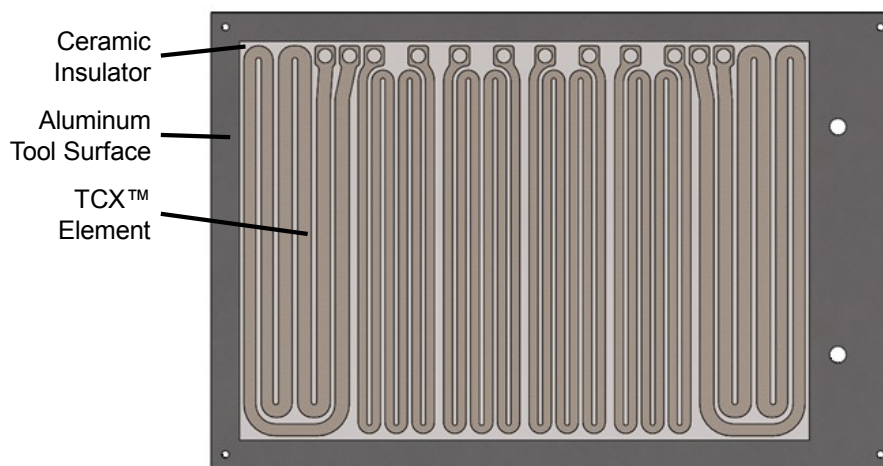


Figure 3.2-2: MZT underside featuring six heating elements

At the centre of each element's area small grooves were machined and thermocouples were embedded in the mid-plane of the MIC6® surface. These thermocouples would allow both control and monitoring of the tool's temperature without having the place a thermocouple at the tool-part interface. This would ensure a smooth tool surface of laminates produced on the MZT, allowing them to be used for mechanical testing in the future.

3.2.2 CONTROL AND MONITORING SYSTEM

To handle the six heating zones of the MZT, a custom power supply was produced. Similar to the system used by the HTP, this power supply used DC controlled SSRs to control the current supplied to each element, with K-type thermocouples providing temperature feedback to PID controllers. The SSRs used in this system were SSRL240DC10s from OMEGA. As the working surface of this tool was larger, the system required more power and was built to run off two separate 120 V / 15 A AC power sources, with each source powering three of the six elements. A schematic of one half of the control system is shown in Figure 3.2-3. An identical circuit was used to control the other three elements power by the second AC source.

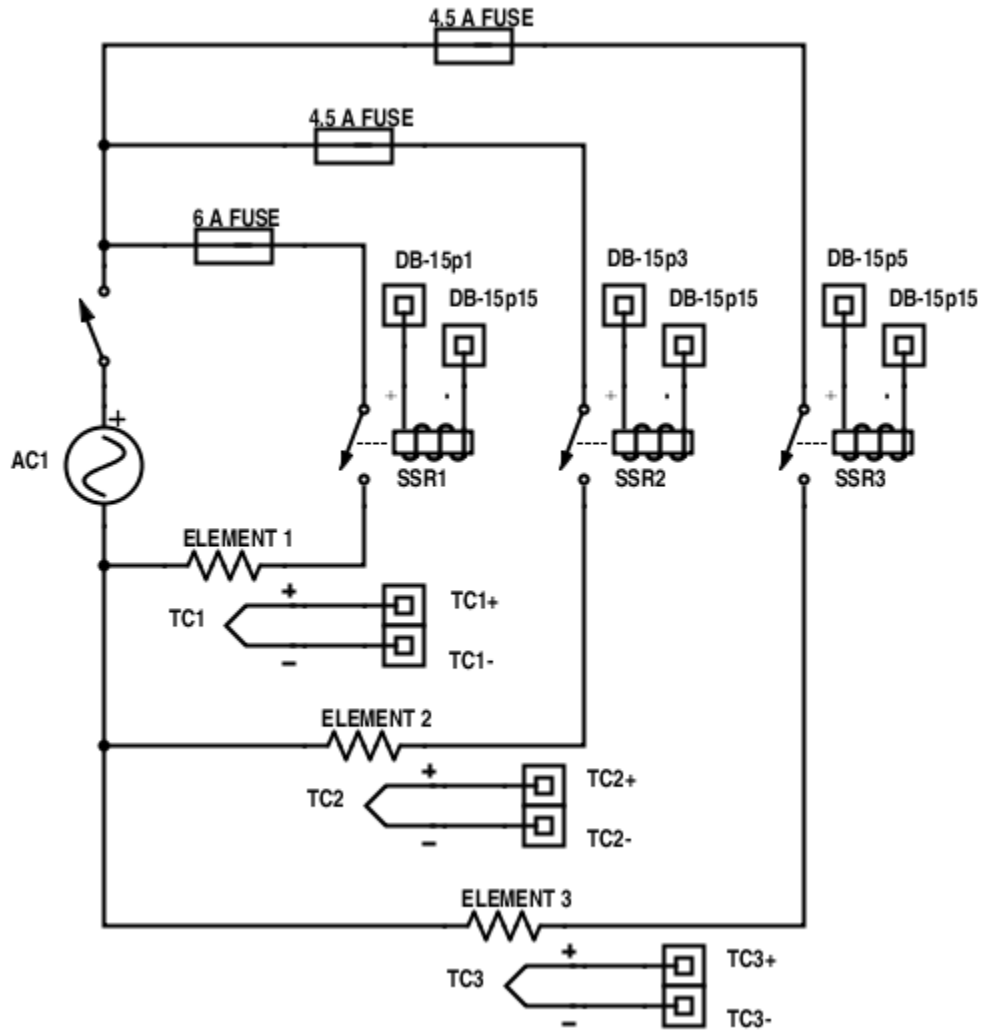


Figure 3.2-3: MZT control system circuit diagram, elements 1-3

Rather than using a standalone PID controller, a LabVIEW program was developed which took advantage of built-in virtual instrument (VI) PID controls. Details of this system are provided in Section 3.2.3. The LabVIEW program was coupled to the power supply by NI 9213 and 9219 input modules, as well as an NI 9472 DC output module to control the SSRs. As shown in Figure 3.2-3, the power supply was linked to the LabVIEW program via a DB-15 connector for the DC controls, and thermocouple terminals for the temperature feedback.

3.2.3 LABVIEW CONTROL PROGRAM

To control the six elements of the MZT prototype, a LabVIEW program was developed. This would allow for simultaneous control and monitoring of the heating zones, as well as provide more flexibility than using standalone PID controllers. In developing this program, LabVIEW's built-in VIs were used where possible for simplicity. Figure 3.2-4 shows a simplified program overview, illustrating the flow of data through the program.

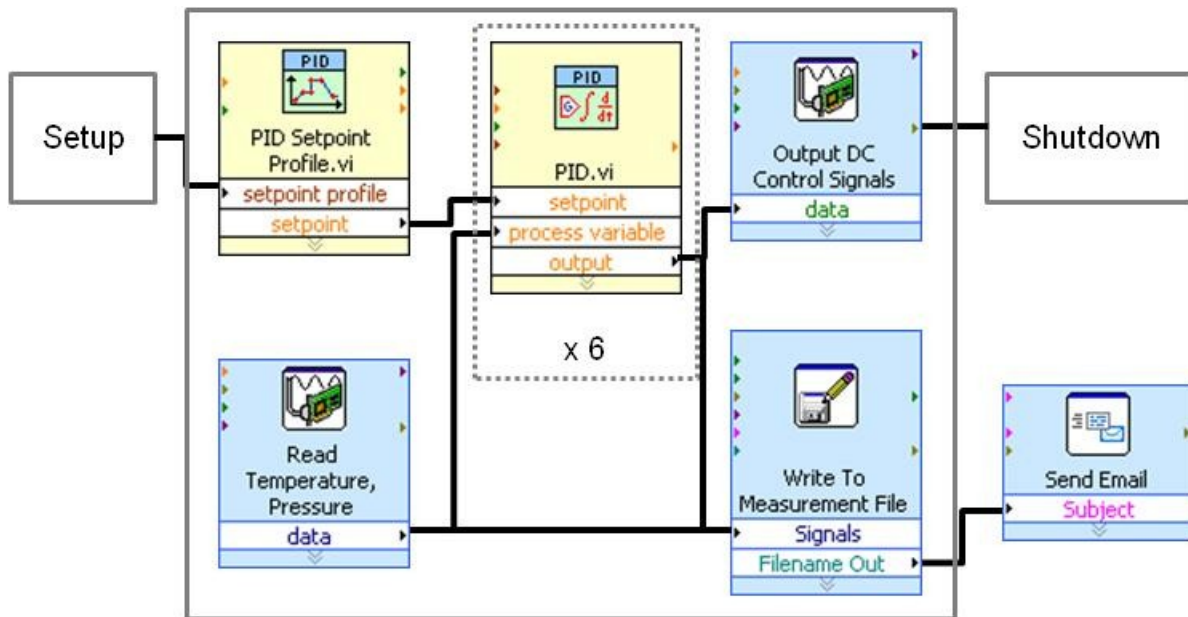


Figure 3.2-4: LabVIEW control program overview

In essence, the program consists of three main sections; setup, control & monitoring, and shut-down. During the setup stage, the user defines the desired cure cycle, configures data acquisition channels, logging settings, and PID gains. In the control & monitoring loop, the program measures temperature and pressure, and determines the temperature setpoint. Current temperature of

each zone is compared to the desired setpoint in PID algorithms, and an output value is set between 0 and 100 for each zone. This output value is converted to a square wave where the output value determines the duty cycle of the wave, which corresponds to the proportion of a cycle where the SSR is closed. These square waves are then sent to the SSRs via the DC output module, opening and closing the relays as required by the PID algorithm. Meanwhile, temperature, pressure, setpoint, and control output values are all sent to measurement files, providing simultaneous control and data logging for the system. This loop iterates once per second, updating the desired setpoint for each iteration. After the cure profile is complete, the measurement file is sent by email to the operator, and a shutdown procedure is initiated. This shutdown stage consists of ensuring all SSRs are set to open, and that all LabVIEW channels are closed.

During the development of this tool, a power logging function was added to the code to allow for real-time monitoring of the current being drawn by each element. To accomplish this, a correlation was made between the PID output signals representing the square waves duty cycle, and the actual current being drawn measured using a Fluke a3000 FC wireless current clamp module. Figure 3.2-5 shows the data obtained by plotting the PID output values against the RMS current measured by the clamp meter, which was then fit to a square-root function to link the two variables. The LabVIEW code uses this equation to convert PID output values to current, and allow for instantaneous determination of current and power drawn by each element.

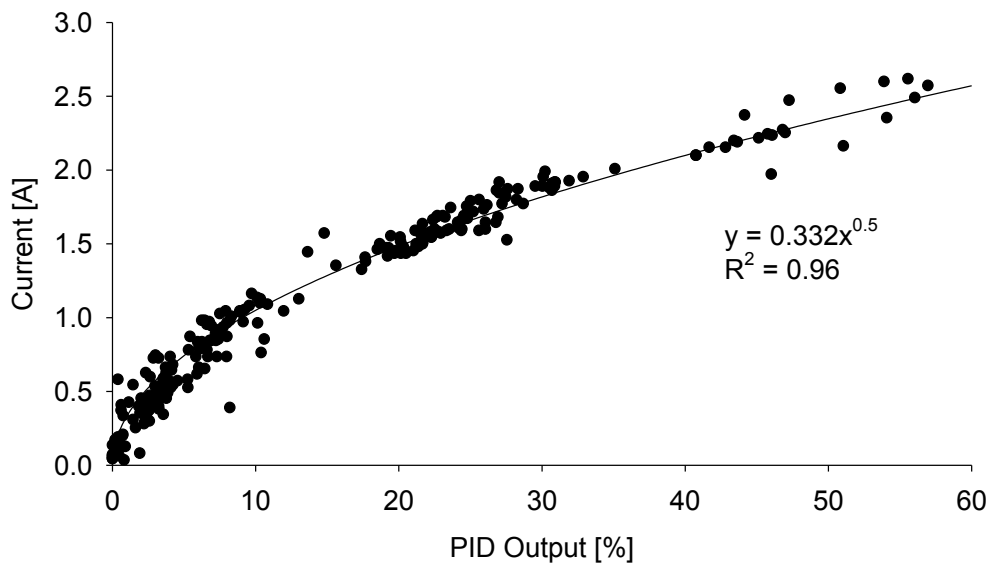


Figure 3.2-5: MZT controller PID output vs. current drawn

Not shown in Figure 3.2-4 are several charts and indicators which are present on the program's front panel. These include a waveform chart which plots setpoint, temperature, and pressure as the cycle progresses, and a set of vertical bar indicators which show the output value between 0 and 100 being sent to each element in real time. This front panel items allow the user to monitor the cure's progress as well as each element's power draw in real time.

CHAPTER 4: QUALITY BENCHMARKING

In an effort to investigate the ability of TCX™ heated tools to produce high quality composite laminates, a substantial benchmarking regime was performed. This consisted of comparing laminates produced on the HTP system to those produced in a convection oven in terms of several quality metrics, namely void content, short-beam shear strength, and glass transition temperature (T_g). These three metrics would give a good indication of the final part quality obtained. Within this chapter, the experimental procedures used will be explained in detail, with results and relevant discussion highlighted. Several of the experiments presented here were previously presented in *Out-of-Autoclave Manufacturing: Benchmarking of an Integrally Heated Tool-Plate*, a conference paper presented at CAMX 2014 and later published in *SAMPE Journal* [49; 50]. In this chapter, more in-depth experimental details are provided, and several experiments are expanded based on the initial findings originally presented.

4.1 TEST PLAN

As mentioned, three quality metrics were investigated as part of this study. Void content was determined using greyscale thresholding of optical micrographs, while short-beam strength and glass transition temperature were determined according to ASTM D2344 [51] and ASTM D7028 [52] respectively. To provide a direct comparison between the oven and the HTP, a standard cure cycle was used featuring 3 °C/min heating. In addition, the high ramp rate capabilities of the HTP were investigated by curing laminates with 50 °C/min heating for all three quality metrics. A more detailed ramp rate comparison was performed for the void content measurements, featuring heating at 3, 10, 30, and 50 °C/min.

4.2 LAMINATE PREPARATION

All laminates in this study were prepared using a representative OoA resin system, CY-COM®5320 from Cytec Engineered Materials, with an 8-harness satin fibre architecture and 36% resin content. 200 mm x 200 mm panels were produced using in a $[0]_8$ configuration, resulting in a final laminate thickness of approximately 3.2 mm. The bagging scheme presented in Figure 4.2-1 was used to approximate the conditions present when manufacturing large parts, as the

thermal advantages of the TCX™ element are believed to be the most advantageous for larger structures where uniform heating is difficult. This bagging scheme restricts airflow to the through-thickness direction, to represent a worst-case scenario for air evacuation. OoA prepregs typically benefit from in-plane air evacuation; however, this strategy has been shown to be difficult to implement for large parts, as the lengthy room temperature vacuum hold required for complete air evacuation is unacceptable in many production environments [16; 53]. The consumables used for this configuration consisted of Airweave N-4 polyester breather (2 plies), Airtech A4000RP3 perforated fluoropolymer release film, Wrightlon 6400 nylon vacuum bag, and Airtech GS-213-3 sealant tape.

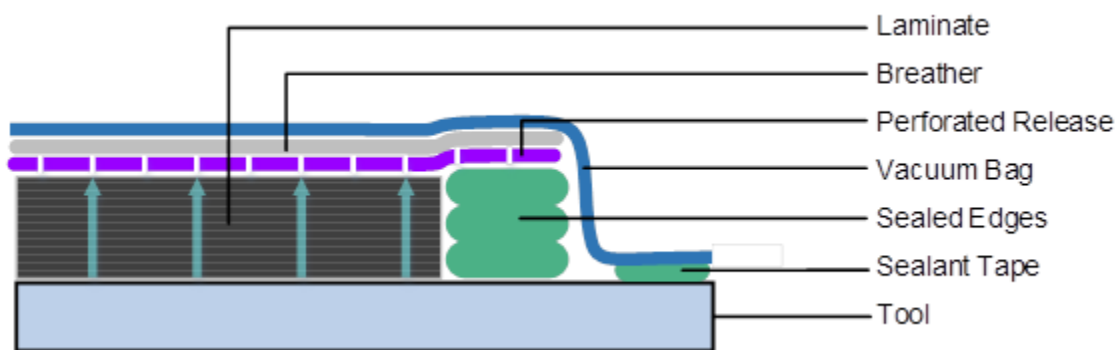


Figure 4.2-1: Flat laminate bagging scheme, arrows indicating air evacuation direction

Prior to cure, all laminates were held under vacuum at room temperature for 16 hours. Laminates were then cured at the manufacturer recommended temperature of 121 °C, followed by a post-cure at 177 °C [54]. Using characterization data presented by Kratz *et al.* [38], a 2 hour cure and a 3 hour post-cure were selected to achieve maximum degree of cure. The cure and post-cure were completed sequentially, to represent the one-shot processing of a large component. Following the work of Smith *et al.* [32], the baseline cure cycle included a ramp rate of 3 °C/min for both heat-up stages. Later trials featured heating rates of 10, 30, and 50 °C/min. All cures featured 1°C/min cooling. These cure cycles are shown in Figure 4.2-2.

For oven cured laminates, a Blue M model 256 oven from SPX® Thermal Product Solutions was used. The oven was controlled by a PRO550 controller with a J-type thermocouple monitoring air temperature. For this stage of the project, all heated tool laminates were produced using the HTP prototype with a K-type thermocouple placed at the centre of the tool surface for tempera-

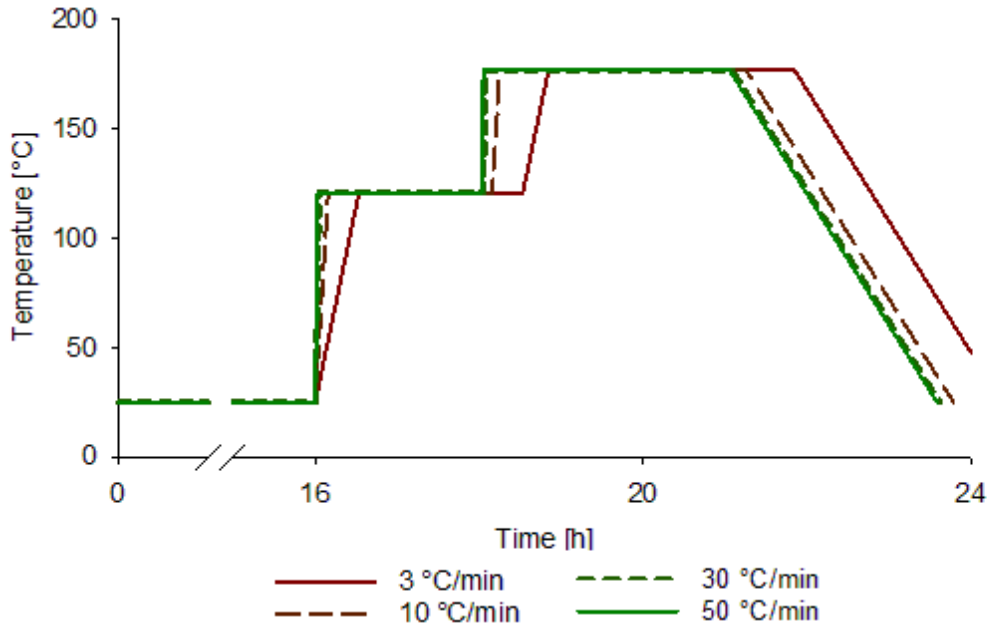


Figure 4.2-2: Quality benchmarking cure cycles

ture control. Polyester insulation was included on the bag-side to limit the through-thickness thermal gradient, while fibreglass insulation was placed under the TCX™ element to improve in-plane temperature uniformity. This led to very good thermal control of all laminates produced at this stage, as shown in Figures 4.2-3 and 4.2-4. These graphs indicate that for the low ramp rate, nearly perfect heating was achieved, while for the aggressive ramp rate the top of the laminate lagged slightly behind the bottom, and a slight overshoot was observed.

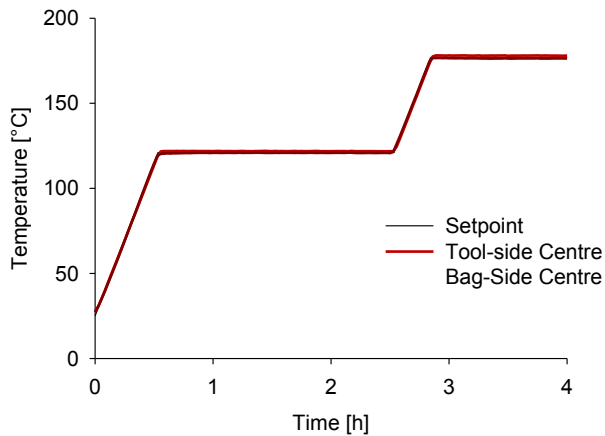


Figure 4.2-3: Typical thermal profile for 3 °C/min HTP heating

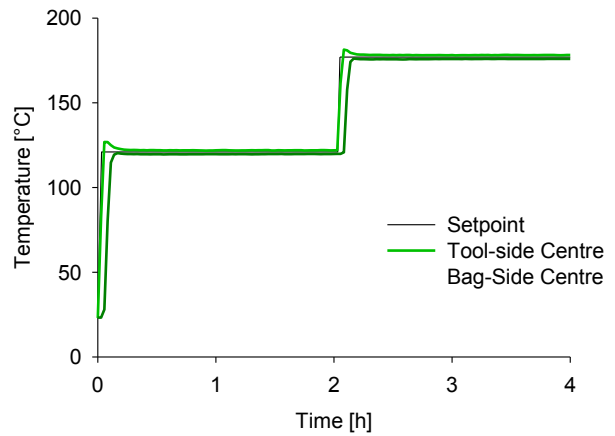


Figure 4.2-4: Typical thermal profile for 50 °C/min HTP heating

4.3 VOID CONTENT

Void content is often used as a simple measure of part quality, as the presence of voids has been shown to severely deteriorate mechanical properties [55; 56; 57]. Here, it is used as the first quality metric to compare heated tool processing of OoA prepregs to a convection oven cure.

4.3.1 METHODOLOGY

At this stage, two comparisons were performed. First, the heated tool was compared to the oven in a direct comparison. Second, the effect of ramp rate on void content was studied using different heating rates on the HTP. For the first comparison, three laminates from each configuration were produced. For the second comparison, five laminates were produced for each heating rate. From each laminate, three samples of approximately 40 mm x 20 mm were cut as indicated in Figure 4.3-1. All cutting was done using a Rubi wet-cutting diamond blade saw.

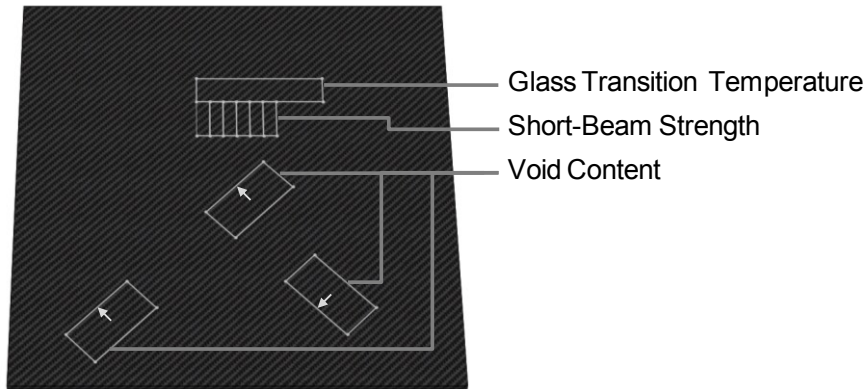


Figure 4.3-1: Quality assessment sample locations, arrows indicating micrographed edges

Samples were then mounted using Epothin™ 2 epoxy resin from Buehler, and polished up to 0.3 μm using a metkon FORCIPOL polisher equipped with a FORCIMAT automatic head. The samples were imaged using a Nikon optical microscope equipped with Marzhauser motorized stage, at 50x magnification. The void content of each sample was determined via greyscale thresholding using the image processing software ImageJ. The thresholding results from 3 independent operators were averaged to minimize the impact of operator bias on the final results.

4.3.2 BASELINE OVEN COMPARISON

Figure 4.3-2 shows the void content results obtained for each laminate, using both oven and heated tool processing with 3 °C/min heating. The error bars shown correspond to the standard deviations observed between the three samples taken from each laminate. As shown in this figure, there was a fair amount of variability within a laminate, as well as between the laminates.

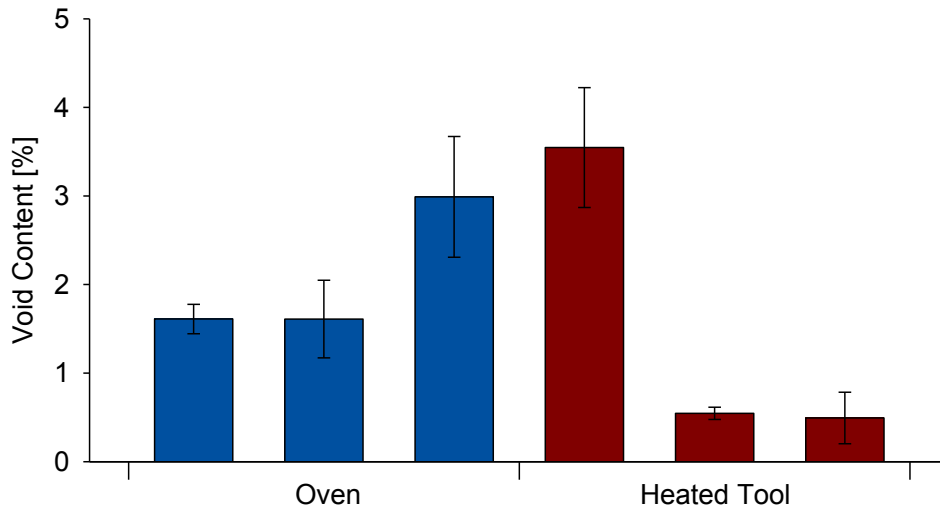


Figure 4.3-2: Average laminate void contents, oven vs. HTP at 3 °C/min

Examining the overall void content per heating method, as shown in Figure 4.3-3, several observations can be made. Firstly, overall void contents are very close to the typically accepted limit of 2 % [13; 58]. The elevated void contents are a result of the restricted airflow bagging scheme implemented throughout this study. As mentioned, these materials typically benefit from in-plane air evacuation as their effective in-plane air permeabilities are orders of magnitude greater than their transverse permeabilities [53]. This leads to difficulty in evacuating air in the through-thickness direction, which is often required for large parts, and was implemented here. Second, there is significant variation from laminate to laminate which can be attributed to operator inconsistencies during layup, as well as the high variability in the through-thickness permeability of woven prepregs. The through-thickness permeability of these materials has been shown to vary by nearly an order of magnitude, indicating that one laminate's permeability could have been vastly different from the next [53]. Finally, the two heating methods appear to yield similar void contents overall for the baseline cure cycle, indicating that heating with the HTP does not affect

void content compared to the oven. This was confirmed using an analysis of variance (ANOVA) technique with a 95 % confidence level.

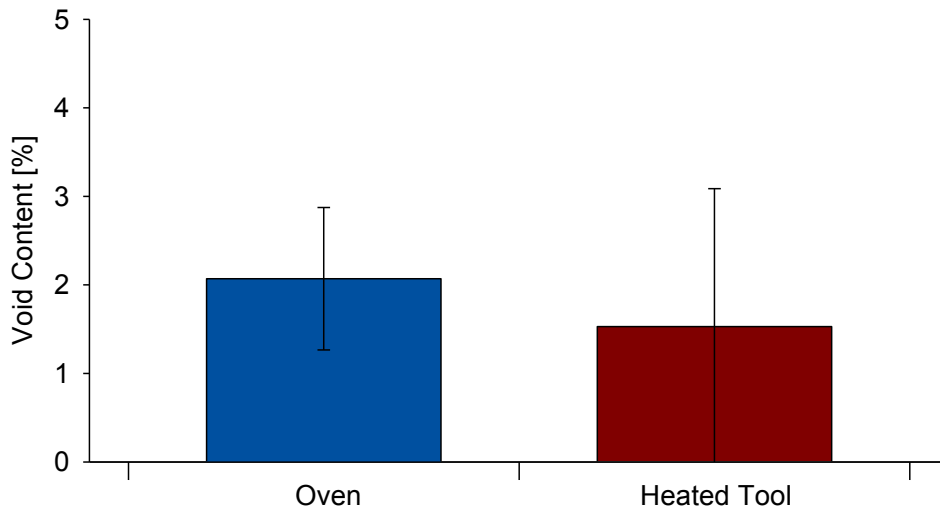


Figure 4.3-3: Average heating method void contents, Oven vs. HTP at 3 °C/min

4.3.3 HEATED TOOL RAMP RATE TRIALS

Along with the original laminates produced for the baseline oven comparison, three laminates were also produced on the HTP using an aggressive ramp rate of 50 °C/min, which is approximately the maximum heating rate the tool is capable of. These laminates showed an average void content of 2.92 %, with a standard deviation of 0.79 %. When compared to the baseline HTP values with 3 °C/min heating (1.53 ± 1.52 %), it was unclear whether the aggressive heating had an effect on void content. The average values indicated a difference, but the high standard deviation made drawing any conclusions difficult.

A previous study by Agius *et al.* on the effect of ramp-rate on void content in OoA prepregs indicated that the increased heating rate would not result in higher void contents [59]. However, their study was limited to a unidirectional material, with every ply debulked during layup, and an in-plane air evacuation strategy used during cure. Here, in the absence of debulks and in-plane air evacuation, the main difficulty comes from evacuating inter-laminar voids. While an increased ramp-rate reduces tow impregnation time, and thus the presence of intra-tow voids [37], it also decreases the length of time at which the resin is maintained at low viscosity [38]. These two effects would have the opposite effect on overall void content, and the initial results indi-

cated that the reduced low viscosity time may have been the dominant effect. Based on these initial results, the test plan was expanded to include testing of additional laminates, to give a final dataset of 5 laminates cured with heating rates of 3, 10, 30, and 50 °C/min. Void content results for this expanded set are shown in Figure 4.3-4 below. Figures 4.3-5 through 4.3-8 provide a representative micrograph for each heating rate.

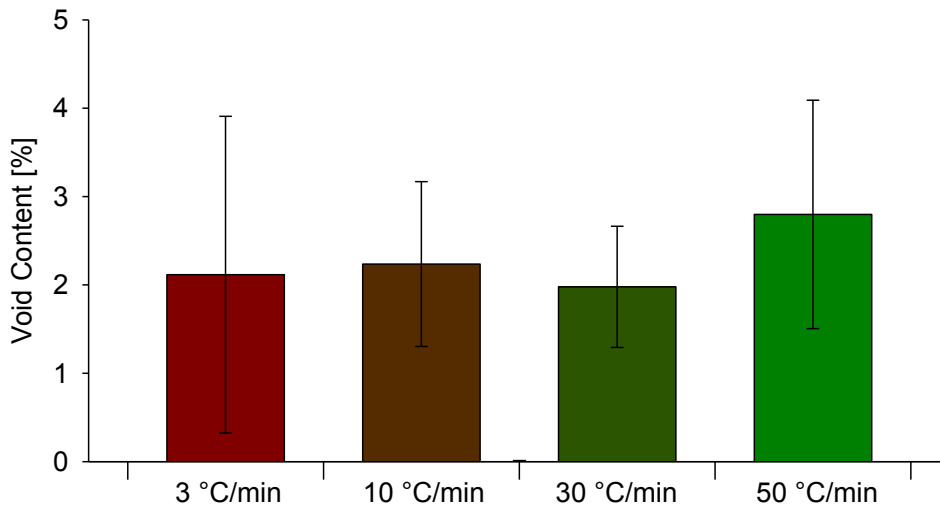


Figure 4.3-4: Average void contents, HTP cure with 3, 10, 30, and 50 °C/min heating

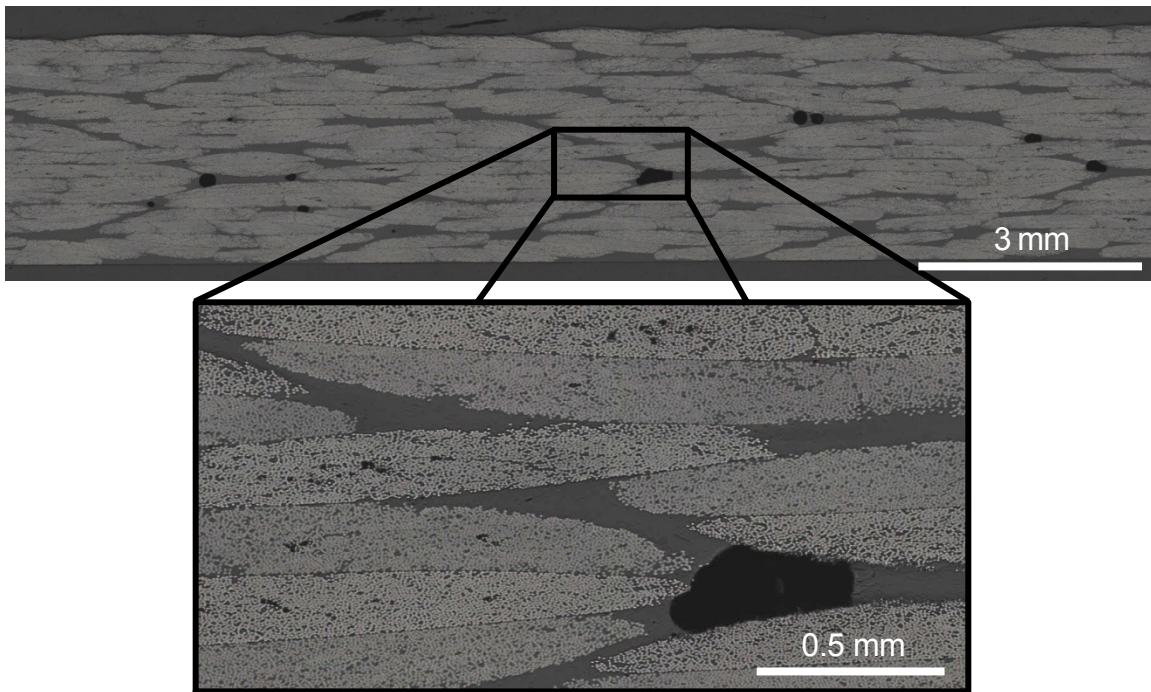


Figure 4.3-5: Representative micrograph, HTP 3 °C/min, 1.42% void content

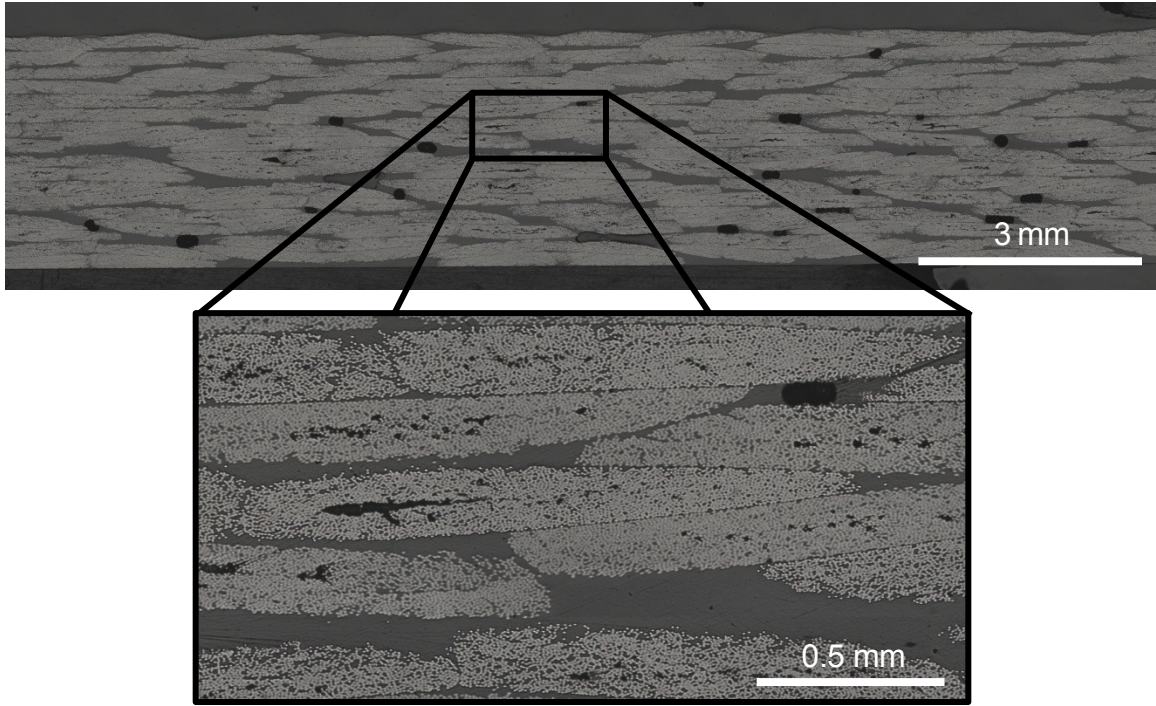


Figure 4.3-6: Representative micrograph, HTP 10 °C/min, 2.33% void content

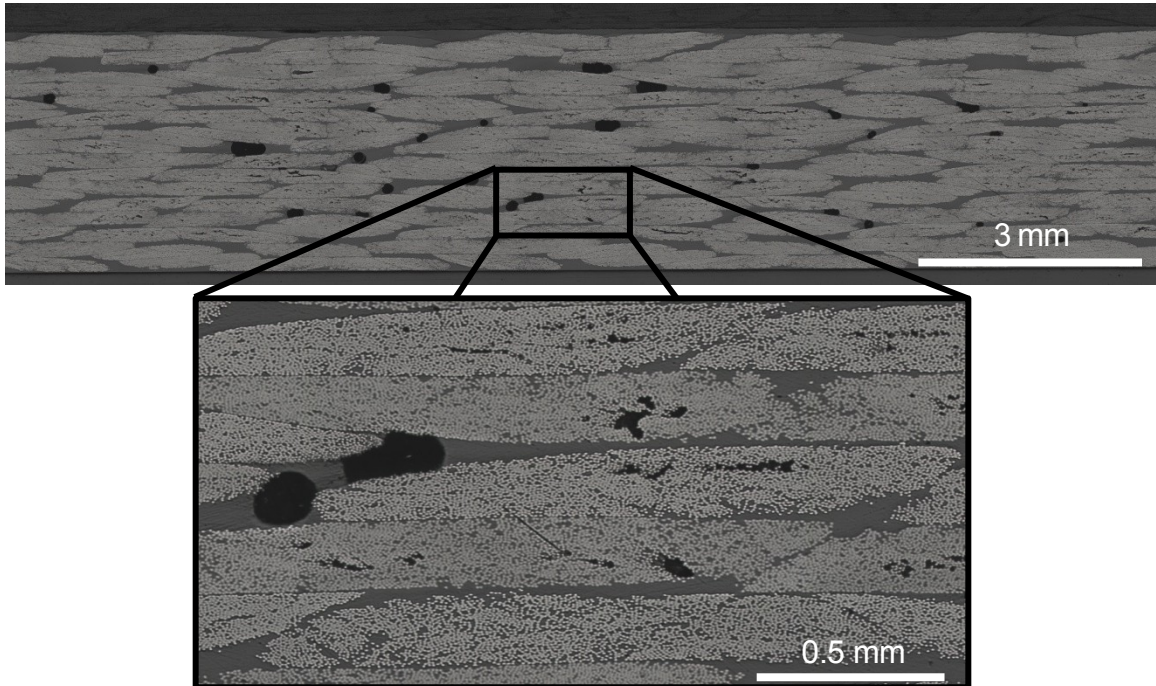


Figure 4.3-7: Representative micrograph, HTP 30 °C/min, 1.98% void content

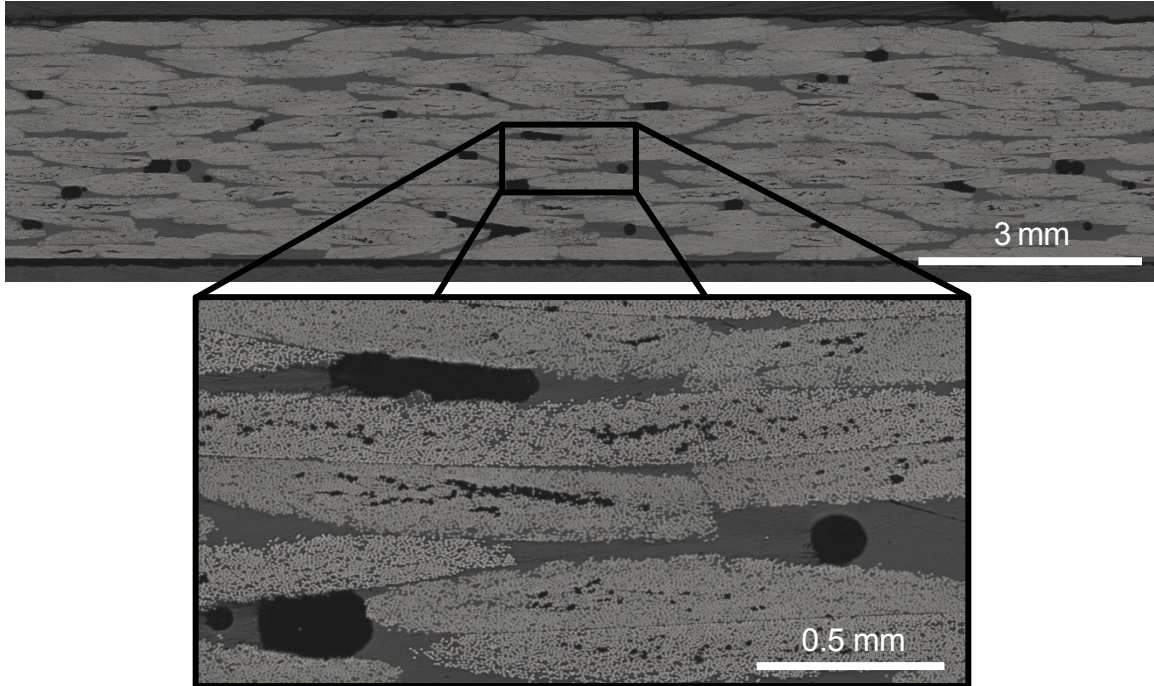


Figure 4.3-8: Representative micrograph, HTP 50 °C/min, 3.35% void content

From the above figures it is clear that in this configuration ramp rate does not have an effect on void content. While the 50 °C/min heating still results in a higher mean void content, there is no trend in the intermediary heating rates. The high standard deviations within each set of results indicate that ramp rate and void content are not linked. This was confirmed using ANOVA with a 95% confidence level, which yielded $F < F_{crit}$, confirming the null hypothesis that the means of this data set are not different. This indicates that the two effects mentioned above appear to effectively balance each other out, resulting in uniform void content regardless of heating rate.

4.4 SHORT-BEAM SHEAR STRENGTH

Short-beam strength is commonly used as a quality control test, as it provides a good indication of a part's inter-laminar strength [60]. Sample dimensions are small, and test durations are short, which are part of the reason why short-beam strength is popular in quality control. Here, it was investigated to provide an indication of a laminate's mechanical performance in a simple and quick manner.

4.4.1 METHODOLOGY

In this second stage of the quality assessment, short-beam strength was evaluated per ASTM D2344 [52], using an MTS Insight Electromechanical Testing System equipped with a 5 kN load cell, and a Short-Beam Shear fixture from Wyoming Test Fixtures, Inc. Samples were cut using a Struers Accutom-5 precision saw with a diamond cut-off wheel, as shown in Figure 4.3-1. Three heating conditions were considered here: the baseline cure for both the oven and the HTP, as well as a high ramp rate HTP cure featuring 50 °C/min heating. Taking 6 samples per laminate, and 3 laminates per heating condition, resulted in a total of 18 samples per heating condition.

4.4.2 OVERALL COMPARISON

Examining the average results over each heating condition (Figure 4.4-1), we see an apparent increase in short-beam strength for the heated tool baseline cure cycle. An ANOVA test indicated that the oven and heated tool 50 °C/min results were the same with 95 % confidence, but that the heated tool 3 °C/min trials yielded different short-beam strengths.

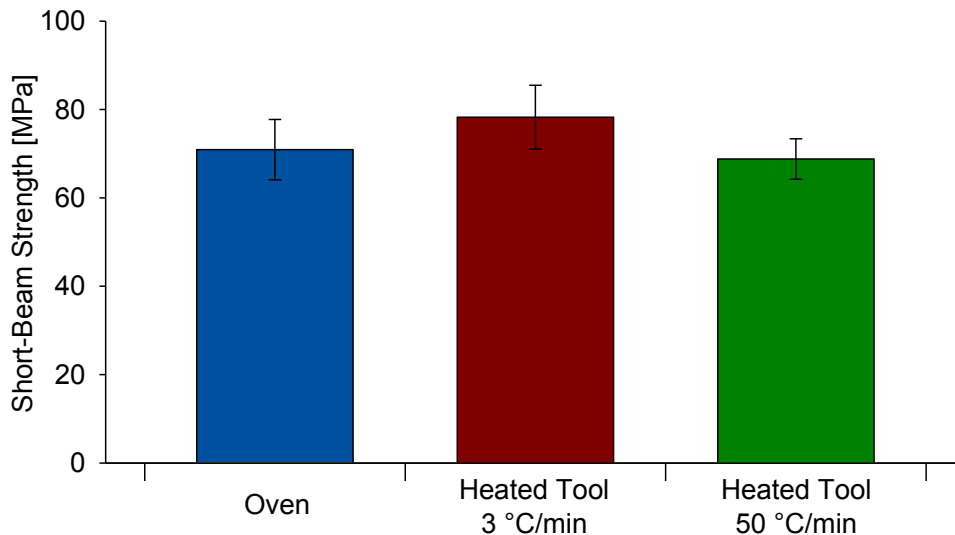


Figure 4.4-1: Average short-beam strengths for 3 heating conditions

These results contradict initial expectations, as the short-beam strengths were expected to be similar across all three heating conditions. However, short-beam strength has been shown to depend highly on void content, as researchers have observed in a number of studies [56; 57]. Examining the relationship between void content and short-beam strength of the individual samples

tested here, it is clear that the samples demonstrated the expected drop in short-beam strength as void content increased.

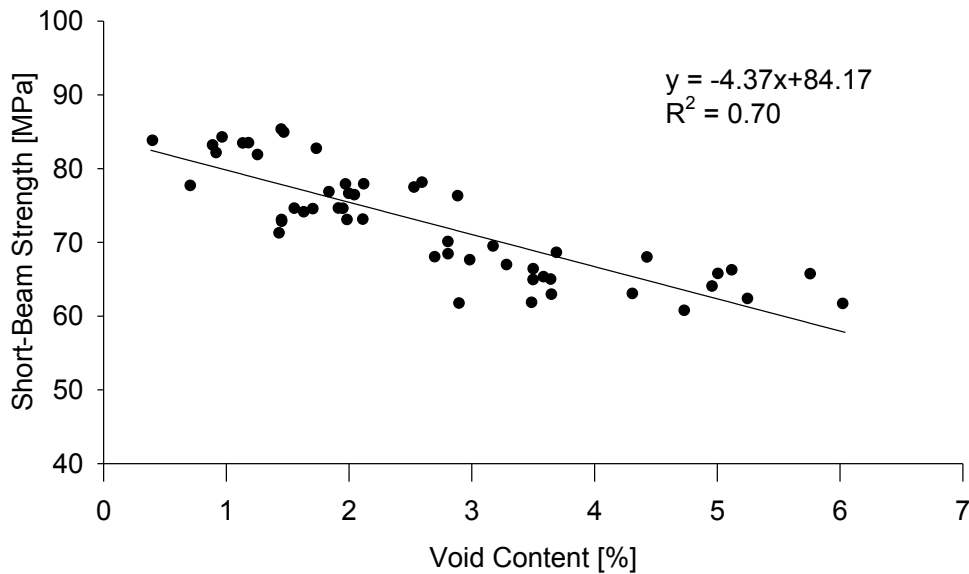


Figure 4.4-2: Short-beam strength vs. void content

The unexpected mean short-beam strength results can be explained as the result of two factors. First, the laminate to laminate variation in void content discussed earlier could be at fault. Second, the specimen dimensions for these tests are set as a function of laminate thickness. Here, an average value for thickness was used, resulting in specimens of approximately 18.9 mm x 6.3 mm for all heating configurations. It is possible that using an average thickness throughout skewed the individual results, leading to the unexpected mean values. Overall, the results indicate that switching to a heated tool cure did not negatively impact the short-beam strength of specimens tested here.

4.5 GLASS TRANSITION TEMPERATURE

Glass transition temperature (T_g) is typically used in industry to establish a maximum service temperature for a composite part, as it corresponds to the temperature at which a polymeric material changes from a rigid glassy solid into a softer, rubbery material [5]. Around this point, there is a significant drop in stiffness. However, given that T_g displays a well established link with the degree of polymerization of polymer matrices, it can also be used an indicator of the extent to

which laminates have cured [61]. Here, T_g was used to examine the different cure conditions' effects on laminate degree of cure.

4.5.1 METHODOLOGY

Glass transition temperature was determined by Dynamic Mechanical Analysis (DMA) according to ASTM D7028 [51], using the dual cantilever setup on a TA Q800 DMA. Per the standard, the intercept of the two tangent lines on the storage modulus curve was reported as the T_g . Three samples were tested per heating condition, with a span of 35 mm, heating rate of 5 °C/min, frequency of 1 Hz, and displacement amplitude of 100 μm. Samples were cut to 60 mm x 13 mm using a Struers Accutom-5 precision saw with a diamond cut-off wheel, from the locations indicated in Figure 4.3-1.

4.5.2 OVERALL COMPARISON

Glass transition temperature testing yielded consistent results for all three heating conditions, indicating that a similar degree of cure was achieved in all cases [61]. To verify these results, they were compared with the model developed by Kratz *et al.* [38], which predicted glass transition temperatures of 198.03 °C for the baseline cure cycle, and 197.80 °C for the high ramp rate trials. The results are given in Table 4.5-1, as well as the predicted values. This comparison confirms that the heated tool cure achieved similar heating to the standard oven process, resulting in uniform T_g across all three heating conditions.

Table 4.5-1: Glass transition temperature results with standard deviations

Glass Transition Temperature	Oven	Heated tool	
	3 °C/min	3 °C/min	50 °C/min
DMA [°C]	200.98 ± 0.24	201.54 ± 0.45	200.58 ± 0.75
Kratz <i>et al.</i> prediction [°C]	198.03	198.03	197.80

4.6 SUMMARY OF RESULTS AND DISCUSSION

Table 4.6-1 summarizes the results of this quality assessment. Overall, these results indicate that the HTP produces laminates of similar quality to a standard oven cure, regardless of the heating rate implemented. The short-beam strength and T_g testing illustrate that the heated tool cure,

even when using 50 °C/min heating, does not negatively impact laminate quality. Despite initial signs indicating that aggressive heating may be detrimental to void content, the detailed ramp rate studies show no trend between heating rate and void content.

Table 4.6-1: Quality benchmarking average results with standard deviations

Quality Metric	Oven	Heated Tool			
	3 °C/min	3 °C/min	10 °C/min	30 °C/min	50 °C/min
Void Content [%]	2.07 ± 0.80	2.11 ± 1.79	2.23 ± 0.93	1.98 ± 0.69	2.80 ± 1.29
Short-Beam Strength [MPa]	70.92 ± 6.84	78.65 ± 7.22	N/A	N/A	68.80 ± 4.58
T _g [°C]	200.98 ± 0.24	201.54 ± 0.45	N/A	N/A	200.58 ± 0.75

These results indicate that implementing a TCX™ heated tool cure within an industrial setting should not impact quality. Additionally, the fact that ramp rate does not seem to have an effect on the quality metrics investigated here indicates that manufacturers could safely make use of the aggressive heating made possible by implementing these types of cures. In terms of cycle time savings, switching from 3 °C/min heating to 50 °C/min results in approximately 48 minutes for the cure implemented throughout this study. This represents a significant reduction in cure time, on the order of 10%. As manufacturers are always seeking to shorten cycle times, this type of cure cycle could be highly attractive to companies seeking to produce more parts without sacrificing quality.

CHAPTER 5: ENERGY CONSUMPTION

In all manufacturing processes, an understanding of the energy consumption inherent to that process is required when evaluating its applicability. A comparison between energy consumption of heating methods can be quite complicated, as scale very quickly becomes an issue. As the TCX™ element is believed to be well suited for large, complex parts, lab scale tests alone do not tell a complete story. That said, they can be used to gain an understanding of the method's energy requirements, and a basic comparison of the scale-up issues can be performed to theorize how the methods would compare on the industrial scale. In this chapter, a comparison of the energy requirements of the two heated tool prototypes and a laboratory scale convection oven is performed. Several methods are considered to investigate the issue of scale, and provide the fairest comparison between these methods to illustrate the potentially energy savings available when replacing a convection oven with a TCX™ heated tool. Some of the experiments presented here were previously presented as part of the work done in *Out-of-Autoclave Manufacturing: Benchmarking of an Integrally Heated Tool-Plate* [49; 50]. This chapter provides greater experimental details, as well as incorporating the MZT prototype into the energy comparisons.

5.1 METHODOLOGY

To compare energy consumption required for TCX™ heated tools, the current drawn during cure by the respective systems (Oven, HTP, and MZT) was monitored using Fluke a3000 FC wireless current clamp modules. In all cases, the current meters logged Root Mean Square (RMS) current for the AC source, at a sampling period of 1 s. As the HTP prototype was powered by single phase 120 V AC, a single meter was used. For the MZT, two single phase 120 V AC power supplies feed the tool, requiring two clamp meters. For the oven, three clamp meters were used simultaneously to monitor the 3-phase 208 V AC source. The current measurements were then used to determine both power and energy consumption.

In the case of the HTP, Equations 9 and 10 were used where $P(t)$ is the power, $E(t)$ is the energy, V_{RMS} is the 120 V supplied to the tool, I_{RMS} is the current measured by the Fluke meter, and

Δt is the sampling period of 1 s. For the MZT, these calculations were performed for both power sources, and simply summed to determine the total values.

$$P(t) = V_{RMS} \times I_{RMS}(t) \quad (9)$$

$$E(t) = \sum_0^t P(t) \times \Delta t \quad (10)$$

For the 3-phase power supply of the oven, equations 11 and 12 were used to determine the total power and energy consumption, where V_{LL} is the line-to-line voltage measured as 208 V, I_{phase} is the current measured by the Fluke meter for each phase, and Δt is the sampling period of 1 s. These equations assume that the oven is dominated by its resistive elements, and neglect any inductive or capacitive effects. This is a fairly safe assumption made to simplify the calculations performed here, but could lead to a slight under estimation of energy consumption.

$$P_{total}(t) = \frac{V_{LL}}{\sqrt{3}} (I_{phase1} + I_{phase2} + I_{phase3}) \quad (11)$$

$$E_{total}(t) = \sum_0^t P_{total}(t) \times \Delta t \quad (12)$$

For the purpose of this study, four heating conditions were evaluated. These conditions are listed in Table 5.1-1. Five trials were performed for each heating condition. The cure cycle imposed for these trials was a standard two-dwell cycle, featuring a 2 hour dwell at 121 °C followed by a 3 hour dwell at 177 °C. Heating rates changed depending of the heating condition, and cooling rates were constant at 1 °C/min for every case.

Table 5.1-1: Heating conditions for energy consumption trials

Heating Condition	Heat Source	Heating Rates
Oven-3C	Oven	3 °C/min
HTP-3C	HTP	3 °C/min
HTP-50C	HTP	50 °C/min
MZT-3C	MZT	3 °C/min

5.2 ENERGY TRIAL RESULTS

For the four heating conditions evaluated, the power drawn as a function of time was plotted. Examples are shown in Figures 5.2-1 to 5.2-4. As the power varies greatly from one measurement to the next, a moving average filter with a span of 50 measurements was used to better illustrate the trends in power consumption. All four heating conditions display a similar trend, where power consumption peaks at the end of the temperature ramp sections, and the drops rapidly to a steady-state value during the dwells.

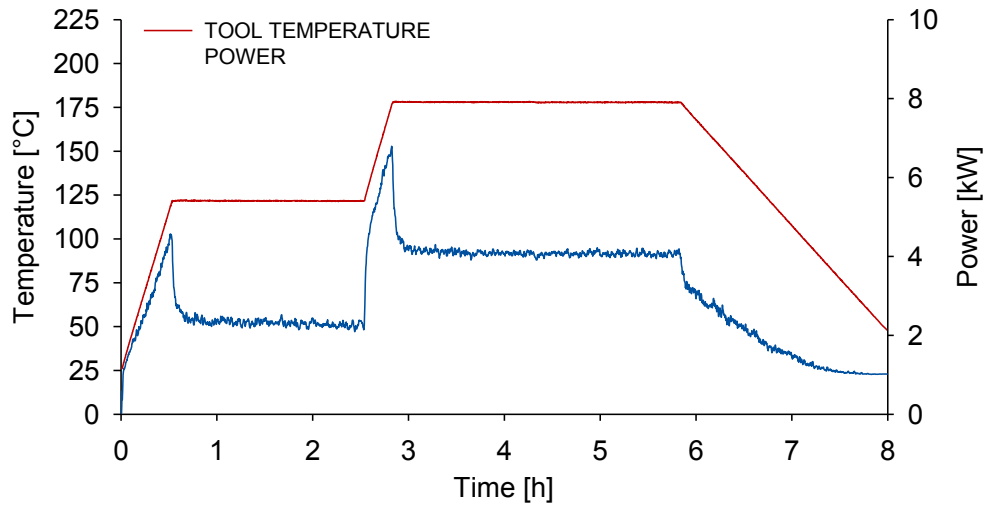


Figure 5.2-1: Representative power vs. time for Oven-3C condition

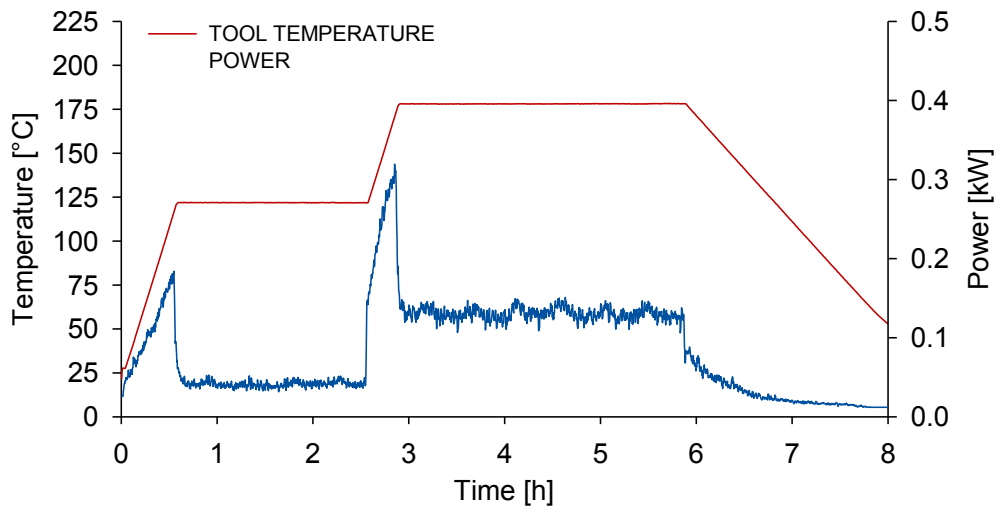


Figure 5.2-2: Representative power vs. time for HTP-3C condition

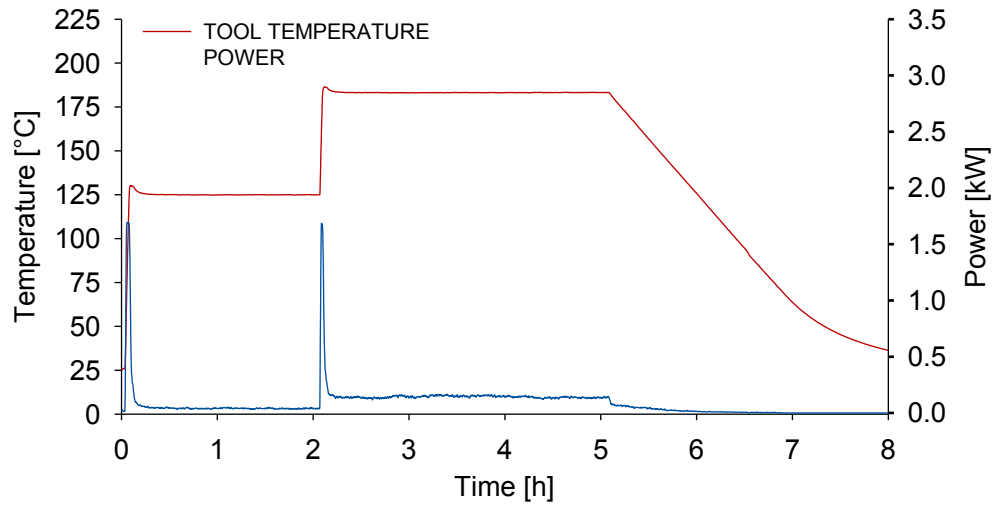


Figure 5.2-3: Representative power vs. time for HTP-50C condition

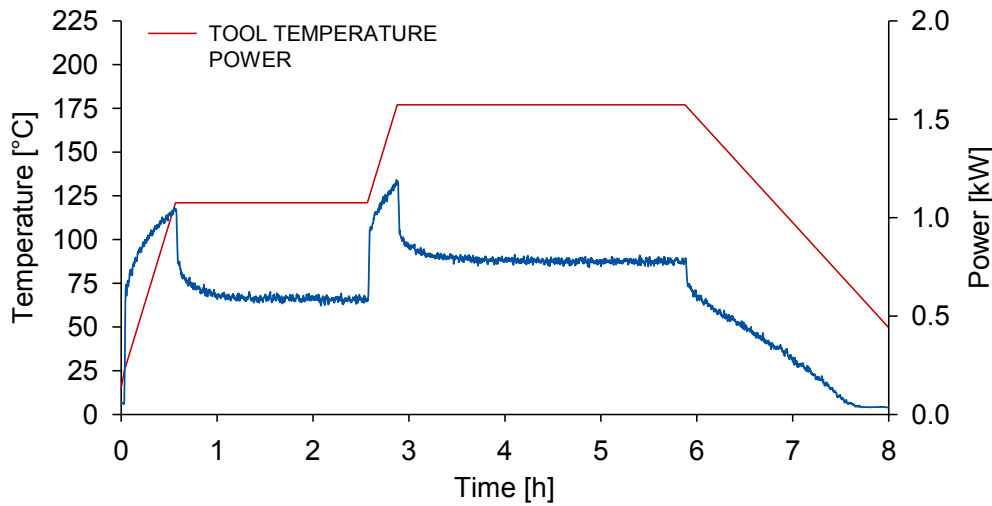


Figure 5.2-4: Representative power vs. time for MZT-3C condition

From the power data gathered, three metrics were determined for each of the heating conditions: total energy consumption, average power consumption, and peak power consumption. These values are summarized in Table 5.2-1.

Table 5.2-1: Energy trial average results with standard deviations

Heating Condition	Energy Consumption [MJ]	Average Power [kW]	Peak Power [kW]
Oven-3C	86.73 ± 3.18	3.024 ± 0.111	6.842 ± 0.205
HTP-3C	2.46 ± 0.14	0.086 ± 0.005	0.304 ± 0.009
HTP-50C	2.55 ± 0.22	0.099 ± 0.009	1.706 ± 0.023
MZT-3C	18.32 ± 0.21	0.636 ± 0.007	1.210 ± 0.012

5.2.1 DIRECT COMPARISON OF HEATING SYSTEMS

Comparing the three heating systems considered here (Oven, HTP, and MZT), it is clear that for the same cure cycle featuring 3 °C/min heating, each requires a vastly different amount of energy. This is illustrated graphically in Figure 5.2-5. However, these are very different systems, capable of processing different amount of material, and a direct comparison is not strictly fair. A scaled comparison will be performed in Section 5.3.

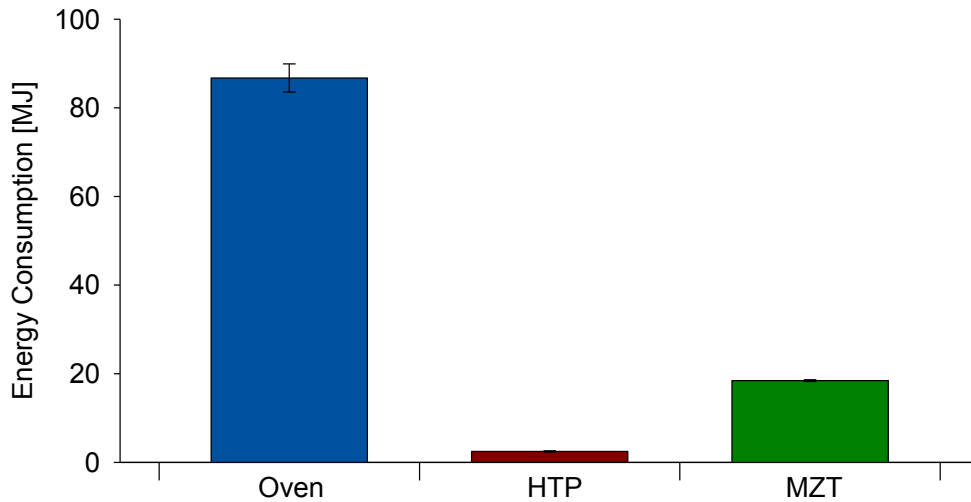


Figure 5.2-5: Energy consumption per heating system using 3 °C/min heating

5.2.2 EFFECT OF HEATING RATE

As the heated tooling systems are capable of much more rapid heating than the convection oven, an understanding of the effect of heating rate on both energy consumption and power draw is required. To that end, the HTP was evaluated for both 3 and 50 °C/min heating. From the results shown Table 5.2-1, we see that heating rate does not greatly influence the overall energy consumption, but does have a marked effect on the peak power observed. The 50 °C/min heating required approximately 6 times more available power, indicating that while energy consumption remains mostly unchanged, increasing heating rates will require larger, more robust power supplies to deliver the required power.

5.3 SCALED COMPARISONS

Each heating system considered here is capable of handling a different load, and as such the results obtained for energy consumption must be scaled to better compare their energy requirements. In order to produce a more representative comparison, two scaling methods were considered.

5.3.1 OVEN POWER FUNCTION SCALING

The first scaling method considered involved developing a relationship between an oven's heater wattage and its cavity volume, using published manufacturer data [62; 63; 64]. Figure 5.3-1 shows the manufacturer data for convection ovens rated for a maximum temperature of 343 °C, for volumes ranging from 0.045 to 14 m³. While the volumes considered in these trials are quite small, the fact that the relationship held across a wide range of volumes provided some confidence in the method's validity. This data set includes the values for the Blue M model 265 oven used during these trials.

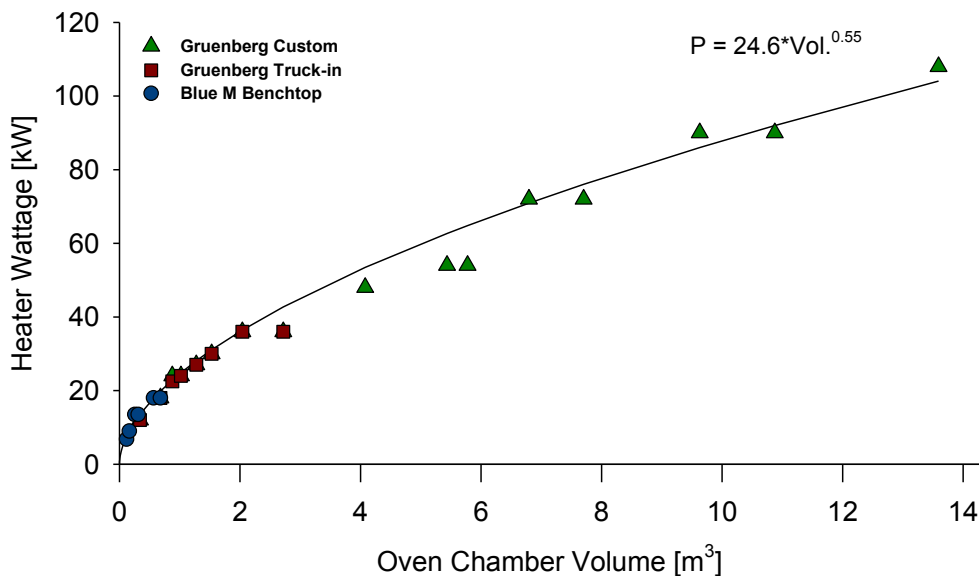


Figure 5.3-1: Cavity volume vs. maximum power for commercially available ovens

From Figure 5.3-1, the relationship between cavity volume and heater wattage was determined to be $P_{heater\ wattage} = 24.6 * Vol.^{0.55}$. This relationship would allow the heater wattage for an oven of a given volume to be estimated. For the cure cycle imposed in these trials, earlier results

indicated that the Blue M model 265 oven used an average power equal to 34% of its heater wattage. Taking this average to hold constant for ovens of any volume, total energy required for a theoretical oven could be estimated using Equation 13.

$$E_{scaled\ oven} = 0.34 \times P_{heater\ wattage} \times t_{cycle} \quad (13)$$

To compare the heated tooling options to the Blue M model 265 oven using this relationship, theoretical ovens just large enough to process the same amount of material as the HTP and the MZT were considered. Table 5.3-1 provides the details of this comparison, including the cavity volume required by each heating method, and the corresponding heater wattage and theoretical energy consumption.

Table 5.3-1: Theoretical oven energy consumption based on power function scaling

Tool	Cavity Dimensions [mm]	Cavity Volume [m ³]	$P_{heater\ wattage}$ [kW]	$E_{scaled\ oven}$ [MJ]
HTP	381 x 381 x 153	0.022	2.98	29.15
MZT	711 x 508 x 153	0.055	4.93	48.28

Finally, to compare the heated tools against the theoretical oven values, the experimental results were divided by the theoretical oven energy consumptions, and the percentage of energy saved was determined. These results are shown in Table 5.3-2. This scaling method indicates the HTP and the MZT to represent 91.6% and 62.1% energy savings respectively.

Table 5.3-2: Oven power function scaling results

Heating Method	$E_{experimental}$ [MJ]	$E_{scaled\ oven}$ [MJ]	Normalized	% Savings
Oven	86.73	86.73	1.00	N/A
HTP	2.46	29.15	0.084	91.6
MZT	18.32	48.28	0.379	62.1

5.3.2 LAMINATE AREA SCALING

A second, more conservative scaling approach was also considered. This method consisted of simply dividing a heating method's energy consumption by the corresponding area of a laminate which could be manufactured by the process. The heated tooling results were then normalized against the oven and the percentage energy savings determined. The HTP and MZT laminate ar-

areas were determined based off the tool surface dimensions, subtracting a suitable amount of space to account for bagging consumables. This yields laminate areas of 0.041 and 0.139 m² respectively. The oven laminate area was determined to be 0.483 m² based on using 3 shelves with the largest possible tool plates placed in the model 256 oven. The results of this second scaling approach are given in Table 5.3-3 below.

Table 5.3-3: Laminate area scaling results

Heating Method	$E_{experimental}$ [MJ]	Laminate Area [m ²]	Energy per Area [MJ/m ²]	Normalized	% Savings
Oven	86.73	0.488	177.82	1.00	N/A
HTP	2.46	0.041	59.58	0.335	66.5
MZT	18.32	0.139	131.47	0.739	26.1

5.3.3 SCALE UP CONSIDERATIONS

While scaling down the energy results provides a more meaningful comparison than the raw data presented, this type of technology is of more interest for large, complex structures which are difficult to heat effectively in a convection oven. When considering scaling up to larger parts, several factors indicate that losses associated with a heated tool will scale more favourably than those of the oven. As an oven is scaled up in volume, the oven structure, duct work, fans, insulation, and mass of air are all increased. As a heated tool is scaled up, the only additional material required is tooling insulation. In both cases, the part and tool themselves will scale identically. This logic indicated that due to the the additional thermal mass present as the oven scales up for large scale components, the gap between the two systems will only become more significant. As such, the potential energy savings presented in Sections 5.3.2 and 5.3.3 should be considered conservative estimations.

5.4 RESULTS AND DISCUSSION

Overall, it was shown that both heated tools considered here require significantly less energy than the convection oven. Attempting to account for the difference in scale between heating methods, the savings for the HTP were determined to be between 66.5 and 91.6 percent, while the MZT showed between 26.1 and 62.1 percent savings. The two scaling methods considered here yield very different results, but provide an indication of the possible savings.

Between the HTP and the MZT, there is a significant difference in the energy requirements, even when scaled appropriately. This difference is due to a number of different contributing factors. Firstly, the HTP represents a very simple tooling system, with minimal substructure. The MZT on the other hand is a more real-world system, with significantly more mass that is indirectly heated by the tool. Heat transfers from the tool surface into the surrounding frame, heating all of the various components to some extent. This results in an increase in power consumption, as there are more thermal sinks drawing heat away from the tool. Second, as the HTP is a simpler setup, it was more easily insulated. Both the top and the bottom of the HTP surface are accessible and easily insulated, with no limit to the thickness of insulation used. The MZT has geometric restrictions on the amount of insulation used, and is less well insulated overall.

Based on these results, several design suggestions can be put forward for future TCX™ heated tool systems. First, an effort should be made to thermally isolate the tool surface from the rest of the substructure. Using non-conductive substructure materials, or adding insulating materials to minimize conductive heat transfer from the surface to the substructure could greatly reduce the energy requirements. Second, where possible the mass of substructure and support systems in thermal contact with the surface should be minimized. Substructure design will likely be driven by structural rather than thermal requirements, but thermally speaking it is logical to minimize the substructure mass as much as possible. Third, insulation will play a key role in the energy efficiency of a heated tool, by preventing convective losses to the surrounding environment. Incorporating good insulation both above and below the tool surface will greatly reduce energy losses. In a production environment, it may be logical to place a heated tool inside an insulated chamber where the convective heat losses can be limited.

CHAPTER 6: PROCESSING FLEXIBILITY

Previous chapters presented here have focused on OoA processing of flat, monolithic, prepreg laminates. This type of part represents a simple structure suitable of laboratory scale investigations, but they do not represent a suitably diverse set of components to meet the needs of the aerospace industry. To that end, three sets of experiments were performed to expand the processing flexibility of TCX™ heated tools. The goal of these experiments was to demonstrate that the prototypes developed during this project are capable of handling parts of a more complicated nature than flat, prepreg panels. This was done by investigating a different processing technique, resin film infusion (RFI), as well as two alternate prepreg structures, specifically tapered laminates and sandwich structures. The experiments on these alternate structures were done as part of a conference paper prepared for CANCOM 2015, titled *Multi-Zoned Heated Tooling for Out-of-Autoclave Processing of Variable Thickness Composite Laminates* [48]. This chapter expands upon the initial results presented in this paper, as well as providing details on the resin film infusion (RFI) trials performed as a third method of increasing processing flexibility for TCX™ heated tools.

6.1 RESIN FILM INFUSION

As a first step in expanding the TCX™ elements processing flexibility, several trials were performed to investigate using a TCX™ heated tool for RFI. This was done both to demonstrate the heated tool's capacity to handle alternative manufacturing techniques, and to demonstrate a potential manufacturing technique which could greatly reduce cycle times. As mentioned previously, OoA prepregs typically require a lengthy vacuum hold prior to cure to produce parts with low void contents, in the range of 4 to 16 hours [54; 65]. The RFI process, which combines B-staged resin films with dry unimpregnated fibres, does not normally require this manufacturing step. The resin film and the fibre reinforcement are initially separate, and are combined by the application of heat and pressure, which melts the resin and forces it into the fibres [5]. As the fibres are completely unimpregnated at the beginning of the process, air can be evacuated very quickly, removing the need for an extended vacuum hold. In this study, RFI panels were pro-

duced using the HTP prototype, investigating several different layup and cure configurations and their effect on void content.

6.1.1 METHODOLOGY

To evaluate RFI as an alternative to preregs, two layup configurations and three cures were evaluated. The two layup configurations studied varied only in the placement of the resin. In the first case, resin films were placed directly in contact with the tool surface, with the fibre bed placed on top. In the second case, resin films were placed between each ply of fabric. These configurations, denoted as Tool-Side and Interspaced, as shown in Figures 6.1-1 and 6.1-2.

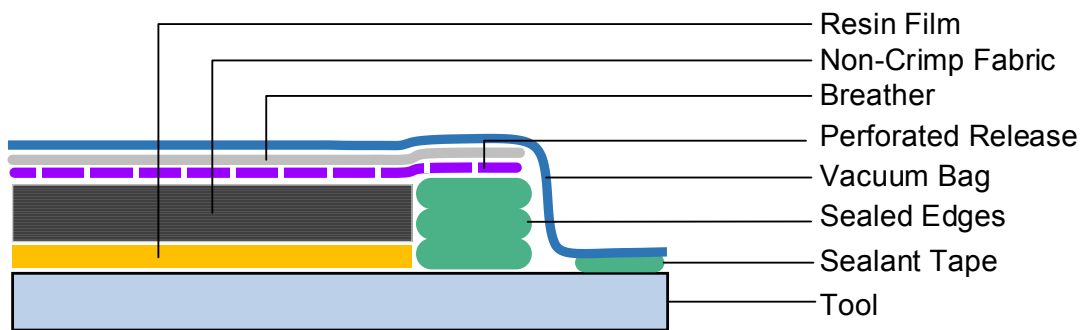


Figure 6.1-1: Tool-Side RFI layup configuration

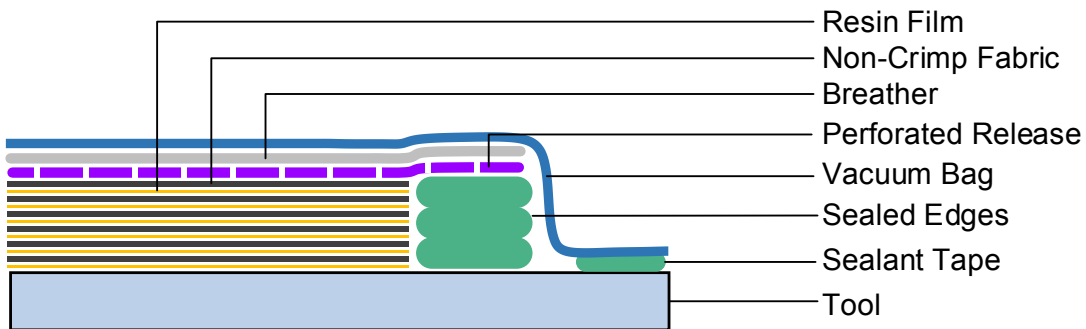


Figure 6.1-2: Interspaced RFI layup configuration

The consumables used for both configurations consisted of Airweave N-4 polyester breather (2 plies), Airtech A4000RP3 perforated fluoropolymer release film, Wrightlon 6400 nylon vacuum bag, and Airtech GS-213-3 sealant tape. The resin film used was 112 g/m^2 MTM[®]45-1 from Cytec, a toughened epoxy system optimized from vacuum-bag only processing [66]. The reinforcement used was a non-crimp fabric from SAERTEX, with an areal weight of 440 g/m^2 . In all

case 6 plies of fabric were combined with 12 plies of resin film, resulting in a final resin content of approximately 33.8%.

As mentioned, three cures were evaluated. In all cases, a 2 hour cure at 121 °C and 3 hour post-cure at 177°C were used based on the model developed by Kratz *et al.* [38]. The first cure established a baseline by using 3 °C/min heating, while the second used 50 °C/min to evaluate the impact of aggressive heating. Both of the cures featured no room temperature vacuum hold. The third cure again used 50 °C/min, but added in a 30 minute room temperature hold prior to starting the first heating phase.

Combining these 2 layup configurations and 3 cures resulted in a total of 6 test configurations, with 1 laminate produced for each. For each configuration, void content was used as the main measure of quality, once again evaluating it by greyscale thresholding of optical micrographs. Cutting, polishing, and micrograph preparation were done following the same procedure outlined in Section 4.3, with three samples of approximately 40 mm x 20 mm taken from each laminate in the same manner as shown in Figure 4.3-1.

6.1.2 VOID CONTENT RESULTS

For the six configurations mentioned above, void content results are included in Table 6.1-1.

Table 6.1-1: RFI trial void content results

Trial	Resin Film Position	Room Temperature Hold [min]	Heating Rate [°C/min]	Void Content [%]
1	Tool-Side	0	3	0.47 ± 0.19
2	Tool-Side	0	50	0.22 ± 0.14
3	Tool-Side	30	50	0.74 ± 0.29
4	Interspaced	0	3	0.76 ± 0.27
5	Interspaced	0	50	2.27 ± 0.81
6	Interspaced	30	50	0.57 ± 0.22

These results indicate that the void contents of these RFI panels were generally quite low, mostly well below 1%. The notable exception is Trial 5, which combined the interspaced resin film configuration with no room temperature hold and 50 °C/min heating. Figures 6.1-3 and 6.1-4 provide a direct comparison between the two layup configurations for 50 °C/min with no room tem-

perature hold. Observing the micrographs as a whole, typically more inter-tow voids were present than intra-tow voids. The large standard deviations across the results can be attributed to the presence of these very large voids, where a single void can greatly change the results obtained for a given micrograph.

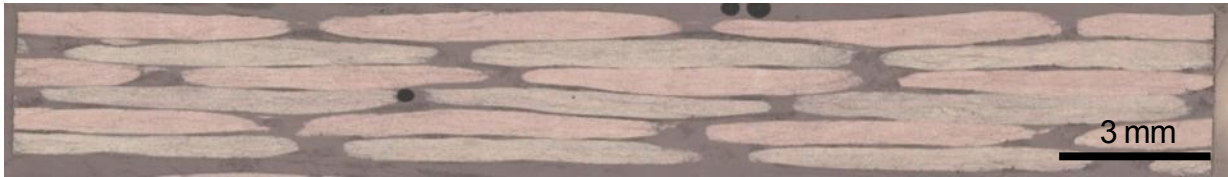


Figure 6.1-3: RFI trial 2 sample micrograph, 0.26 % void content



Figure 6.1-4: RFI trial 5 sample micrograph, 2.31 % void content

6.1.3 DISCUSSION

Based on the three parameters which were varied here, several observations can be made from these results. First, it appears that the tool-side resin configuration results in lower void content than the interspaced configuration. From a practical standpoint, it is also much easier in terms of layup as handling the thin, tacky resin film is not easy. By combining all the resin films into one thick stack they become easier to handle. The interspaced configuration has many interfaces between fibre and resin, which tends to result in fibres being sheared when backing films are removed from the resin, potentially impacting fibre alignment. Grouping the resin on the tool side appears to be the more common approach [5], and was shown here to produce better results while being easier to implement.

Second, the implementation of an aggressive heating rate had a very different effect between the two layup configurations. In the tool-side tests, the 50 °C/min heating appeared to improve void content, although it is hard to state that with confidence given the limited size of the data set. More interesting is that the interspaced panel featuring 50 °C/min heating had the highest void

content of any of the tests. One possible explanation for this is that in this configuration, the presence of resin films between each ply makes air evacuation prior to the onset of gelation very difficult. Using the model developed by Kratz *et al.* for MTM[®]45-1, a quick examination of the cure kinetics shows that the 50 °C/min heating reaches gelation in approximately 110 minutes, whereas the 3 °C/min heating takes 135 minutes [38]. Prior to gelation, air can still be evacuated from the fibres, indicating that reaching gelation sooner could negatively impact the void content.

The third noteworthy observation is the effect of adding in a 30 minute room temperature hold. In the tool-side layup configuration, the addition of a room temperature hold appears to negatively impact laminate quality. That said, the high standard deviations make it more likely that there is little to no effect and that the apparent difference is caused by insufficient data. When comparing Trials 5 and 6 however, it appears that for the interspaced configuration, adding the room temperature hold greatly improved quality. As the fibres are initially unimpregnated, air evacuation happens very quickly, which normally removes the need for an extended room temperature hold. In the interspaced configuration, with 50 °C/min heating, it is believed that the layers of resin between plies, coupled with the reduced time to gelation, make it challenging to fully evacuate the air. The addition of a short room temperature hold appears to provide enough extra time to bring void content back to acceptable levels.

Overall, these experiments have shown that the HTP is capable of processing material forms other than prepregs. In fact, coupling the TCX[™] elements rapid heating capabilities with a simple process like RFI appears to be a promising way to reduce cycle times for composites manufacturing. When compared to an oven-cured OoA prepreg with a 16 hour room temperature vacuum hold, the RFI process studied here requires approximately 1/3 of the time from the end of layup until final debuggging.

6.2 TAPERED LAMINATES

As a second step in expanding the TCX[™] heating element's processing flexibility, the curing of variable thickness tapered laminates was investigated. Previous chapters have focused exclu-

sively on flat structures of uniform thickness, but real-world structures are rarely so simple. Aircraft manufacturers make use of complex geometries and layups to achieve the highest performance with the lowest weight. In many cases, designers use thickness changes to tailor a laminate's elastic properties to a given application. This can be achieved by using partial plies which terminate within the laminate [67]. A good example is a helicopter rotor blade, which is designed thick at the root, and tapers along its length, changing in stiffness as required by the design [68].

These types of structures can be challenging to process when using one-sided heating, such as the heating provided by the prototypes developed in this project. As thickness varies, so does the amount of heat required to cure a part. In addition, it is critical that the various sections progress simultaneously through the stages of cure, to avoid developing residual stresses due to a non-uniform degree of cure [68]. For one-sided heating of tapered laminates, this problem becomes doubly important. As heat is transferred via conduction through the thickness of a part, a cure gradient can develop if the tool side material heats up more quickly than material on the bag side of a laminate. If there are also thickness variations in-plane to contend with, a second cure gradient can develop if the thicker sections do not follow the same temperature profile as the thinner sections. To assess the TCX™ heating elements ability to handle parts of this nature, the Multi-zoned tool (MZT) prototype was developed with multiple heating zones arranged along its length. This would allow for the temperature profile to be accurately controlled and for each zone of the tool to provide the necessary heat to a part regardless of its thickness.

6.2.1 METHODOLOGY

To investigate the processing of tapered laminates, parts featuring aggressive ply drop-offs were produced using the MZT prototype. Laminates were also produced in a convection oven to provide a baseline comparison. To eliminate the possibility of the in-plane thermal conductivity of the carbon fibres dominating the heat transfer on these lab scale experiments, the same cure was also applied to two separate laminates of different thicknesses, co-cured simultaneously on the tool.

To evaluate the performance of each trial, three thermal metrics were tracked; thermal lag (t_{lag}), mid-plane temperature deviation (ΔT_{mp}), and through-thickness temperature difference (ΔT_{tt}).

Thermal lag was taken as the difference in time between the cure cycle setpoint reaching a dwell temperature, and a section of the laminate reaching 98% of its steady-state dwell temperature at the mid-plane. The mid-plane temperature deviation was taken as the difference between the cure cycle dwell temperature and the mid-plane steady-state temperature. The through-thickness temperature difference was taken as the difference between the tool surface and the bag-side temperatures at steady-state. The t_{lag} was recorded for both the first and second ramp sections, while ΔT_{mp} and ΔT_{tt} were recorded for both dwell sections. A schematic of these metrics is given in Figure 6.2-1.

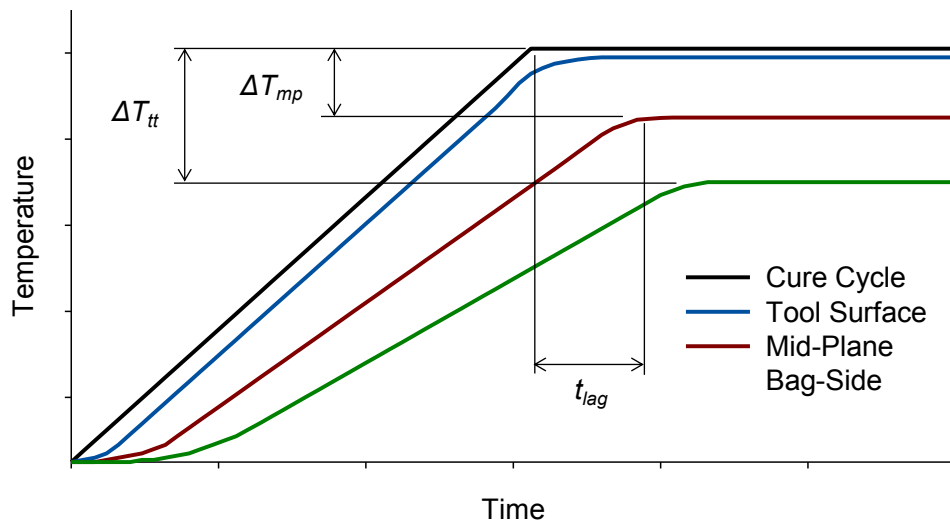


Figure 6.2-1: Thermal performance metrics illustrated for a typical one-sided heating cure

6.2.2 LAMINATE PREPARATION

Tapered laminates were produced as shown in Figure 6.2-2. Thermocouples were placed on the bag-side, the laminate mid-plane, and within the multi-zoned tool itself to monitor the thermal evolution during cure and evaluate the uniformity of temperature during the processing cycle. Laminate dimensions were 450 mm by 100 mm, with the ply count progressing from 4 plies to 24 plies along the length of the laminate. During layup, a 10 minute debulk was performed after ply 1, ply 4, and every subsequent 4 plies. All laminates were held under vacuum for 4 hours at room temperature, and then cured using the standard 2 dwell cycle used in Chapter 4, featuring 3 °C/min heating, a 2 hour dwell at 121 °C, a 3 hour dwell at 177 °C, and 1 °C/min cooling.

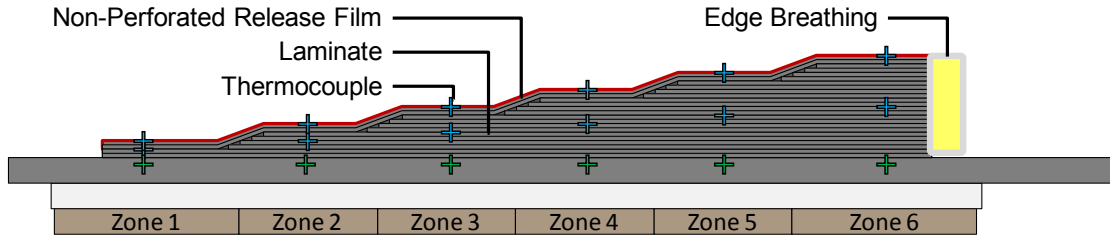


Figure 6.2-2: Tapered laminate layup configuration

For comparison, 4 and 24 ply laminates were co-cured simultaneously in zones 1-2 and 5-6 of the MZT's tooling surface. This would eliminate the role of the in-plane thermal conductivity of the prepreg, to verify that the tapered laminates were representative of larger scale components. A schematic of this configuration is shown in Figure 6.2-3.

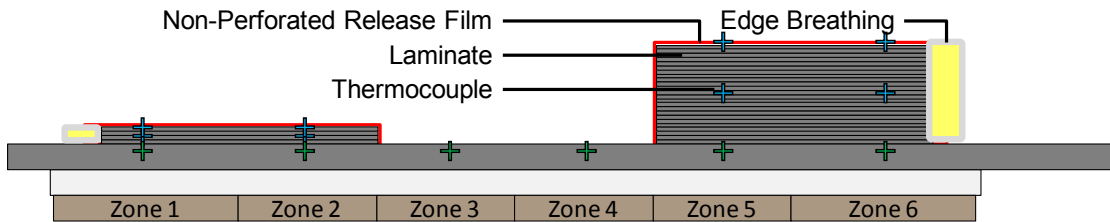


Figure 6.2-3: Co-cured laminate layup configuration

All laminates in this study were prepared using a modified version of CYCOM[®] 5320 from Cytec Engineered Materials, featuring an 8-harness satin fibre architecture and 36% resin content. Where applicable, standard consumables were used, including Airweave N-4 polyester breather, Airtech fluoropolymer release films (A4000R and A4000RP3), OptiSpray OS2400F glass roving edge breathing, Wrightlon 6400 nylon vacuum bag, and Airtech GS-213-3 sealant tape.

6.2.3 DIRECT COMPARISON OF HEATING SYSTEMS

As a first comparison, the oven and the MZT were compared according to the metrics outlined in Section 6.2.1. The results are shown in Figures 6.2-4, 6.2-5, and 6.2-6.

From Figure 6.2-4 we see a marked difference between the oven and MZT trials. The oven laminate lagged between 33 and 43 minutes during the first ramp, and by approximately 19 minutes in the second ramp. The MZT laminate lagged between 20 seconds and 8 minutes during the first ramp, and by approximately 1 minute during the second ramp. From these results, three noteworthy observations were made. First, there is a notable difference in the average lag between the

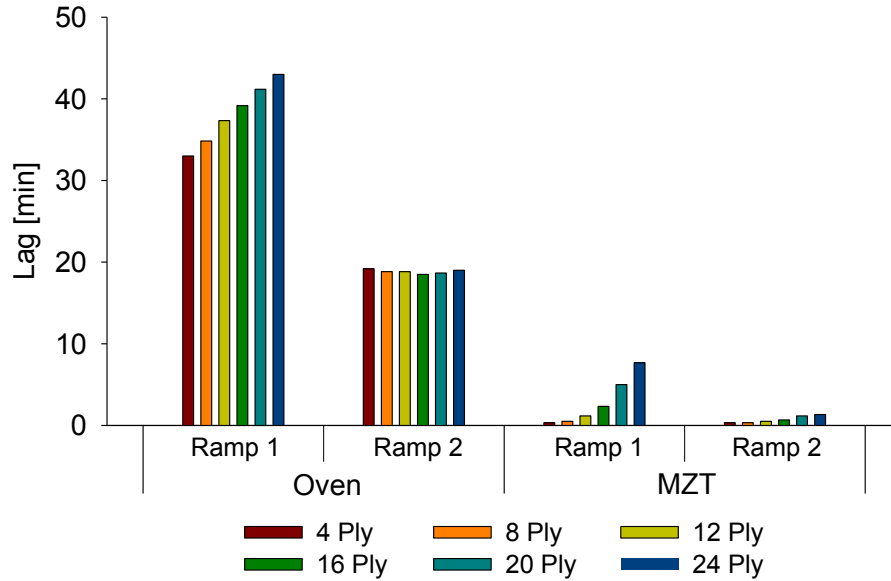


Figure 6.2-4: Tapered laminate thermal lag results

first and second ramps. This can be explained by the low thermal conductivity of the prepreg when uncured. During cure, the resin is able to flow and the ply stack consolidates. Prior to that, the ply stack is less well compacted and heat does not transfer as easily through the thickness. This explains why the second ramp shows less lag, as the material will have gelled by that stage and will have increased its thermal conductivity. The second observation is the difference in lag between the thin and thick sections of each laminate, noticeable only for the first ramp. This result agrees with initial expectations, as the thick sections will require more time to heat, and thus lag further behind. This isn't seen in the second ramp, likely due again to the increased thermal conductivity of the material in its cured state. The final observation made here is the difference in total lag between the two heating methods. The MZT is able to reduce the overall thermal lag from 62 minutes to 9 minutes. This indicates that shorter dwells could be implemented for the heated tool cures, reducing the total cure time by 52 minutes. This would represent nearly an 11% reduction in cure time for the cycle implemented here.

From Figure 6.2-5 we see that both heating methods do not precisely match the input cure profile. The oven trial matches very closely during the first dwell, but deviates by approximately 3 °C in the second dwell. The deviation is believed to be the result of the control setup of the oven, as the air temperature is controlled by thermocouples placed towards the top of the cavity. This

could result in a temperature variation within the oven where the bottom is cooler than the top, explaining why the part appears to reach a steady-state temperature lower than the air above it. The first dwell does not show this trend, likely due to the presence of a slight exotherm which keeps the temperature up. The MZT's deviation from the cure cycle is due to the control thermocouples being embedded in the middle of the tool's thickness. With one-sided heating applied from the bottom and control taking place from the middle, the top surface is slightly cooler than the control location, which carries through to the laminate. Again, the first dwell is closer than the second, most likely because of the same light exotherm.

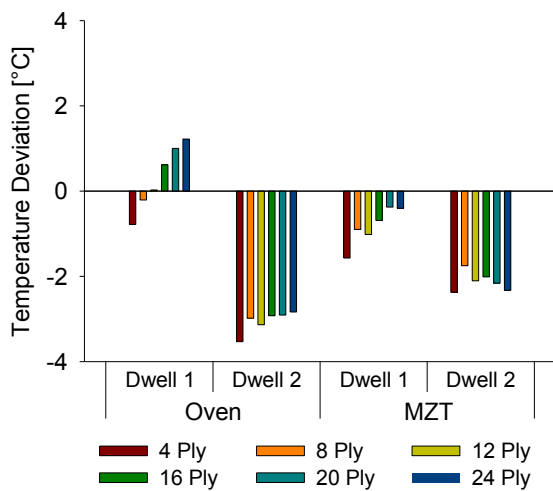


Figure 6.2-5: Tapered laminate mid-plane temperature deviation results

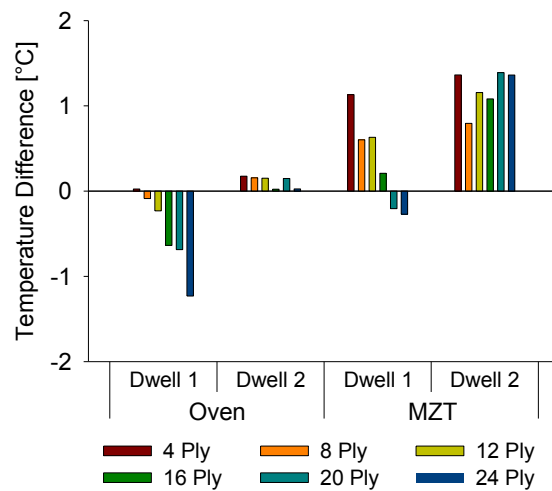


Figure 6.2-6: Tapered laminate through-thickness temperature difference results

Looking at Figure 6.2-6, results indicate that both heating technologies do a good job of minimizing the through-thickness temperature difference within tapered laminates. The thermal lag results indicate that thicker sections take longer to reach the desired dwell temperatures, but Figure 6.2-6 confirms that they do eventually reach the required steady-state temperature.

To verify that the result shown above are applicable to large scale components, the same experiments were performed for co-cured thin and thick laminates.

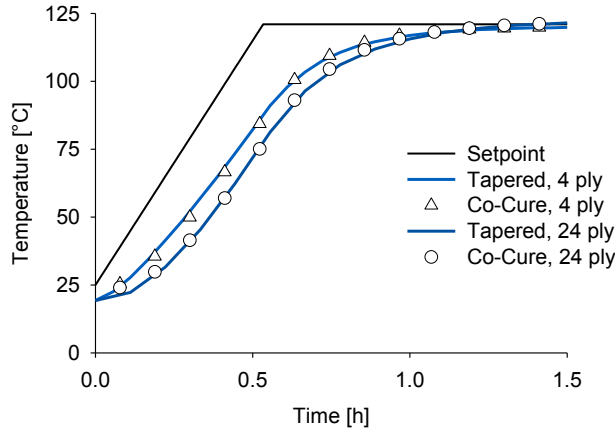


Figure 6.2-7: Comparison of oven processed co-cured and tapered laminates

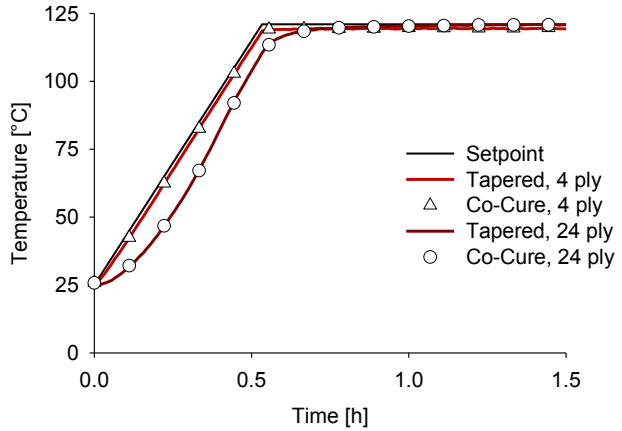


Figure 6.2-8: Comparison of MZT processed co-cured and tapered laminates

As shown in Figures 6.2-7 and 6.2-8, the co-cured laminate cure profile is almost identical to what is seen for the tapered laminates. The overlaid symbols in these plots represent the co-cured laminates, while the solid lines represent the tapered laminates. As the symbols consistently fall on the solid lines, it is clear that the in-plane thermal conductivity does not dominate the temperature evolution, and that the results obtained for the tapered laminates studied here are applicable to larger scale parts.

6.2.4 POWER CONSIDERATIONS

Using the built-in power tracking feature of the MZT, RMS current data was recorded during the cure of the MZT processed laminate. This was done to verify the hypothesis that thicker sections of composite were indeed using more energy during cure. Using the equation shown in Section 3.1.2, the PID outputs fed to each zone of the tool were converted into RMS current values. These were then used to calculate instantaneous power and energy consumption, using Equations 9 and 10, provided in Section 5.1. The overall energy consumption of each zone is shown in Figure 6.2-9, with zone 1 corresponding to the thinnest section, and zone 5 corresponding to the thickest.

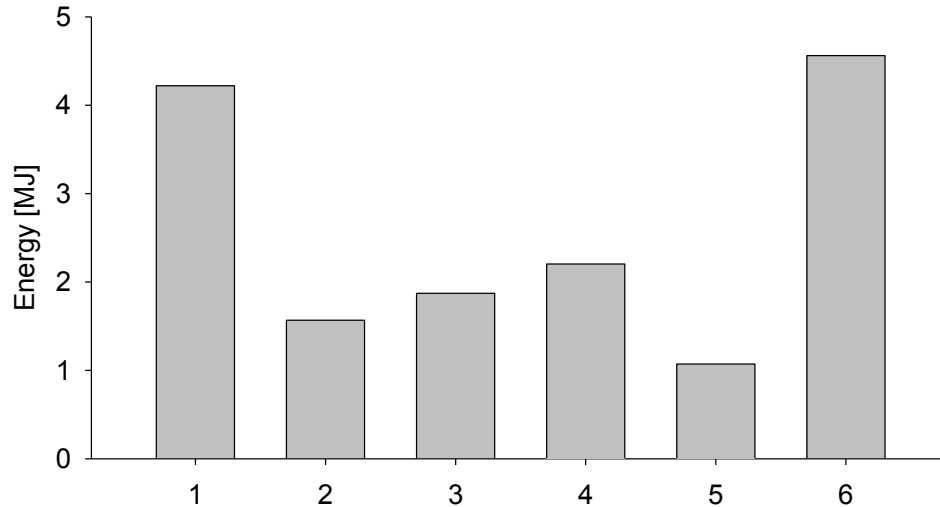


Figure 6.2-9: MZT tapered laminate power consumption per zone

From Figure 6.2-9, the relationship between part thickness and energy consumption is not perfectly clear. In Zones 1 and 6 (see Figure 6.2-2), edge effects result in increased energy consumption as these two elements must combat convective cooling at the edges of the tool, and also bleed heat into the edges of the aluminum surface as well as to the tool's substructure. Zone 6 in particular is responsible for heating the largest amount of aluminum, as the elements are not centred within the tool surface, and Zone 6 provides heat to an extra 2" of the tool's length. Examining Zones 2 through 5, two things are of interest. First, Zones 2 through 4 display the expected behaviour, with power consumption increasing linearly with part thickness. Zone 5, however, does not follow the trend. This is believed to be due to some of the heat from Zone 6 bleeding into Zone 5. As Zone 6 has the largest surface area to heat, it ends up transferring heat to Zone 5 in its effort to maintain temperature. This explains why we see the lowest energy consumption in Zone 5. While these results do not perfectly demonstrate the expected relationship between part thickness and energy consumption, they do indicate that the expected effect is present, but clouded by complicated boundary conditions. To further verify this, a simple test plan could be implemented curing flat parts of varying thickness, and monitoring power drawn during cure. A relationship between a part's thickness or areal density and the power required to process it could then be established.

6.3 SANDWICH STRUCTURES

A second real-world structure worth investigating is sandwich structures, which are parts that feature lightweight core materials as part of their layup. Sandwich structures play an increasingly important structural role due to their exceptionally high flexural stiffness-to-weight ratios [69]. By using a core to greatly increase the thickness of a part, the bending stiffness increases without the same weight penalty that would be required were the part made purely of CFRP. Sandwich structures can be challenging to produce for a number of reasons, but are particularly difficult in OoA applications [70].

In terms of heating, sandwich structures present an interesting challenge. When a low thermal conductivity core is used, such as foam or a Nomex honeycomb, the two composite skins are thermally decoupled to some degree. The core material acts as insulation, reducing conductive heat transfer between the skins. This means that the boundary conditions faced by each skin are very different, and can lead to each skin experiencing a significantly different thermal profile. In an OoA heated tooling application, this poses a problem as these tools typically rely on one-sided heating, which exacerbates the issue in that the desired cure profile is only accurately applied to the skin in contact with the tool.

6.3.1 METHODOLOGY

To address the processing of sandwich structures, three heating strategies were considered. First, a baseline oven trial was performed. Next, a heated tool trial relying on one-sided heating was performed. Finally, the multi-zoned heated tool was coupled with a silicone heating blanket to evaluate a hybrid heating solution. These three trials would illustrate the challenges of processing sandwich structures in a convection oven as well as with one-sided heated tooling, and demonstrate a novel solution to these issues.

6.3.2 LAMINATE PREPARATION

Laminates featuring honeycomb core were produced as shown in Figure 6.3-1. Ply dimensions were 450 mm by 100 mm, with a chamfered core 150 mm long placed in the middle of the length parts length.

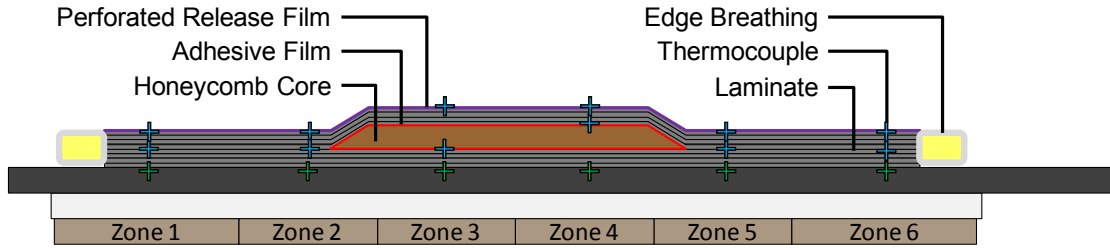


Figure 6.3-1: Sandwich structure laminate configuration

All laminates in this study were prepared using a modified version of CYCOM[®] 5320 from Cytec Engineered Materials, featuring an 8-harness satin fibre architecture and 36% resin content. Four plies of prepreg were used for both the top and bottom skins. A 19 mm thick over-expanded cell aramid honeycomb core (ECA-R 3/16-4.0) from Euro-Composites[®] was bonded to the skins using Cytec FM[®] 300-2M adhesive film. Where applicable, standard consumables were used, including Airweave N-4 polyester breather, Airtech fluoropolymer release films (A4000R and A4000RP3), OptiSpray OS2400F glass roving edge breathing, Wrightlon 6400 nylon vacuum bag, and Airtech GS-213-3 sealant tape.

In this configuration, a 10 minute debulk was performed after ply 1 and ply 4. Before placing the adhesive, it was perforated using a spiked roller to promote through-thickness air evacuation. Each ply placed after the core was debulked for 10 minutes. Prior to cure, all laminates were held under vacuum for 16 hours at room temperature, and then cured using the standard 2 dwell cycle used in Chapter 4, featuring 3 °C/min heating, a 2 hour dwell at 121 °C, a 3 hour dwell at 177 °C, and 1 °C/min cooling.

For the hybrid heating system, a heating blanket was placed above the breather and the vacuum bag, below a layer of fibreglass insulation. Ideally, the heating blanket would be placed within the vacuum bag to better conform to the laminate. However, as a first attempt at this heating strategy, the heating blanket was placed above the vacuum bag for simplicity. A thermocouple placed above the vacuum bag and in direct contact with the heating blanket was used for control, ensuring the heating blanket followed the desired temperature profile as accurately as possible. The heating blanket was powered and controlled by the system developed by Bujun, described in Section 3.1.2 [33].

To evaluate the performance of each heating configuration, the same thermal metrics were used as described in Section 6.2.1. More specifically, both the thermal lag, and through-thickness temperature difference were monitored and reported, as defined in Figure 6.2-1.

6.3.3 RESULTS AND DISCUSSION

Each of the three heating configurations showed its own strengths and weaknesses, as illustrated in Figures 6.3-2, 6.3-3, and 6.3-4, which show the first 6 hours of the cure for each configuration.

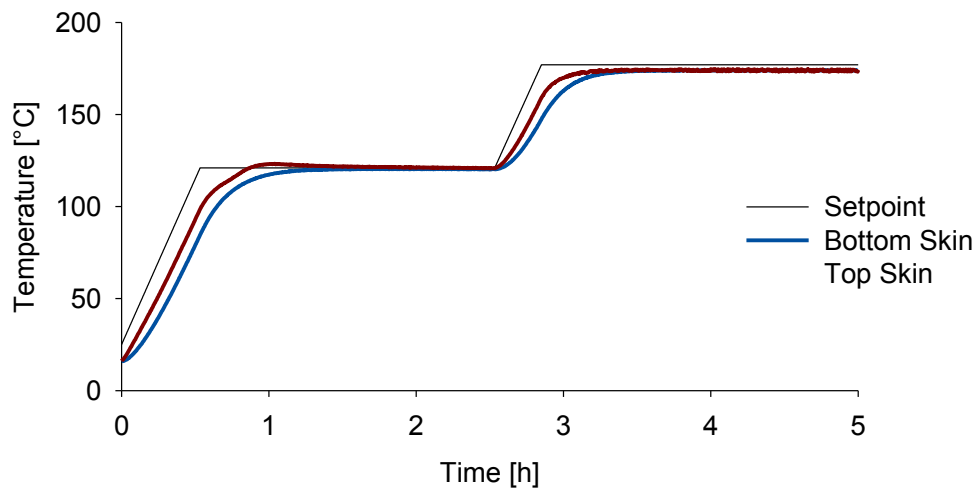


Figure 6.3-2: Sandwich structure oven cure thermal profile

Figure 6.3-2 illustrates the challenges in oven processing of sandwich structures. As is typical for this configuration, the top skin lags slightly behind the setpoint profile, while the bottom skin lags further behind. The relatively high thermal mass of the tool makes it challenging to heat the bottom skin effectively, and causes it to lag behind the top skin. At the lab scale, this results in a thermal lag of approximately 17 minutes for the top skin, and 30 minutes for the bottom. This difference in lag indicates an uneven cure, where the two skins may gel and vitrify at different times. Were larger, more difficult to heat tools considered, this effect would likely be amplified by the increased thermal mass of the tool. The large invar tools seen throughout the aerospace industry would be especially challenging.

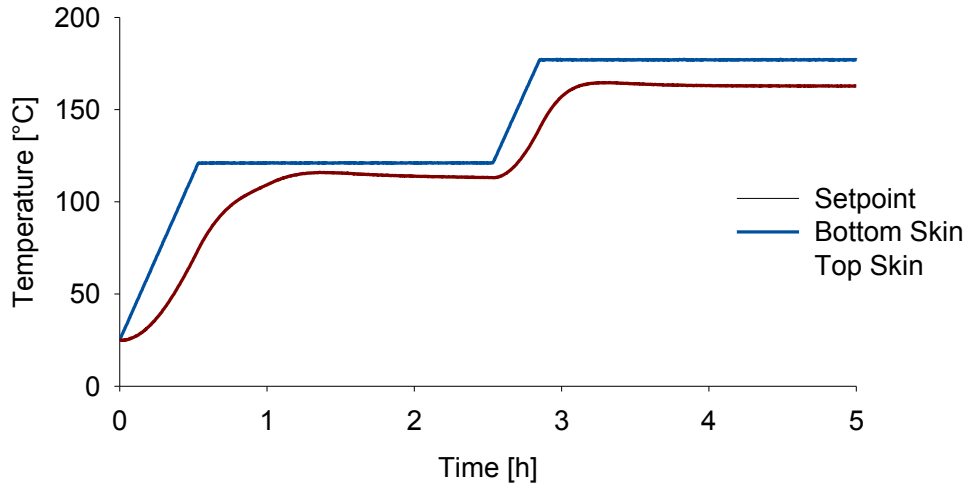


Figure 6.3-3: Sandwich structure heated tool cure thermal profile

From the heated tool trial shown in Figure 6.3-3, we see the issue of applying one-sided heating to sandwich structures. The bottom skin which is in contact with the tool, follows the desired setpoint very closely. However, with the Nomex core material separating the top skin from the heated tool's surface, it is vulnerable to natural convection and receives significantly less heat. Here, the top skin is shown to lag by 33 minutes during the first ramp, and to reach dwell temperatures of only 114 °C and 163 °C, compared to the desired values of 121 °C and 177 °C. This results in a very different cure progression between the two skins. Different core materials and thicknesses would have an effect on this, but this experiment successfully demonstrates that applying one-sided heating to sandwich structures is extremely unlikely to yield good results.

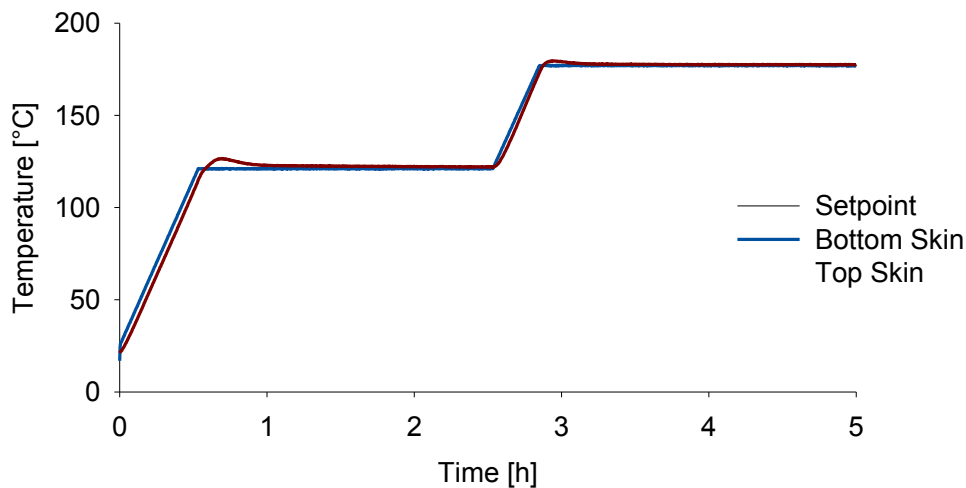


Figure 6.3-4: Sandwich structure hybrid cure thermal profile

To address the challenges shown in Figure 6.3-3, the hybrid heating system added a heating blanket above the top skin, to force it to follow the desired setpoint. From Figure 6.3-4, it is clear that the addition of the heating blanket helps solve both the lag and the through-thickness temperature difference seen in the heated tool cure. The heating blanket is able to keep the top skin close to the desired profile, even when placed above the vacuum bag. Lag is reduced to 3 minutes in the first ramp, and the top skin reaches the desired dwell temperatures. The one apparent issue with this cure is the presence of small temperature overshoot after each ramp section. This is most likely due to poor PID tuning values input into the controller, and could be easily eliminated in future trials.

Table 6.3-1 summarizes the thermal results obtained in these three trials.

Table 6.3-1: Sandwich structure thermal performance results

Phase	Metric	Oven	Heated Tool	Hybrid
Ramp 1	Bottom Skin t_{lag} (min)	30.23	0.46	0.54
	Top Skin t_{lag} (min)	17.29	32.58	2.83
Dwell 1	ΔT_{tt}^* (°C)	1.71	6.40	1.63
Ramp 2	Bottom Skin t_{lag} (min)	19.23	0.33	0.38
	Top Skin t_{lag} (min)	10.88	12.58	1.50
Dwell 3	ΔT_{tt}^* (°C)	1.59	12.74	1.63

**Through-thickness temperature difference*

These trials illustrate some of the typical challenges in processing composite sandwich structures. Having both skins experience the same temperature cycle is a non-trivial challenge due to the effects of tooling, the lightweight core material, and the varied heating conditions. Overall, it's clear that both the oven and a one-sided TCX™ heated tool struggle to have both skins ramp up to temperature without one lagging behind the other. In the case of this heated tool, the lag isn't the most pressing issue, as a large temperature difference between skins results from the one-sided heating. The hybrid heating solution presented here manages to mitigate both of these issues, but requires further work to achieve the best possible thermal control. That said, eliminating lag promises to decrease cycle times by over 45 minutes, and will result in uniformly cured parts with the best possible properties.

6.4 SUMMARY OF PROCESSING FLEXIBILITY EXPERIMENTS

In this chapter, three different challenges were addressed in an effort to expand the processing flexibility of heated tooling for OoA processing. First, the use of an alternate material form and processing technique, specifically RFI, was explored. These experiments illustrated that heated tooling is not limited to prepregs, and that there exists an interesting possibility of coupling fast heating rates with processes that employ dry fibres to achieve shorter cycle times.

Second, experiments were performed to address the challenge of processing tapered laminates with significant thickness variations. Implementing a multi-zoned heated tool allowed for an improved thermal response compared to the oven baseline, with the heated tool trials showing decreased thermal lag, and similar through-thickness temperature uniformity to the oven cure. This was confirmed to be a scalable conclusion by co-curing laminates of greatly different thicknesses to remove any effects of the fibres in-plane thermal conductivity. The similarity between these results and those of the tapered laminated indicates that the findings presented here should apply to larger scale components.

Finally, the processing of sandwich structures was investigated. These trials illustrated the challenge of processing these structures both using a conventional oven, and using one-sided heated tooling. A hybrid heating solution was proposed which succeeded in improving the thermal response of this type of structure, although work remains to optimize this setup.

Overall, these experiments have shown that TCX™ heated tools are capable of being used for more than the production of flat, monolithic laminates. Through a combination of intelligent multi-zoned control and an innovative hybrid heating solution, these tools can be used to tackle a number of challenges. These experiments serve primarily as a first step in investigating these various challenges, to demonstrate the advantages of TCX™ heated tools and motivate further work exploring in more detail the potential of these tools.

CHAPTER 7: CONCLUSIONS AND FUTURE WORK

7.1 CONCLUSIONS AND CONTRIBUTIONS

The main theme of this work was explore the application of the TCX™ heating element to OoA processing of composite materials. To this end, three objectives were put forth: to develop prototype heated tools, to compare these tools against the convection oven, and to expand the range of parts and processes for which heated tooling could be used. Within that context, the main conclusions and contributions of this research are summarized as follows:

1. Two prototype heated tools featuring TCX™ heating elements were developed.

As a first step in working with this technology, two prototypes were produced. The first demonstrated a very simple, laboratory scale processing solution, while the second provided a glimpse at a more real-world product. A novel control system was developed using LabVIEW, providing real time monitoring of temperature, pressure, and power consumption for a multi-zoned heated tool. Coupled with the second prototype, this system serves as a proof of concept for what can be done using TCX™ heating elements.

2. Heated tool processing of OoA prepregs was determined to achieve similar quality to oven processing, regardless of the heating rate imposed.

Laminate quality experiments showed that the heated tool processing of CYCOM®5320 OoA prepreg produces parts of similar quality to those cured in an oven. Void content, short-beam strength, and T_g analysis confirmed this conclusion. The effect of heating rates on void content was explored, and was determined to have little to no impact. This allows future users to confidently take advantage of the TCX™ elements ability to provide rapid heating, and reduce cycle times.

3. Heated tools were shown to require significantly less energy for the curing of composite structures.

Experimental results showed the energy savings made possible by providing a more direct heating solution. Two scaling methods were considered to provide a fair comparison between three systems capable of handling different amounts of material. This scaled comparison indicates possible savings of between 26.1 and 91.6 percent, and led to recommendations for future tool designs to best achieve these savings.

4. Resin film infusion, tapered laminates, and sandwich structures were all successfully demonstrated using heated tooling.

Three challenges were addressed to expand the processing flexibility of heated tooling. These alternate materials and structures demonstrated some of the challenges in OoA manufacturing, and how heated tooling can be used to address these issues. Overall, these experiments demonstrated that heated tooling, through the use of multiple heating zones and heat sources, is capable of processing a wide range of parts.

7.2 FUTURE WORK

This work serves primarily as a first exploration of the TCX™ element for OoA processing. As such, during the course of this project several possible avenues for future work were identified.

1. The TCX™ element could be applied to moulds featuring complex geometries and alternate tooling materials.

As a first step, this heating technology was applied only to flat aluminum tools. A logical progression of this technology would be to demonstrate its suitability for more real-world systems, by investigating its application to both alternate tooling materials and more complex shapes. To be used within the aerospace industry, this technology must be shown to be applicable to common tooling materials such as steel, invar, and CFRP. It must also be shown to be applicable to tools which feature both gradual and sharp radii, to cover the range of part shapes required by the industry.

2. A cost analysis of this technology could be performed.

While this work presents the possible energy savings this technology promises, a more complete cost study would better determine its suitability for industrial application. Companies are driven primarily by their bottom lines, and for this technology to be implemented on a larger scale it must be shown to achieve equal or better results at a lower cost.

3. The innovative heating systems developed here could be optimized to provide improved thermal control.

For the multi-zoned heating system, an intelligent system could be developed which takes part thickness into account, and automatically adjusts power output in an effort to improve temperature uniformity during ramp sections. For the hybrid heating blanket / heated tool system, further testing could be done to better tune the PID values and provide an extremely accurate two-sided heating solution.

REFERENCES

- [1] American Composites Manufacturers Association. "What Are Composites?". 2015. June 4 2015. <<http://www.acmanet.org/composites/what-are-composites>>.
- [2] Paul, D., and Pratt, D. "History of Flight Vehicle Structures 1903-1990." *Journal of Aircraft* 41(5) (2004): 969-977.
- [3] Deo, R. B., Starnes, J. H., and Holzwarth, R. C. "Low-Cost Composite Materials and Structures for Aircraft Applications." *NATO RTO AVT Panel Spring Symposium and Specialists' Meeting*. May 7-11, 2001. Leon, Norway.
- [4] Roeseler, W. G., et al. "Composite Structures: The First 100 Years." *16th International Conference on Composite Materials*. July 8-13, 2007. Kyoto, Japan.
- [5] Campbell, F. C. *Manufacturing Processes for Advanced Composites*. Ed. Campbell, F. C. Kidlington, UK: Elsevier Advanced Technology, 2003.
- [6] McCormick, C. "How Nickel Contributes to More Sustainable Air Transportation." *Nickel* 23 (2008).
- [7] Hubert, P., Fernlund, G., and Poursartip, A. "Autoclave Processing for Composites." *Manufacturing Techniques for Polymer Matrix Composites*. Eds. Advani, S. and Hsiao, K.-T. Cambridge: Woodhead Publishing Limited, 2012.
- [8] Mazumdar, S. *Composites Manufacturing: Materials, Product, and Process Engineering*. Boca Raton, FL: CRC Press LCC, 2001.
- [9] Hubert, P. "Lecture Notes Module 1.2." *Mech 544 Processing of Composite Materials*. 2015.
- [10] Holman, J. P. *Heat Transfer*. 10 ed. New York, NY: McGraw-Hill, 2009.
- [11] Johnston, A., et al. "An Investigation of Autoclave Convective Heat Transfer". *Design and Manufacturing of Composites, Proceedings of the Second Joint Canada-Japan Workshop on Composites*. 1998. Technomic Publishing Company, Inc. pp. 106-113.
- [12] Monaghan, P. F., Brogan, M. T., and Oosthuizen, P. H. "Heat Transfer in an Autoclave for Processing Thermoplastic Composites." *Composites Manufacturing* 2(3-4) (1991): 233-242.
- [13] U.S. Department of Defense. "Composite Materials Handbook - Polymer Matrix Composites: Materials Usage, Design, and Analysis." MIL-HDBK-17-3F. 2002.
- [14] Witik, R., et al. "Assessing the Economic and Environmental Potential of out of Autoclave Processing." *The 18th International Conference on Composite Materials*. August 21-26, 2011. Jeju, South Korea.
- [15] Ridgard, C. "Next Generation out-of-Autoclave Systems." *SAMPE 2010 Conference and Exhibition*. May 17-20, 2010. Seattle, Washington.
- [16] Centea, T., et al. "Scaling Challenges Encountered with out-of-Autoclave Prepregs." *53rd AIAA/ASME/ASCE/ AHS/ASC Structures, Structural Dynamics, and Materials Conference*. April 23-26, 2012. Honolulu, Hawaii.
- [17] Kaufmann, C. "Nickel Coated Graphite Fiber Advantages for Integrally Heated Tooling Applications." *Industrial Heating* (1988): 14-15.

- [18] Arney, M. W., et al. "Integrally-Heated Tooling for the Manufacture of Fibre-Reinforced Composites." *Composites Processing 2004 Conference*. April 23, 2004. Bromsgrove, UK.
- [19] Stewart, R. "New Mould Technologies and Tooling Materials Promise Advances for Composites." *Reinforced Plastics* 54(3) (2010): 30-36.
- [20] Blacker, J. M., Merriman, D. J., and Lucas, R. D. "Out-of-Autoclave Composites Manufacturing with Electrically Heated Carbon Foam Tooling." *SAMPE 2010 Conference and Exhibition*. May 17-20, 2010. Seattle, Washington.
- [21] Coenen, V., et al. "A Feasibility Study of Quickstep Processing of an Aerospace Composite Material." *SAMPE-EUROPE 2005 Conference*. April 5-7, 2005. Paris, France.
- [22] Davies, L., et al. "Effect of Cure Cycle Heat Transfer Rates on the Physical and Mechanical Properties of an Epoxy Matrix Composite." *Composites science and technology* 67(9) (2007): 1892-1899.
- [23] Khan, L. A., et al. "Cure Characterization of CYCOM 977-2a Carbon/Epoxy Composites for Quickstep Processing." *Polymer Engineering & Science* 54(4) (2014): 887-898.
- [24] Ruiz, E., et al. "Flexible Injection: A Novel LCM Technology for Low Cost Manufacturing of High Performance Composites. Part I-Experimental Investigation." *The 9th International Conference on Flow Processes in Composite Materials*. July 7-9, 2008. Montreal, Canada.
- [25] Trochu, F., Soukane, S., and Touraine, B. "Flexible Injection: A Novel Lcm Technology for Low Cost Manufacturing of High Performance Composites. Part II: Numerical Model." *The 9th International Conference on Flow Processes in Composite Materials*. July 7-9, 2008. Montreal, Canada.
- [26] Schlimbach, J., Ogale, A., and Schimmel, S. "Quickstep Processing to Control Exothermic Reaction During the Manufacture of Thick Laminates." 38(9-10) (2009): 374-8.
- [27] Sommers, J., Clawson, D., and Mori, G. "Selected Patents Related to Thermal Spraying." *Journal of Thermal Spray Technology* 14(1) (2005).
- [28] Nelson, W., Aunemo, H., and Demers, A. "Selected Patents Related to Thermal Spraying." *Journal of Thermal Spray Technology* 16(2) (2007).
- [29] Abbott, R. C., Magnant, G. P., and Glenn, W. A. "Resistive Heaters and Uses Thereof." U.S. Patent 20,030,121,906. 2003.
- [30] Smith, A. W., et al. "Development of a Heated Tooling Solution to Improve Process Flexibility for out-of-Autoclave Prepregs." SAMPE Tech 2013 Conference: Powerpoint. 2013.
- [31] Twardowski, T. E., Lin, S. E., and Geil, P. H. "Curing in Thick Composite Laminates: Experiment and Simulation." *Journal of Composite Materials* 27(3) (1993): 216-250.
- [32] Smith, A. W., et al. "Development of a Heated Tooling Solution to Improve Process Flexibility for out-of-Autoclave Prepregs." *SAMPE Tech 2013 Conference*. October 21-24, 2013. Wichita, Kansas.
- [33] Bujun, K. "Processing Study of in-Situ Bonded Scarf Repairs for Composite Structures." Thesis. McGill University, 2014.
- [34] Quinlan, E. P. "Thermal and Crystallinity Profiles in Laminates Manufactured with Automated Thermoplastic Tow Placement Process." Thesis. McGill University, 2011.

- [35] Painter, P. C., and Coleman, M. M. *Fundamentals of Polymer Science: An Introductory Text*. 2 ed. Lancaster, PA: Technomic Publishing Company, Inc., 1997.
- [36] Enns, J. B., and Gillham, J. K. "Time–Temperature–Transformation (TTT) Cure Diagram: Modeling the Cure Behavior of Thermosets." *Journal of Applied Polymer Science* 28(8) (1983): 2567-2591.
- [37] Centea, T., and Hubert, P. "The Effect of Material and Process Parameters on Tow Impregnation and Micro-Void Formation in out-of-Autoclave Prepregs". *26th Annual Technical Conference of the American Society for Composites 2011 and the 2nd Joint US-Canada Conference on Composites*. September 26-28, 2011. DEStech Publications Inc. pp. 1279-1298.
- [38] Kratz, J., et al. "Thermal Models for MTM45-1 and CYCOM 5320 out-of-Autoclave Prepreg Resins." *Journal of Composite Materials* 47(3) (2013): 341-352.
- [39] Cole, K., Hechler, J., and Noel, D. "A New Approach to Modeling the Cure Kinetics of Epoxy/Amine Thermosetting Resins. 2. Application to a Typical System Based on Bis [4-(Diglycidylamino) Phenyl] Methane and Bis (4-Aminophenyl) Sulfone." *Macromolecules* 24(11) (1991): 3098-3110.
- [40] Kamal, M., and Sourour, S. "Kinetics and Thermal Characterization of Thermoset Cure." *Polymer Engineering & Science* 13(1) (1973): 59-64.
- [41] Khoun, L., Centea, T., and Hubert, P. "Characterization Methodology of Thermoset Resins for the Processing of Composite Materials-Case Study: CYCOM 890RTM Epoxy Resin." *Journal of Composite Materials* (2009).
- [42] Huang, Y., et al. "Influence of Ultrasonic Treatment on the Characteristics of Epoxy Resin and the Interfacial Property of Its Carbon Fiber Composites." *Composites science and technology* 62(16) (2002): 2153-2159.
- [43] Centea, T., and Hubert, P. "Modelling the Effect of Material Properties and Process Parameters on Tow Impregnation in out-of-Autoclave Prepregs." *Composites Part A: applied science and manufacturing* 43(9) (2012): 1505-1513.
- [44] Kim, J. S. "Development of an Autoclave Cure Cycle with Cooling and Reheating Steps for Thick Thermoset Composite Laminates." *Journal of composite materials* 31(22) (1997): 2264-2282.
- [45] Oh, J. H. "Cure Cycle for Thick Glass/Epoxy Composite Laminates." *Journal of composite materials* 36(1) (2002): 19-45.
- [46] White, S., and Hahn, H. "Cure Cycle Optimization for the Reduction of Processing-Induced Residual Stresses in Composite Materials." *Journal of Composite Materials* 27(14) (1993): 1352-1378.
- [47] Alcoa Global Aerospace Transportation and Industrial Rolled Products. "Precision Machined Cast Aluminum Plate." Pamphlet. 2012.
- [48] Payette, S., et al. "Multi-Zoned Heated Tooling for out-of-Autoclave Processing of Variable Thickness Composite Laminates." *CANCOM 2015*. August 18-20, 2015. Edmonton, Alberta.
- [49] Payette, S., et al. "Out-of-Autoclave Manufacturing: Benchmarking of an Integrally Heated Tool-Plate." *CAMX 2014*. October 13-16, 2014. Orlando, Florida.

- [50] Payette, S., et al. "Out-of-Autoclave Manufacturing: Benchmarking of an Integrally Heated Tool-Plate." *SAMPE Journal* 51(1) (2015): 27-35.
- [51] ASTM Standard D7028, 2007, "Standard Test Method for Glass Transition Temperature (DMA Tg) of Polymer Matrix Composites by Dynamic Mechanical Analysis (DMA)." ASTM International, West Conshohocken, PA, 2007. DOI: 10.1520/D7028-07E01. www.astm.org.
- [52] ASTM Standard D2344 / D2344M, 2013, "Standard Test Method for Short-Beam Strength of Polymer Matrix Composite Materials and Their Laminates." ASTM International, West Conshohocken, PA, 2013. DOI: 10.1520/D2344_D2344M. www.astm.org.
- [53] Kratz, J., and Hubert, P. "Anisotropic Air Permeability in out-of-Autoclave Prepregs: Effect on Honeycomb Panel Evacuation Prior to Cure." *Composites Part A: Applied Science and Manufacturing* 49 (2013): 179-191.
- [54] Cytec Engineered Materials. "CYCOM 5320 Toughened Epoxy for Structural Applications." Information Sheet: Revision 1.3. 2009.
- [55] Ghiorse, S. R. "Effect of Void Content on the Mechanical Properties of Carbon/Epoxy Laminates." *S.A.M.P.E. quarterly* 24(2) (1993): 54-59.
- [56] Muller de Almeida, S. F., and dos Santos Nogueira Neto, Z. "Effect of Void Content on the Strength of Composite Laminates." *Composite Structures* 28(2) (1994): 139-48.
- [57] Zhan-Sheng, G., et al. "Critical Void Content for Thermoset Composite Laminates." *Journal of Composite Materials* 43(17) (2009): 1775-90.
- [58] U.S. Department of Defense. "Composite Materials Handbook - Polymer Matrix Composites: Materials Properties." MIL-HDBK-17-2F. 2002.
- [59] Agius, S. L., Magniez, K. J. C., and Fox, B. L. "Cure Behaviour and Void Development within Rapidly Cured out-of-Autoclave Composites." *Composites Part B: Engineering* 47 (2013): 230-237.
- [60] Hoecker, F., et al. "Effects of Fiber/Matrix Adhesion on Off-Axis Mechanical Response in Carbon-Fiber/Epoxy-Resin Composites." *Composites Science and Technology* 54(3) (1995): 317-327.
- [61] Schiraldi, A., Baldini, P., and Pezzati, E. "Epoxy Polymers: Glass Transition/Cure Degree Correlation." *Journal of Thermal Analysis* 30(6) (1985): 1343-1348.
- [62] Thermal Product Solutions. "Blue M 146 Series Standard Oven." Product Brochure.
- [63] Thermal Product Solutions. "Gruenberg Truck-in Industrial Ovens." Product Brochure.
- [64] Thermal Product Solutions. "Gruenberg Cabinet Ovens." Product Brochure.
- [65] Levy, A., Kratz, J., and Hubert, P. "Air Evacuation During Vacuum Bag Only Prepreg Processing of Honeycomb Sandwich Structures: In-Plane Air Extraction Prior to Cure." *Composites Part A: Applied Science and Manufacturing* 68 (2015): 365-376.
- [66] Cytec Industrial/Aerospace Materials. "MTM45-1." Product Data Sheet: Issue 8a. 2012.
- [67] He, K., Hoa, S. V., and Ganesan, R. "The Study of Tapered Laminated Composite Structures: A Review." *Composites Science and Technology* 60(14) (2000): 2643-2657.
- [68] Thomas, D. M., and Webber, J. P. H. "A Design Study into the Delamination Behaviour of Tapered Composites." *Composite Structures* 27(4) (1994): 379-388.

- [69] Vinson, J. R. *The Behavior of Sandwich Structures of Isotropic and Composite Materials*. CRC Press, 1999.
- [70] Kratz, J. "Processing Composite Sandwich Structures Using out-of-Autoclave Technology." Thesis. McGill University, 2009.

APPENDIX I – QUALITY BENCHMARKING DATA

Table AI-1: Initial void content study complete results

		Operator				Laminate		Condition	
		1	2	3	Avg	Avg	StDev	Avg	StDev
Oven 3C	HTP-E_QUAL-001-L1-S1	1.56	1.31	1.59	1.49	1.61	0.17	2.07	0.80
	HTP-E_QUAL-001-L1-S2	1.82	1.64	1.93	1.80				
	HTP-E_QUAL-001-L1-S3	1.75	1.42	1.46	1.55				
	HTP-E_QUAL-002-L1-S1	2.12	1.69	1.93	1.91	1.61	0.44		
	HTP-E_QUAL-002-L1-S2	1.88	1.73	1.82	1.81				
	HTP-E_QUAL-002-L1-S3	1.11	1.07	1.15	1.11				
	HTP-E_QUAL-003-L1-S1	3.97	3.50	3.69	3.72	2.99	0.68		
	HTP-E_QUAL-003-L1-S2	3.11	2.68	2.88	2.89				
	HTP-E_QUAL-003-L1-S3	2.38	2.22	2.50	2.36				
HTP 3C	HTP-E_QUAL-006-L1-S1	0.23	0.25	0.22	0.23	0.49	0.29	1.53	1.56
	HTP-E_QUAL-006-L1-S2	0.39	0.46	0.48	0.44				
	HTP-E_QUAL-006-L1-S3	0.77	0.79	0.86	0.81				
	HTP-E_QUAL-007-L1-S1	0.43	0.49	0.51	0.47	0.55	0.07		
	HTP-E_QUAL-007-L1-S2	0.63	0.54	0.48	0.55				
	HTP-E_QUAL-007-L1-S3	0.59	0.54	0.71	0.61				
	HTP-E_QUAL-008-L1-S1	3.02	2.75	3.30	3.02	3.55	0.68		
	HTP-E_QUAL-008-L1-S2	3.50	3.16	3.27	3.31				
	HTP-E_QUAL-008-L1-S3	4.70	3.90	4.32	4.31				
HTP 50C	HTP-E_QUAL-012-L1-S1	1.58	1.40	1.49	1.49	2.16	0.59	2.74	1.27
	HTP-E_QUAL-012-L1-S2	2.62	2.21	2.90	2.58				
	HTP-E_QUAL-012-L1-S3	2.52	2.37	2.33	2.41				
	HTP-E_QUAL-025-L1-S1	3.14	3.30	3.58	3.34	3.01	0.42		
	HTP-E_QUAL-025-L1-S2	2.36	3.17	2.06	2.53				
	HTP-E_QUAL-025-L1-S3	3.00	3.21	3.24	3.15				
	HTP-E_QUAL-026-L1-S1	3.20	3.01	2.71	2.98	3.60	0.64		
	HTP-E_QUAL-026-L1-S2	3.57	3.62	3.49	3.56				
	HTP-E_QUAL-026-L1-S3	4.02	3.79	4.98	4.26				

Anova: Single Factor, Oven 3C and HTP 3C

SUMMARY

Groups	Count	Sum	Average	Variance
Column 1	18	37.26303	2.070169	0.700372
Column 2	18	27.5163	1.528683	2.328363

ANOVA

Source of Variation	SS	df	MS	F	P-value	F crit
Between Groups	2.638856	1	2.638856	1.742547	0.195635	4.130018
Within Groups	51.4885	34	1.514368			
Total	54.12735	35				

Table AI-2: Ramp trials complete void content results

		Operator				Laminate		Condition	
		1	2	3	Avg	Avg	StDev	Avg	StDev
HTP 3C	HTP-E_QUAL-006-L1-S1	0.23	0.25	0.22	0.23	0.49	0.29	2.12	1.79
	HTP-E_QUAL-006-L1-S2	0.39	0.46	0.48	0.44				
	HTP-E_QUAL-006-L1-S3	0.77	0.79	0.86	0.81				
	HTP-E_QUAL-007-L1-S1	0.43	0.49	0.51	0.47	0.55	0.07		
	HTP-E_QUAL-007-L1-S2	0.63	0.54	0.48	0.55				
	HTP-E_QUAL-007-L1-S3	0.59	0.54	0.71	0.61				
	HTP-E_QUAL-008-L1-S1	3.02	2.75	3.30	3.02	3.55	0.68		
	HTP-E_QUAL-008-L1-S2	3.50	3.16	3.27	3.31				
	HTP-E_QUAL-008-L1-S3	4.70	3.90	4.32	4.31				
	HTP-E_QUAL-034-L1-S1	1.04	1.43	1.80	1.42	1.32	0.10		
	HTP-E_QUAL-034-L1-S2	0.78	1.03	2.12	1.31				
	HTP-E_QUAL-034-L1-S3	0.97	1.03	1.65	1.22				
	HTP-E_QUAL-038-L1-S2	5.14	5.31	5.76	5.40	4.68	0.63		
HTP-E_QUAL-038-L1-S3	4.13	4.08	4.94	4.38					
HTP-E_QUAL-038-L1-S1	4.03	4.07	4.63	4.24					
HTP 10C	HTP-E_QUAL-028-L1-S1	0.66	0.62	0.61	0.63	0.78	0.13	2.24	0.93
	HTP-E_QUAL-028-L1-S2	0.83	0.86	0.88	0.86				
	HTP-E_QUAL-028-L1-S3	0.83	0.86	0.89	0.86				
	HTP-E_QUAL-029-L1-S1	3.36	3.24	4.20	3.60	3.33	0.24		
	HTP-E_QUAL-029-L1-S2	3.39	3.50	2.90	3.26				
	HTP-E_QUAL-029-L1-S3	3.25	3.06	3.06	3.12				
	HTP-E_QUAL-030-L1-S1	2.35	2.43	2.33	2.37	2.34	0.02		
	HTP-E_QUAL-030-L1-S2	2.40	2.23	2.37	2.33				
	HTP-E_QUAL-030-L1-S3	2.19	2.34	2.46	2.33				
	HTP-E_QUAL-035-L1-S1	2.53	2.72	3.19	2.81	2.88	0.39		
	HTP-E_QUAL-035-L1-S2	2.23	2.54	2.83	2.53				
	HTP-E_QUAL-035-L1-S3	3.08	3.16	3.69	3.31				
	HTP-E_QUAL-039-L1-S1	1.42	1.74	2.19	1.78	1.84	0.08		
	HTP-E_QUAL-039-L1-S2	1.52	1.94	2.34	1.93				
HTP-E_QUAL-039-L1-S3	1.48	1.74	2.24	1.82					
HTP 30C	HTP-E_QUAL-031-L1-S1	1.43	1.59	1.62	1.55	1.69	0.21	1.98	0.69
	HTP-E_QUAL-031-L1-S2	1.45	1.63	1.67	1.58				
	HTP-E_QUAL-031-L1-S3	1.73	1.99	2.08	1.93				
	HTP-E_QUAL-032-L1-S1	1.49	1.61	1.34	1.48	1.98	0.51		
	HTP-E_QUAL-032-L1-S2	2.51	2.62	2.35	2.49				
	HTP-E_QUAL-032-L1-S3	1.91	2.24	1.79	1.98				
	HTP-E_QUAL-033-L1-S1	2.26	2.96	2.32	2.51	2.74	0.21		
	HTP-E_QUAL-033-L1-S2	2.78	2.98	2.98	2.91				
	HTP-E_QUAL-033-L1-S3	2.51	3.16	2.75	2.81				
	HTP-E_QUAL-036-L1-S1	0.91	1.06	1.36	1.11	1.06	0.23		
	HTP-E_QUAL-036-L1-S2	0.95	1.05	1.80	1.26				
	HTP-E_QUAL-036-L1-S3	0.59	0.92	0.92	0.81				
	HTP-E_QUAL-040-L1-S1	1.95	2.59	4.45	3.00	2.41	0.58		
	HTP-E_QUAL-040-L1-S2	1.47	1.80	2.23	1.83				
HTP-E_QUAL-040-L1-S3	1.88	2.74	2.60	2.41					
HTP 50C	HTP-E_QUAL-012-L1-S1	1.58	1.40	1.49	1.49	2.16	0.59	2.80	1.29
	HTP-E_QUAL-012-L1-S2	2.62	2.21	2.90	2.58				
	HTP-E_QUAL-012-L1-S3	2.52	2.37	2.33	2.41				
	HTP-E_QUAL-025-L1-S1	3.14	3.30	3.58	3.34	3.01	0.42		
	HTP-E_QUAL-025-L1-S2	2.36	3.17	2.06	2.53				
	HTP-E_QUAL-025-L1-S3	3.00	3.21	3.24	3.15				
HTP-E_QUAL-026-L1-S1	3.20	3.01	2.71	2.98	3.60	0.64			

	Operator				Laminate		Condition	
	1	2	3	Avg	Avg	StDev	Avg	StDev
HTP-E_QUAL-026-L1-S2	3.57	3.62	3.49	3.56	0.99	0.18		
HTP-E_QUAL-026-L1-S3	4.02	3.79	4.98	4.26				
HTP-E_QUAL-041-L1-S1	0.79	0.89	1.27	0.98				
HTP-E_QUAL-041-L1-S2	0.67	0.93	0.84	0.81	4.24	1.01		
HTP-E_QUAL-041-L1-S3	0.85	1.31	1.33	1.16				
HTP-E_QUAL-042-L1-S1	3.01	3.36	3.67	3.35				
HTP-E_QUAL-042-L1-S2	4.87	5.30	5.86	5.34				
HTP-E_QUAL-042-L1-S3	3.72	4.06	4.34	4.04				

Anova: Single Factor, Ramp Rate Trials

SUMMARY

Groups	Count	Sum	Average	Variance
Column 1	15	30.2813	2.018753	3.088463
Column 2	15	32.4034	2.160227	0.862924
Column 3	15	28.2017	1.880113	0.451377
Column 4	15	41.16027	2.744018	1.605483

ANOVA

Source of Variation	SS	df	MS	F	P-value	F crit
Between Groups	6.49069	3	2.163563	1.440396	0.240738	2.769431
Within Groups	84.11547	56	1.502062			
Total	90.60616	59				

Table AI-3: Short-beam strength complete results

	Thick ness (mm)	Width (mm)	Peak Load (N)	Short-Beam Strength (MPa)					
				Sample	Laminate		Condition		
					Avg	StDev	Avg	StDev	
Oven 3C	HTP-E_QUAL-001-L1-S1	3.18	6.27	2044.59	76.86	77.44	0.72		
	HTP-E_QUAL-001-L1-S2	3.18	6.29	2033.14	76.31				
	HTP-E_QUAL-001-L1-S3	3.18	6.29	2080.03	77.92				
	HTP-E_QUAL-001-L1-S4	3.17	6.32	2071.12	77.48				
	HTP-E_QUAL-001-L1-S5	3.18	6.28	2071.91	77.91				
	HTP-E_QUAL-001-L1-S6	3.16	6.29	2072.99	78.15				
	HTP-E_QUAL-002-L1-S1	3.22	6.14	1920.61	72.84	73.43	1.29	70.92	6.84
	HTP-E_QUAL-002-L1-S2	3.18	6.30	1980.50	74.14				
	HTP-E_QUAL-002-L1-S3	3.18	6.30	1994.03	74.56				
	HTP-E_QUAL-002-L1-S4	3.20	6.32	1920.03	71.27				
	HTP-E_QUAL-002-L1-S5	3.19	6.29	1997.19	74.63				
	HTP-E_QUAL-002-L1-S6	3.15	6.29	1933.90	73.13				
	HTP-E_QUAL-003-L1-S1	3.20	6.32	1636.65	60.77	61.90	0.73		
	HTP-E_QUAL-003-L1-S2	3.19	6.30	1655.47	61.70				
	HTP-E_QUAL-003-L1-S3	3.20	6.30	1657.77	61.75				
HTP-E_QUAL-003-L1-S4	3.19	6.29	1668.92	62.38					

	Thick ness (mm)	Width (mm)	Peak Load (N)	Short-Beam Strength (MPa)					
				Sample	Laminate		Condition		
					Avg	StDev	Avg	StDev	
	HTP-E_QUAL-003-L1-S5	3.19	6.31	1690.42	62.96				
	HTP-E_QUAL-003-L1-S6	3.19	6.30	1658.28	61.85				
HTP 3C	HTP-E_QUAL-006-L1-S1	3.08	6.32	2174.79	83.82	82.22	2.33	78.26	7.22
	HTP-E_QUAL-006-L1-S2	3.05	6.30	2132.62	83.19				
	HTP-E_QUAL-006-L1-S3	3.05	6.30	1992.14	77.71				
	HTP-E_QUAL-006-L1-S4	3.08	6.29	2113.61	81.88				
	HTP-E_QUAL-006-L1-S5	3.04	6.31	2150.03	83.95				
	HTP-E_QUAL-006-L1-S6	3.03	6.30	2107.30	82.74				
	HTP-E_QUAL-007-L1-S1	3.08	6.30	2204.24	85.34	83.95	1.16		
	HTP-E_QUAL-007-L1-S2	3.10	6.30	2210.37	84.94				
	HTP-E_QUAL-007-L1-S3	3.11	6.31	2180.91	83.46				
	HTP-E_QUAL-007-L1-S4	3.11	6.30	2180.43	83.49				
	HTP-E_QUAL-007-L1-S5	3.10	6.30	2194.00	84.28				
	HTP-E_QUAL-007-L1-S6	3.12	6.29	2149.21	82.16				
	HTP-E_QUAL-008-L1-S1	3.15	6.31	1815.68	68.62	68.61	1.00		
	HTP-E_QUAL-008-L1-S2	3.14	6.31	1797.10	68.03				
	HTP-E_QUAL-008-LI-S3	3.17	6.31	1853.84	69.49				
	HTP-E_QUAL-008-L1-S4	3.19	6.31	1815.62	67.63				
	HTP-E_QUAL-008-L1-S5	3.16	6.31	1860.87	70.11				
	HTP-E_QUAL-008-L1-S6	3.13	6.29	1781.16	67.77				
HTP 500C	HTP-E_QUAL-012-L1-S1	3.13	6.32	2019.34	76.46	74.75	1.55	68.80	4.58
	HTP-E_QUAL-012-L1-S2	3.13	6.33	2025.15	76.64				
	HTP-E_QUAL-012-L1-S3	3.11	6.30	1947.24	74.60				
	HTP-E_QUAL-012-L1-S4	3.12	6.32	1921.54	73.09				
	HTP-E_QUAL-012-L1-S5	3.13	6.32	1966.61	74.64				
	HTP-E_QUAL-012-L1-S6	3.11	6.32	1917.70	73.09				
	HTP-E_QUAL-025-L1-S1	3.11	6.31	1674.10	64.05	66.27	1.71		
	HTP-E_QUAL-025-L1-S2	3.12	6.32	1784.04	68.00				
	HTP-E_QUAL-025-L1-S3	3.12	6.30	1723.86	65.77				
	HTP-E_QUAL-025-L1-S4	3.14	6.32	1717.08	64.93				
	HTP-E_QUAL-025-L1-S5	3.14	6.32	1807.67	68.44				
	HTP-E_QUAL-025-L1-S6	3.10	6.32	1734.42	66.41				
	HTP-E_QUAL-026-L1-S1	3.11	6.31	1721.89	65.74	65.39	1.34		
	HTP-E_QUAL-026-L1-S2	3.15	6.32	1670.37	63.05				
	HTP-E_QUAL-026-L1-S3	3.13	6.30	1741.62	66.25				
	HTP-E_QUAL-026-L1-S4	3.11	6.32	1710.00	65.33				
	HTP-E_QUAL-026-L1-S5	3.13	6.31	1713.32	65.00				
	HTP-E_QUAL-026-L1-S6	3.14	6.32	1771.47	66.97				

Anova: Single Factor, Short-beam strength

SUMMARY				
Groups	Count	Sum	Average	Variance
Column 1	18	1276.61	70.92278	46.72089
Column 2	18	1408.61	78.25611	52.09521
Column 3	18	1238.46	68.80333	20.97972

ANOVA

Source of Variation	SS	df	MS	F	P-value	F crit
Between Groups	885.749	2	442.8745	11.09073	0.0001	3.178799
Within Groups	2036.529	51	39.93194			
Total	2922.278	53				

Table AI-4: Glass transition temperature complete results

Heating Condition	Laminate	Sample	Thickness (mm)	Length (mm)	Width (mm)	Span (mm)	DMA Tg (°C)	Average Tg (°C)
Oven 3C	HTP-E/QUAL-004-L1	S1	3.142	50.68	12.98	35	200.74	200.98
		S2	3.141	50.64	12.99	35	201.00	
		S3	3.158	50.58	12.99	35	201.21	
HTP 3C	HTP-E/QUAL-009-L1	S1	3.115	51.75	13.01	35	201.35	201.54
		S2	3.176	51.81	13.00	35	202.06	
		S3	3.139	51.86	13.01	35	201.22	
HTP 50C	HTP-E/QUAL-027-L1	S1	3.134	57.27	13.01	35	199.71	200.58
		S2	3.084	60.62	13.02	35	200.99	
		S3	3.129	60.90	13.02	35	201.03	

APPENDIX II – ENERGY BENCHMARKING DATA

Table AII-1: Energy consumption complete data

Heating Method	Trial	Energy Consumption		
		Sample (MJ)	Average (MJ)	Standard Deviation
Oven 3C	HTP-E/QUAL-015	83.15	86.73	3.18
	HTP-E/QUAL-016	86.16		
	HTP-E/QUAL-017	89.77		
	HTP-E/QUAL-018	90.24		
	HTP-E/QUAL-019	84.34		
HTP 3C	HTP-E/QUAL-006	2.54	2.46	0.14
	HTP-E/QUAL-007	2.23		
	HTP-E/QUAL-008	2.52		
	HTP-E/QUAL-009	2.43		
	HTP-E/QUAL-010	2.57		
MZT 3C	HTP-MZT-E001	18.09	18.32	0.21
	HTP-MZT-E002	18.29		
	HTP-MZT-E003	18.21		
	HTP-MZT-E004	18.40		
	HTP-MZT-E005	18.63		
HTP 50C	HTP-E/QUAL-012	2.43	2.55	0.22
	HTP-E/QUAL-020	2.83		
	HTP-E/QUAL-021	2.65		
	HTP-E/QUAL-022	2.27		
	HTP-E/QUAL-023	2.57		

Table AII-2: Average power complete data

Heating Method	Trial	Power		
		Sample (kW)	Average (kW)	Standard Deviation
Oven 3C	HTP-E/QUAL-015	2.899	3.02	0.11
	HTP-E/QUAL-016	3.004		
	HTP-E/QUAL-017	3.130		
	HTP-E/QUAL-018	3.147		
	HTP-E/QUAL-019	2.941		
HTP 3C	HTP-E/QUAL-006	0.089	0.086	0.005
	HTP-E/QUAL-007	0.078		
	HTP-E/QUAL-008	0.088		
	HTP-E/QUAL-009	0.085		
	HTP-E/QUAL-010	0.090		
MZT 3C	HTP-MZT-E001	0.628	0.636	0.007
	HTP-MZT-E002	0.635		
	HTP-MZT-E003	0.632		
	HTP-MZT-E004	0.639		
	HTP-MZT-E005	0.647		
HTP 50C	HTP-E/QUAL-012	0.094	0.099	0.008
	HTP-E/QUAL-020	0.110		
	HTP-E/QUAL-021	0.103		
	HTP-E/QUAL-022	0.088		
	HTP-E/QUAL-023	0.099		

Table AII-3: Peak power complete data

Heating Method	Trial	Peak Power		
		Sample (kW)	Average (kW)	Standard Deviation
Oven 3C	HTP-E/QUAL-015	6.590	6.842	0.205
	HTP-E/QUAL-016	6.817		
	HTP-E/QUAL-017	7.028		
	HTP-E/QUAL-018	7.068		
	HTP-E/QUAL-019	6.705		
HTP 3C	HTP-E/QUAL-006	0.311	0.304	0.009
	HTP-E/QUAL-007	0.292		
	HTP-E/QUAL-008	0.303		
	HTP-E/QUAL-009	0.316		
	HTP-E/QUAL-010	0.300		
MZT 3C	HTP-MZT-E001	1.203	1.210	0.012
	HTP-MZT-E002	1.200		
	HTP-MZT-E003	1.212		
	HTP-MZT-E004	1.205		
	HTP-MZT-E005	1.230		
HTP 50C	HTP-E/QUAL-012	1.680	1.706	0.023
	HTP-E/QUAL-020	1.716		
	HTP-E/QUAL-021	1.698		
	HTP-E/QUAL-022	1.740		
	HTP-E/QUAL-023	1.694		